MODEL REFERENCE ADAPTIVE CONTROL OF WEB GUIDES

By

ARAVIND SESHADRI

Bachelor of Engineering
University of Madras
Tamil Nadu, India
2003

Submitted to the Faculty of the
Graduate College of the
Oklahoma State University
in partial fulfillment of
the requirements for
the Degree of
MASTER OF SCIENCE
May 2007

MODEL REFERENCE ADAPTIVE CONTROL

OF WEB GUIDES

Thesis Approved:

Dr. Prabhakar R. Pagilla

Thesis Advisor

Dr. Karl N. Reid

Dean of the College of Engineering, Architecture & Technology

Dr. Gary E. Young

Committee Member

Dr. A. Gordon Emslie

Dean of the Graduate College

ACKNOWLEDGMENTS

I wish to express my deepest gratitude to my advisor, Dr. Prabhakar R. Pagilla, for his intelligent supervision, friendship and support throughout my graduate program. I am indebted to him for his motivation and encouragement, which kept me focused on my goals. I would like to thank him for supporting me as a research assistant, during which time I was fortunate to learn a lot about the latest advancements in web handling and control systems.

I would like to extend my warmest thanks to my committee members: Dr. Karl N. Reid and Dr. Gary E. Young for their support, suggestions and time.

I would like to thank my colleagues, at Oklahoma State University, Anil Abbaraju, Mauro Cimino, Ramamurthy Dwivedula, Reza Jafari, Seshadri Kuppuswamy, Pranav Kumar Peddi-Ravi, Ryan Ratliff, Nilesh Siraskar, Diao Yu, and Yunfei Zou for their timely support and suggestions.

Finally, I greatly appreciate the support, patience and motivation from my parents and my brother. Without them I would have never reached this level in my life.

TABLE OF CONTENTS

Chapter Page

LIST OF TABLES

Table Page

LIST OF FIGURES

Figure Page

NOMENCLATURE

SYMBOLS

C_m : transmission ratio

e : error

e_1 : tracking error

E : modulus of elastcity of web

ϵ_1 : estimation error

F : friction force

F_c : Coulomb friction coefficient

F_s : static friction coefficient

F_v : viscous friction coefficient

γ : gain

Γ : gain matrix

i : current

I : moment of inertia

J : rotor inertia

k_m : motor parameter or high frequency gain for a reference model

k_p : high frequency gain for a plant model

$K = \sqrt{\frac{T}{EI}}$: web span parameter

K_e : back *e.m.f* constant

K_t : torque constant/sensitivity

SYMBOLS

L : inductance or length of span

L_1 : distance from the guide roller to instant center

$\mathfrak{L}$: Laplace operator

$\mathfrak{L}^{-1}$: inverse Laplace operator

μ : mean

n^* : relative degree

ω : regresor vector

ω_n : natural frequency

$W_m(s)$: reference model transfer function

ϕ : filtered regressor vector

r : reference command

R : resistance

$R_m(s)$: denominator polynomial of reference model

$R_p(s)$: denominator polynomial of plant model

$\mathcal{R}$: set of all real numbers

sgn(.) : signum function

σ : standard deviation

σ^2 : variance

T : torque or Tension

τ : time constant

θ : angular position or parameter vector

θ^* : true parameter vector

θ_0 : roller misalignment

u, U_p : input to a plant

v : velocity

v_s : Stribeck velocity constant

SYMBOLS

x : state variable

x_1 : distance from the guide roller to the instant center

y : output of a plant

$\hat{y}$: estimator output

Y_0 : initial lateral position misalignment

y_L, Y_L : lateral edge position

y_m : output of a reference model

ζ : damping ratio

Z : guide position

$Z_m(s)$: numerator polynomial of reference model

$Z_p(s)$: numerator polynomial of plant model

ABBREVIATIONS

BIBO : Bounded-input bounded-output

I/O : Input-Output

LMS : Least Mean Square

LTI : Linear Time Invariant

MRAC : Model Reference Adaptive Control

OPG : Offset Pivot Guide

P : Proportional

PD : Proportional-Derivative

PE : Persistent Excitation

PI : Proportional-Integral

PR : Positive Real

RLS : Recursive Least Square

RPG : Remotely Pivoted Guide

SISO : Single Input Single Output

SPR : Strictly Positive Real

Chapter 1

Introduction

The term *web* is used to describe materials which have their length considerably larger than their width and width considerably larger than thickness. Webs are materials which are manufactured and processed in a continuous, flexible strip form. Webs consist of a broad spectrum of materials that are used extensively in every day life such as plastics, paper, textile, metals and composites. Typically web materials are manufactured into rolls since it is easy to transport and process the materials in the rolled form. An example of a web material is shown in Figure 1.1.

Figure 1.1: A Web Material used for Packaging

Web handling is a term that is used to refer to the study of the behavior of the web while it is transported and controlled through the processing machinery from an unwind roll to a

rewind roll. A typical operation involves transporting a web in rolled, unfinished form from an unwind roll to a rewind roll through processing machinery where the required processing operations are performed. An example of such a process is commonly seen in the metals industries. The web (metal strip) that is to be processed is transported on rollers to various sections where different operations like coating, painting, drying, slitting, etc., are performed. The process line generally has unwind and rewind rolls, many idle rollers and one or more intermediate driven rollers. An experimental web handling system with unwind and rewind sections is shown in Figure 1.2.

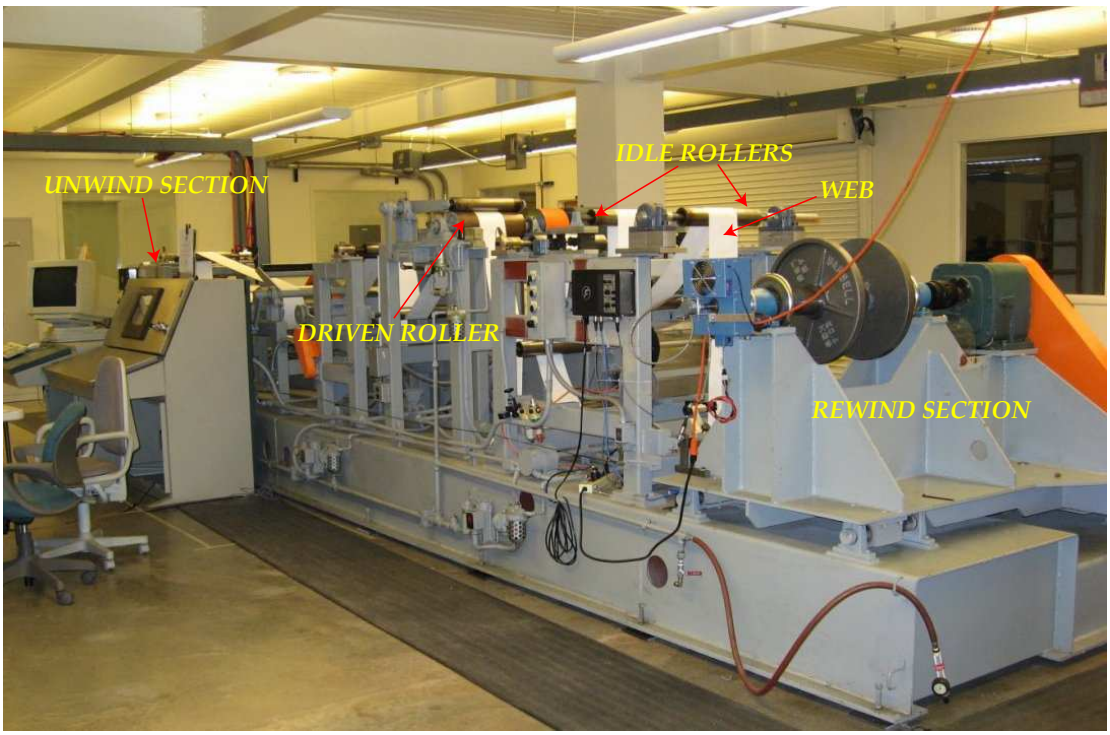

Figure 1.2: Experimental Web Handling System

The longitudinal dynamics of the web is the behavior of the web in the direction of transport of the web. Web transport velocity and web tension are two key variables of interest that affect the longitudinal behavior of the web. The lateral dynamics of the web is the behavior of the web perpendicular to the direction of transport of the web and in the plane of web. Several parameters which affect the lateral web dynamics include web material, tension, transport velocity, and web geometry, etc. The quality of the finished web depends on how well the web is handled on the rollers during transport. The longitudinal and lateral control of the web on rollers play a critical role in the quality of the finished product.

The focus of this work is on control of lateral dynamics of a web. Adaptive control strategies that are capable of providing the required performance in the presence of the variations in the process and web parameters are investigated. The suitability of these control strategies and their ability to provide the required performance are studied in detail, both from theoretical and experimental perspectives.

Web guiding (also called as lateral control) involves controlling web fluctuations in the plane of the web and perpendicular to web travel. Web guiding is important because rollers in any web handling machinery tend to have inherent misalignment problems and this may cause the web to move laterally on the rollers. The lateral movement of the web on the rollers may produce wrinkles or slackness in the web, or the web may completely fall off the rollers. A number of web processes like printing, coating, winding may get affected severely due to the web lateral motion and it becomes important to maintain the lateral position of the web. Web guides are used to maintain the lateral position of the web on rollers during transport.

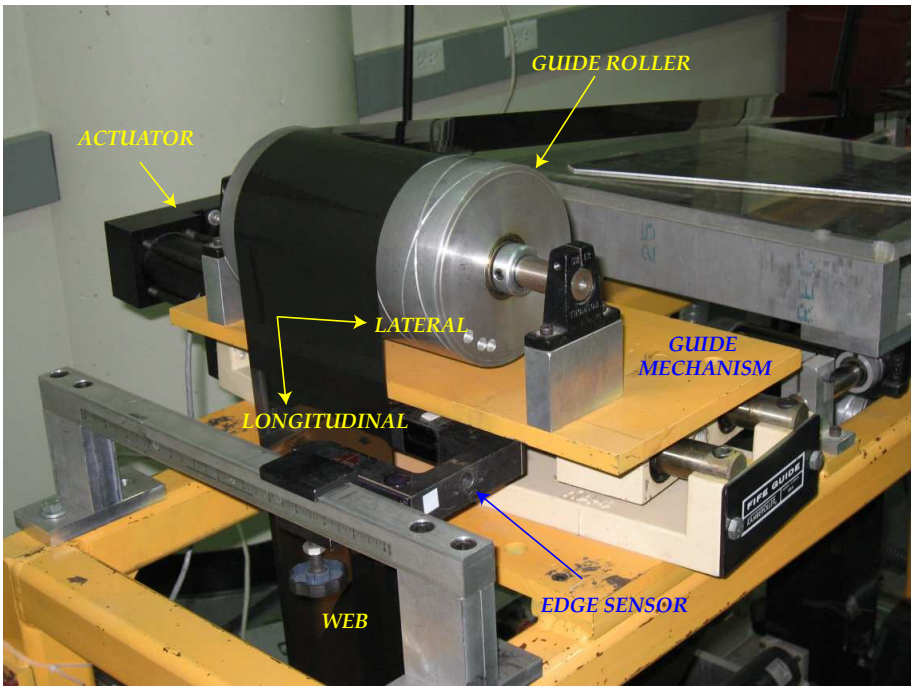

Figure 1.3: An Example of a Web Guide

A web guide mechanism typically consist of a roller sitting on a pivoted base, whose motion is controlled to change the axis of rotation of the roller. The working principle of all web guides is based on a well understood fundamental principle in web handling – *a web approaching a roller*

will always tend to orient itself perpendicular to the axis of rotation of the roller. The lateral motion of the web is controlled by changing the axis of rotation of the guide roller. The lateral position of the web is measured using an edge sensor. Based on this measurement as feedback the axis of rotation of the guide roller is controlled to maintain the lateral position at the required location. Figure 1.3 shows a web guide mechanism with an electromechanical actuator and an infrared sensor.

Web guides are positioned at different locations in an industrial process line where guiding is required. Guides located at either ends in a process line are usually called *terminal guides* [1]. An unwind guide maintains the lateral position of the web which is fed into the processing line, whereas a rewind guide maintains the lateral position of the processed web which is wound onto a roll in the rewind section. Apart from terminal guiding, web guides are extensively used in the intermediate process sections and they are referred to as *intermediate guides*.

The intermediate web guides are classified based on the way in which the axis of rotation of the guide roller is changed. Figure 1.4 shows an *end pivoted guide* where the change in the axis of rotation of the roller is about a pivot point which is at one end of the roller. Similarly the *center pivoted guide* shown in Figure 1.5 has its pivot point in the center of the guide roller. An *offset-pivot guide* (shown in Figure 1.6) utilizes a pair of rollers to change the axis of rotation while in a *remotely pivoted guide* (shown in Figure 1.7) the guide roller moves along a curved path to change its axis. These are some commonly used intermediate web guides in the web handling industry.

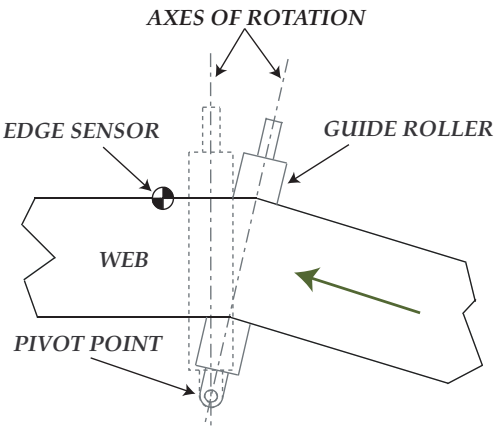

Figure 1.4: End Pivoted Guide

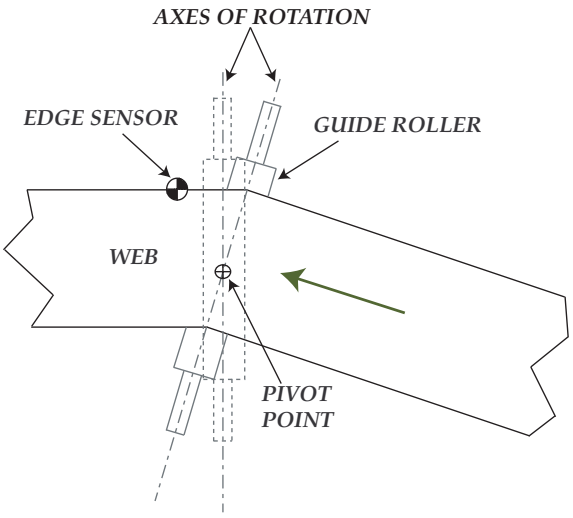

Figure 1.5: Center Pivoted Guide

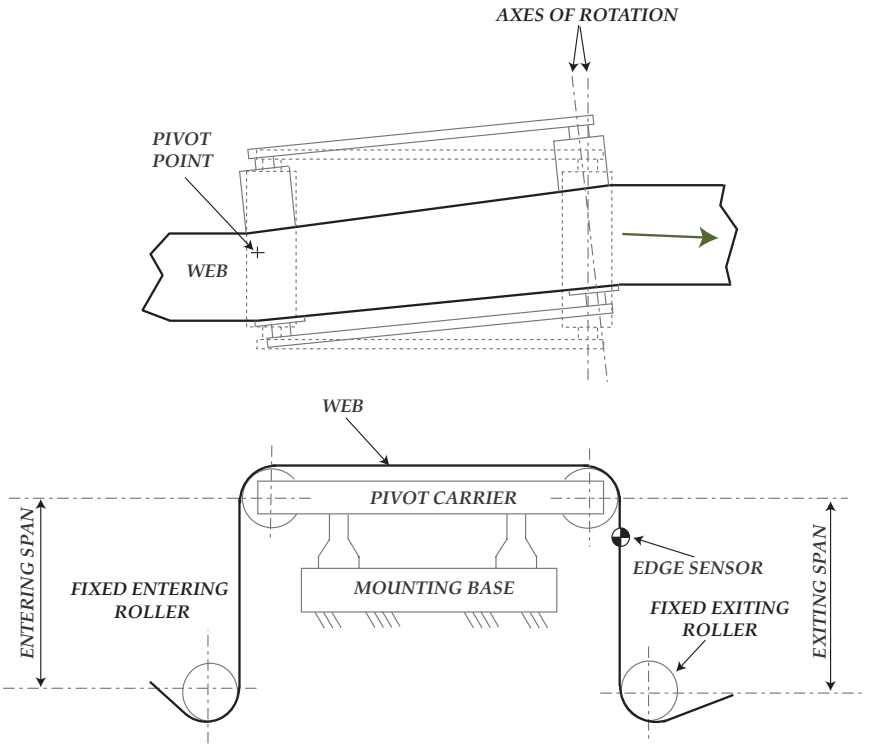

Figure 1.6: Offset Pivot Guide

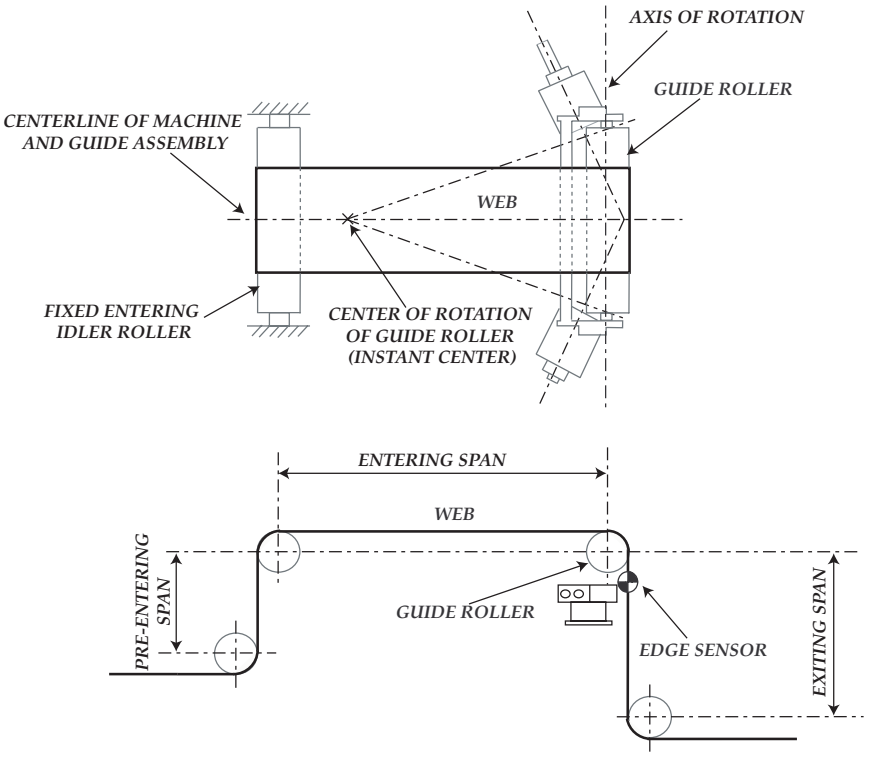

Figure 1.7: Remotely Pivoted Guide or Steering Guide

1.1 Lateral Dynamics

In order to control a web guide it is important to understand the physics behind the transport of web on rollers. Lateral and longitudinal dynamics of a moving web are dependent on various process parameters like transport velocity, web tension, web material, and the geometry of the web material, etc. Understanding the lateral dynamics of the web is important for designing an effective lateral controller for the web guide mechanism. Lateral dynamics of the web was first modeled in [2], based on the assumption that the web behaves like a string. A major improvement to the mathematical model for the lateral dynamics of the web was described by J. J. Shelton [3]. A first order model of an ideal web was presented in [4] followed by a second-order model [5] by considering the web as an Euler beam. A model for the web lateral dynamics for a multiroll system was developed in [6] based on the Timoshenko beam theory. A stochastic modeling formulation for the lateral dynamics was developed in [7]. An overview of the lateral and longitudinal dynamics along with a historic perspective of modeling and control of moving webs was presented in [8]. A detailed modeling of the lateral dynamics of the web for different types of intermediate guides was presented in [9, 10].

The two types of intermediate guides which are considered in this work are a remotely pivoted guide (also called as a *steering guide*) and an offset-pivot guide (also called as a *displacement guide*). The web span lateral dynamics for the two guides are similar and hence the same controller design can be implemented on both the guides. Even though the focus of this research is on these two intermediate guides, the theory developed can be adapted to other guides as well.

1.1.1 Remotely Pivoted Guide (Steering Guide)

The action of the remotely pivoted guide on the lateral position of the web is given by

$$Y_L(s) = G_{1s}(s)Z(s) + G_{2s}(s)\theta_0(s) + G_{3s}(s)Y_0(s) \tag{1.1}$$

where $Y_L(s)$ is the Laplace transform of the web lateral position, $Z(s)$ is the input to the guide in the lateral direction, $\theta_0(s)$ denotes the entering span roller misalignment and $Y_0(s)$ is the initial lateral position misalignment (see Figure 1.8). The transfer functions in equation (1.1) are given by

$$G_{1s}(s) = \frac{s^2 + \beta_2 s + \beta_1}{s^2 + \beta_2 s + \beta_0}, \quad G_{2s}(s) = \frac{\beta_3'}{s^2 + \beta_2 s + \beta_0}, \text{ and } \quad G_{3s}(s) = \frac{-\beta_3 s + \beta_0}{s^2 + \beta_2 s + \beta_0} \tag{1.2}$$

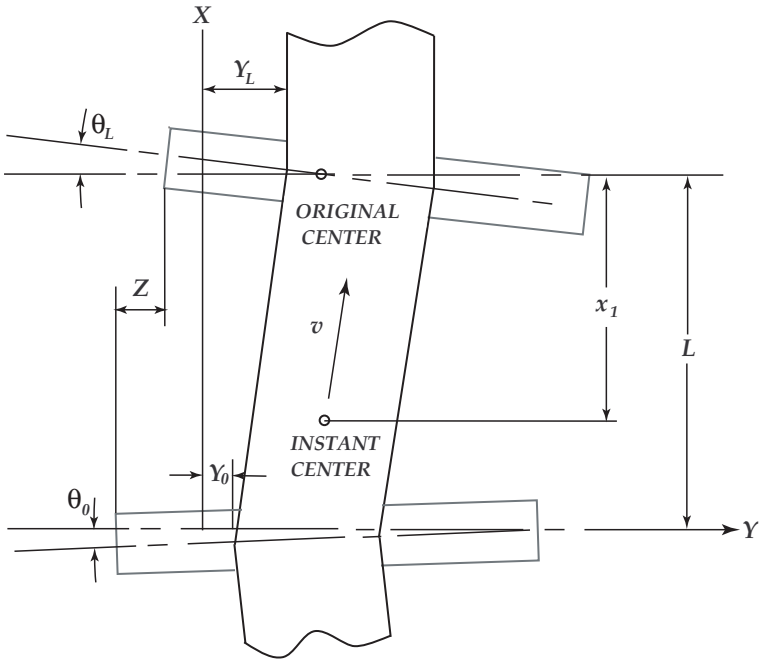

Figure 1.8: A Schematic of a Remotely Pivoted Guide

where

$$\beta_0 = \left(\frac{1}{\tau^2}\right)\frac{(KL)^2(\cosh KL - 1)}{KL\sinh KL - 2(\cosh KL - 1)} \triangleq \left(\frac{1}{\tau^2}\right) f_1(KL)$$
$$\beta_1 = \left(\frac{L}{\tau^2 x_1}\right)\frac{KL(KL\cosh KL - \sinh KL)}{KL\sinh KL - 2(\cosh KL - 1)} \triangleq \left(\frac{L}{\tau^2 x_1}\right) f_2(KL)$$
$$\beta_2 = \left(\frac{1}{\tau}\right)\frac{KL(KL\cosh KL - \sinh KL)}{KL\sinh KL - 2(\cosh KL - 1)} \triangleq \left(\frac{1}{\tau}\right) f_2(KL)$$
$$\beta_3 = \left(\frac{1}{\tau}\right)\frac{KL(\sinh KL - KL)}{KL\sinh KL - 2(\cosh KL - 1)} \triangleq \left(\frac{1}{\tau}\right) f_3(KL)$$
$$\beta_3' = \left(\frac{L}{\tau^2}\right)\frac{KL(\sinh KL - KL)}{KL\sinh KL - 2(\cosh KL - 1)} \triangleq \left(\frac{L}{\tau^2}\right) f_3(KL)$$

where the web span parameter K is defined as $K^2 = \frac{T}{EI}$, E is the modulus of elasticity of web, I is the moment of inertia of the web, T is the web tension, L is the length of the entering span, $\tau = L/v$ is the time constant, v is the web transport velocity, and x_1 is the distance from the guide roller to its instant center of rotation.

The variables $\theta_0(s)$ and $Y_0(s)$ are considered as the disturbances, and the objective of the web guide is to reject these disturbances to maintain the lateral position downstream of the web guide. Thus the effect of the input guide displacement, $Z(s)$, to the lateral position of the web, $Y_L(s)$, is given by

$$Y_L(s) = \frac{s^2 + \beta_2 s + \beta_1}{s^2 + \beta_2 s + \beta_0} Z(s) \tag{1.4}$$

1.1.2 Offset Pivot Guide (Displacement Guide)

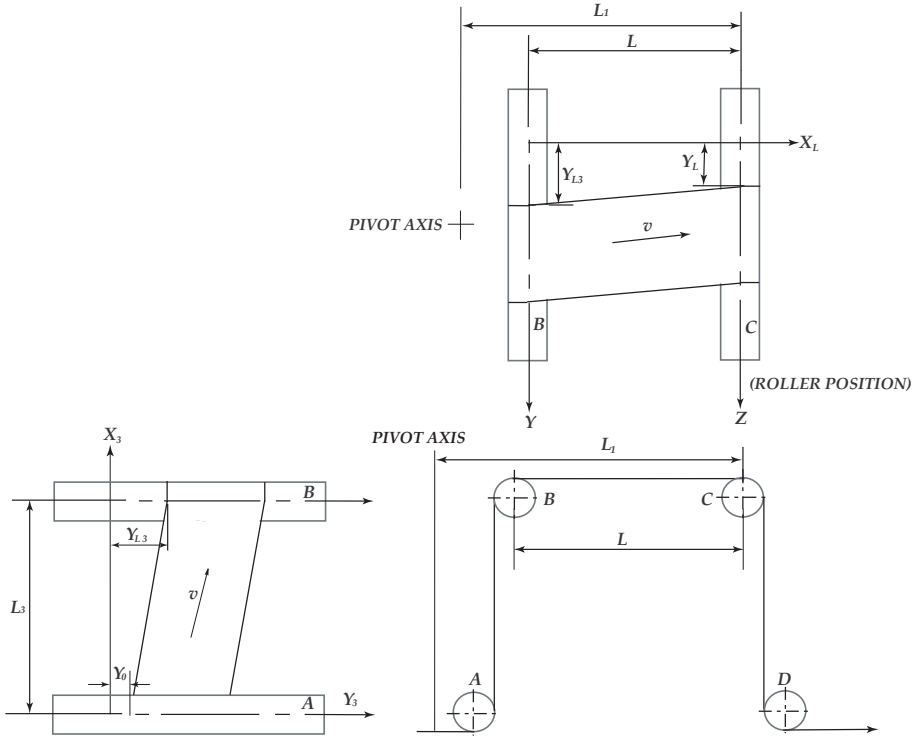

Figure 1.9: A Schematic of an Offset Pivot Guide

The lateral dynamics of the web with a displacement guide is influenced by the input to the guide mechanism, $Z(s)$, and the initial lateral position misalignment, $Y_0(s)$, and is given by

$$Y_L(s) = G_{1d}Z(s) + G_{2d}Y_0(s) \tag{1.5}$$

where

$$G_{1d}(s) = \frac{\left[-\frac{f_3(KL)}{\tau}s + \frac{f_1(KL)}{\tau^2}\right]\left[s^2 + \frac{f_2(KL_3)}{\tau_3}s\right]\frac{L_1 - L}{L_1}}{\left[s^2 + \frac{f_2(KL_3)}{\tau_3}s + \frac{f_1(KL_3)}{\tau_3^2}\right]\left[s^2 + \frac{f_2(KL)}{\tau}s + \frac{f_1(KL)}{\tau^2}\right]} + \frac{s^2 + \frac{f_2(KL)}{\tau}s + \frac{f_2(KL)L}{\tau^2 L_1}}{s^2 + \frac{f_2(KL)}{\tau}s + \frac{f_1(KL)}{\tau^2}}$$

$$G_{2d}(s) = \frac{\left[-\frac{f_3(KL_3)}{\tau_3}s + \frac{f_1(KL_3)}{\tau_3^2}\right]\left[-\frac{f_3(KL)}{\tau}s + \frac{f_1(KL)}{\tau^2}\right]}{\left[s^2 + \frac{f_2(KL_3)}{\tau_3}s + \frac{f_1(KL_3)}{\tau_3^2}\right]\left[s^2 + \frac{f_2(KL)}{\tau}s + \frac{f_1(KL)}{\tau^2}\right]}$$

with L_3 as the span length as shown in Figure 1.9 and $\tau_3 = L_3/v$.

Displacement guides are typically installed such that the length of the guide span (denoted by L) is very close to the distance from the pivot axis to the second guide roller (denoted by L_1)

(see Figure 1.9). When $L \approx L_1$, the transfer function $G_{1d}(s)$ is simplified [9], and the structure is same as the transfer function $G_{1s}(s)$ in the dynamics of the remotely pivoted guide given by equation (1.2). With this simplification, the dynamics from the guide input to the web lateral position is given by

$$Y_L(s) = \frac{s^2 + \beta_2 s + \beta_1'}{s^2 + \beta_2 s + \beta_0} Z(s) \tag{1.6}$$

where $\beta_1' = \dfrac{f_2(KL)L}{\tau^2 L_1}$.

1.2 Lateral Control

Lateral control involves the design of a closed-loop control system for regulating the lateral position of the web in a process line using a web guide mechanism. The guide mechanism includes an actuator which provides the input to the system and a feedback sensor which is used to measure the lateral position of the web.

Current industrial controllers for web guiding are simple and do not consider the web lateral dynamics in the controller design. A typical industrial controller consists of three loops. A very fast current loop, a velocity loop and an outer position loop. The two inner loops are designed based on the actuator dynamics, and they regulate the current and velocity of the actuator. The actuator dynamics is assumed to be completely known. The outer position loop is designed to regulate the lateral position of the web, and the compensation is usually based on a Proportional (P) controller or a Proportional-Integral (PI) controller. The error in the lateral position of the web drives the two inner loops. Hence all the three loops work in unison to regulate the lateral position of the web.

Since the inner two loops are driven by the outer position loop, the lateral position measurement becomes critical. Depending on the web handling application, the type of sensor used to measure the lateral position of the web varies. Applications which handle opaque webs commonly use infrared sensors while transparent film applications employ ultrasonic sensors. The position loop is dependent on this sensor measurement and the sensor gain affects the position loop. Both analog and digital industrial controllers commonly have a manual variable gain, which can be used for tuning the controller gains based on the type of the web. Based on the sensor gain, the controller gain is adjusted appropriately.

A number of strategies have been presented in the literature to control the lateral position of the web. The strategies include Proportional (P) control [11] and [7], Proportional-Derivative

(PD) control [11], a state estimation-proportional gain strategy [12], a state variable feedback control strategy [13], estimated velocity feedback control [14] and [15], controller based on frequency domain design [16], etc. In most of the control strategies cited above, it is assumed that the parameters that affect the lateral dynamics of the web are known. Some of the key parameters that affect the lateral dynamics are the web material properties, web geometry, transport velocity, web tension, etc. These parameters may vary due to process condition variations or due to the processing of different web materials in the same process line. Unless these parameters are measured regularly it is difficult to know the exact dynamic model of the web for each situation.

1.3 Need for a Different Control Strategy

Some potential shortcomings of the existing lateral control strategies are given in the following.

- Existing industrial strategies do not consider the web lateral dynamics in the analysis and design of the lateral controllers. Inclusion of the lateral web dynamics in the control design process has the potential to significantly improve the guiding performance in the presence of process variations as well as many machine induced lateral disturbances.
- Sensor gain changes as a result of web material variations cause poor guiding with existing fixed gain controllers.
- Parameters of the dynamic model are not known. In a model based controller design for lateral guiding, the knowledge of the parameters like tension, web transport velocity, web material geometry, etc., are important to achieve better tracking performance. But in most industrial applications these process parameters are not known to the guide controller. Additionally, most industrial process lines are designed to process different web materials under different operating conditions.

The goal is to find a controller that is capable of providing specified guiding performance which has the ability to overcome many of the limitations of the existing fixed gain controllers, including the ones given above. To achieve this goal, adaptive control strategies are investigated in this thesis.

1.4 Contributions

Two main contributions of this work are summarized below:

1. Model reference adaptive control designs that are applicable to web guiding are developed. A systematic approach for industrial implementation of these new adaptive strategies are developed. Additionally, practical industrial implementation guidelines are proposed.

2. A new performance metric that clearly highlights the web guiding performance is developed. The new metric is based on histograms. Profiles of commonly observed histograms are studied and their occurrence in guiding situations are analyzed. This novel performance metric can be used as a metric for tuning controllers as well as a diagnostic tool for lateral web guiding applications.

In addition to the primary contributions, several other secondary contributions are summarized below:

1. Simplified adaptive controllers are developed based on the approximation of the lateral dynamics by reduced order models.

2. Extensive experimentation of the adaptive strategies on an experimental platform containing various intermediate web guides is carried out. Further, an often used industrial control strategy is simultaneously implemented for all situations, and the results are compared.

3. Commonly used friction models are investigated and an adaptive friction compensation scheme based on static friction model is proposed for web guiding applications. A simplified adaptive controller with friction compensation is proposed and an indirect friction compensation scheme based on recursive least squares is implemented.

4. The output voltage of an optical sensor depends on the opacity of the web. A new method to determine the range of the optical sensor is developed (see Appendix A).

The rest of the document is organized as follows. In Chapter 2, a detailed description of the design of model reference adaptive control strategies suitable for web guiding is given. The results of the experiments carried out on an experimental web handling platform with the

proposed adaptive control strategies are presented in Chapter 3. A detailed discussion of the results along with practical industrial implementation guidelines based on the experimental observations are also presented in Chapter 3. Chapter 4 gives friction compensation techniques that are applicable to web guiding. In Chapter 5, a new performance metric for web guiding based on histograms is discussed. Chapter 6 summarizes the thesis and provides suggestions for future work.

Chapter 2

Adaptive Control Design for Web Guiding

2.1 Introduction to Adaptive Control

To adapt means to change to meet requirements or adjust to new circumstances. An adaptive controller is a scheme that adapts to changes in process dynamics and disturbances. Adaptive controllers are commonly used when there is a considerable change in the process dynamics and disturbances, which may not be compensated by using fixed gain controllers.

One practical application of an adaptive control scheme is the autopilot guidance system in aircrafts. The process dynamics of an aircraft depends on various parameters such as speed, altitude, head wind, tail wind, etc., and the aircraft also experiences various external disturbances. It is difficult to design a linear fixed gain feedback controller which can perform well under different operating conditions and in the presence of various disturbances. In the early autopilot design, the adaptive scheme that was commonly used was *gain scheduling*. Various parameters that affect the process dynamics of an aircraft have a direct relationship with process outputs (or measured variables), and hence these outputs can be used to change the controller parameters directly. Hence it is possible to determine a suitable constant gain linear feedback control strategy for each operating condition. The model is thus linearized around those operating conditions. This is called gain scheduling because the control scheme determines the operating condition based on the process outputs and consequently an appropriate controller is chosen to compensate for the process dynamics (or process gain). The system has basically two loops as shown in Figure 2.1. The inner loop is a standard feedback loop while the outer loop adjusts the controller in the inner loop based on the operating conditions. Gain scheduling can be regarded as a mapping from process parameters to controller parameters [17].

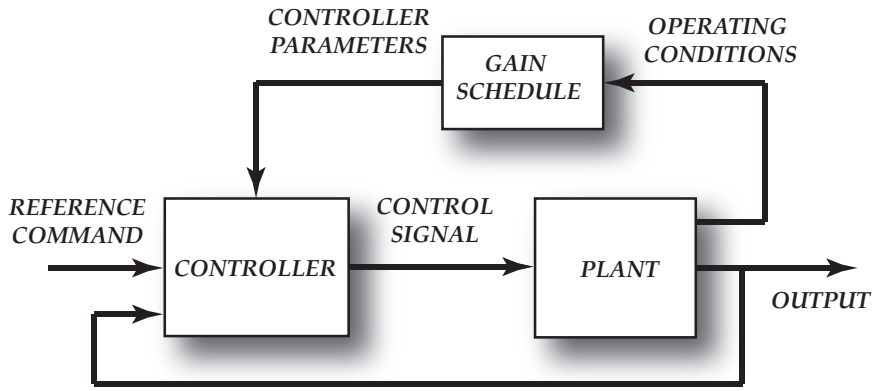

Figure 2.1: Adaptive Gain Scheduling Scheme

Gain scheduling is possible only when the variations (or the process dynamics) are directly correlated to the measured variables. In other words, gain scheduling is possible only when the operating conditions could be characterized based on these measured variables. Variation in disturbance characteristics cannot be compensated using gain scheduling and hence adaptive controllers are used. The modern autopilot for aircrafts employs adaptive controllers to compensate for various disturbances that act on the plane. The modern autopilot system is not limited to level flight. Current systems include different autopilot schemes for taxi, take-off, ascent, level flight, descent, landing and taxi back to the terminal. Since the disturbance changes frequently, it is reasonable to adjust the controller parameters to cope with the disturbance characteristics. A common adaptive control scheme is illustrated in Figure 2.2. Similar to gain scheduling, there are two loops. The inner loop is a standard feedback loop with a controller. The outer loop has a parameter adjustment mechanism which modifies the controller based on variations.

Direct and Indirect Adaptive Control

An adaptive controller consists of two main subsystems. A *parameter estimator* and a *controller* based on the parameter estimator. The parameter adjustment block in Figure 2.2 is the parameter estimator which estimates the unknown parameters, based on the output of the plant, reference command, control signal, etc. The estimated parameters are then used by the controller to compute the control signal to the plant. The way in which the parameters are estimated, also referred to as the *adaptive law*, along with the way in which the control signal is calculated, gives rise to two main kinds of adaptive control schemes, *indirect* and *direct*. *Indirect*

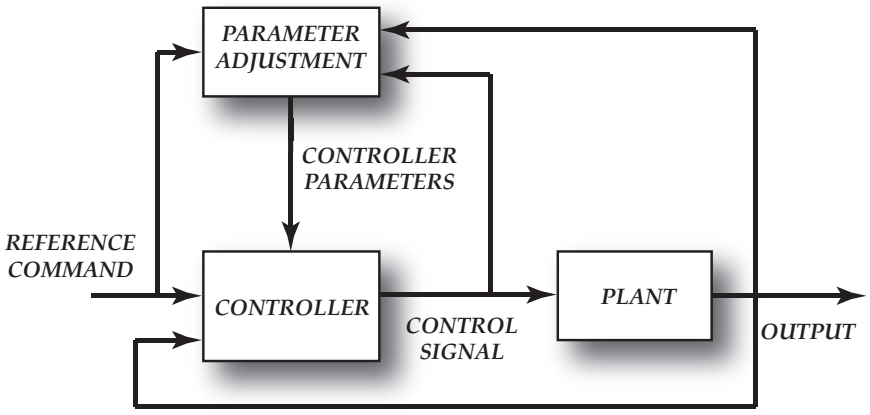

Figure 2.2: Adaptive Control System

adaptive control involves the estimation of actual plant parameters which are used to compute the controller parameters. The controller parameters are computed indirectly and hence the name indirect adaptive control. In *direct adaptive control*, the plant model is parametrized in terms of the controller parameters which are estimated directly without intermediate calculations involving plant parameter estimates [18]. Indirect adaptive control is also referred to as *explicit adaptive control* while direct adaptive control is also referred as *implicit adaptive control* because the control design is based on explicit or implicit plant model estimation. Both types of control schemes can be used for minimum-phase plants, but difficulty arises when designing an indirect adaptive control scheme for nonminimum-phase plants [18]. In direct adaptive control scheme, since the plant parameters are parametrized in terms of the controller parameters, the convergence of parameters to their true values is not of utmost importance. The parameter estimation is usually driven by the output error. Although the parameters do not converge to their true values, the controller is capable of meeting the performance requirement on the output error convergence. On the contrary, convergence of parameters to their true values is of utmost importance while using indirect adaptive control. The convergence of parameters and its importance will be discussed later in this chapter.

Model Reference Adaptive Control

In a *Model Reference Adaptive Control* (MRAC) scheme the control law and adaptive law are designed such that the closed-loop Input/Output (I/O) properties of the plant exactly match a *reference model*. The reference model is any dynamic model which meets a desired closed-loop

performance requirements for the plant. Hence the control law for the plant is designed such that the closed-loop dynamics matches the dynamics of the reference model. There are two kinds of MRAC strategies, direct and indirect MRAC. A schematic of direct MRAC is shown in Figure 2.3.

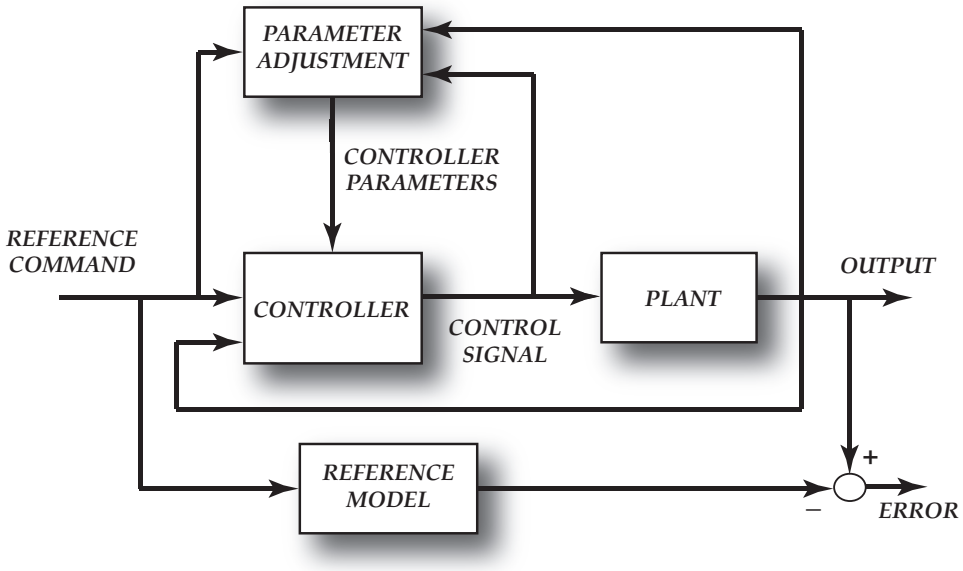

Figure 2.3: Model Reference Adaptive Control System

In this thesis a direct model reference adaptive control scheme is investigated for web guides. In the following sections, the design and analysis of common adaptive control schemes will be presented along with their application to web guides. On-line parameter estimation, a key component in adaptive control design, is discussed in section 2.2. A simple adaptive control example based on on-line parameter estimation is discussed in section 2.3. Model reference adaptive control schemes suitable for web guiding are developed in sections 2.4 and 2.5. Model reference adaptive control schemes, based on a simplified models for the web dynamics, are proposed in section 2.4. A model reference adaptive scheme based on the complete web dynamic model is presented in 2.5.

2.2 On-line Parameter Estimation

On-line parameter estimation is required for any adaptive controller design. Both in direct and indirect adaptive control schemes some form of parameter estimation is carried out. In

indirect adaptive control the plant parameters are estimated. But in direct adaptive control the controller parameters are estimated. In both the cases parameters are estimated in real-time and the controller is adjusted appropriately.

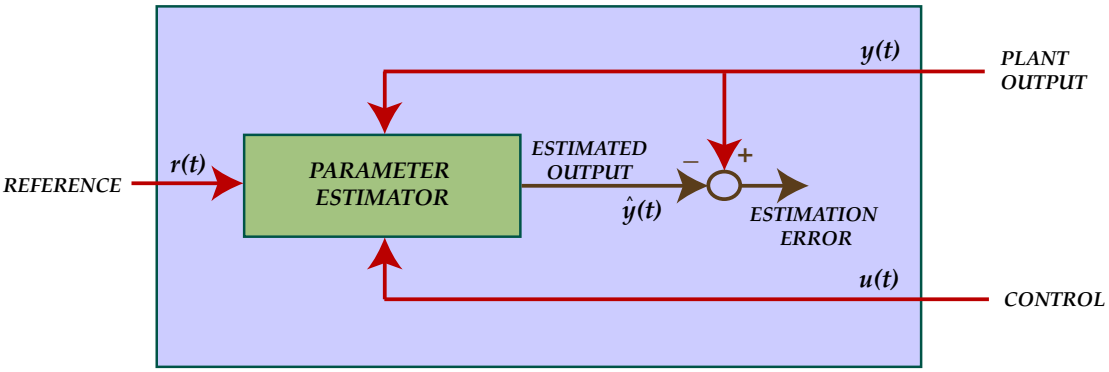

Figure 2.4: On-line Parameter Adjustment Mechanism

In an on-line parameter estimation problem a parameter adjustment mechanism is utilized to estimate the unknown plant parameters, as shown in Figure 2.4. The parameter estimator is designed such that its structure is similar to the plant structure. The estimator is driven by the input to the plant $u(t)$, reference command $r(t)$ and the output of the plant $y(t)$. The output of the estimator $\hat{y}(t)$ is constantly compared with the output of the plant. The difference between the estimator output and the actual plant output is called the *estimation error*. The parameters in the estimator are constantly adjusted so that the estimation error is minimized. Standard optimization techniques like the gradient-descent, least-squares, Newton's method, etc., can be used to minimize the estimation error in real-time (see Appendix B in [18]).

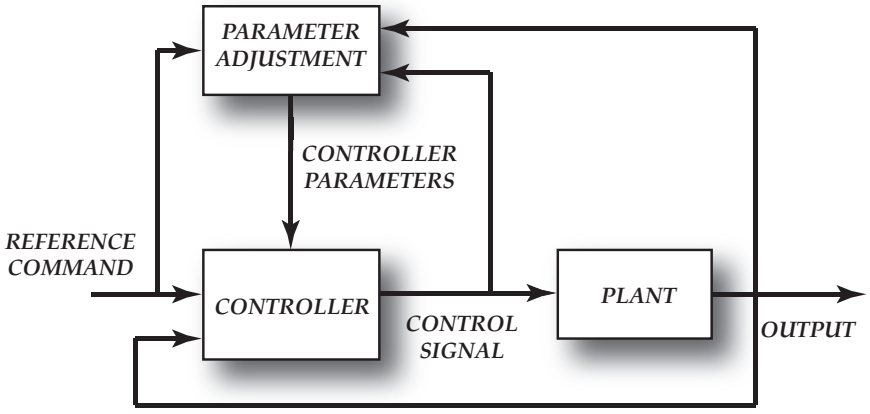

Figure 2.5: Adaptive Control System

An on-line estimation problem involve three key steps. First the parameter estimator has to be parametrized appropriately in terms of the unknown parameters. The second step involves the design of the adaptive law which defines the way in which the parameters are updated. The adaptive law is designed such that the optimization techniques used to minimize the estimation error results in a stable system. The final step involves the design of the plant inputs such that the estimates converge to their true values. The final step is important only for identification problems. For direct adaptive control problems the minimization of the output error is important rather than the convergence of parameters.

In the following section a simple scalar plant of unknown parameters will be considered and the procedure for designing an on-line parameter estimation scheme will be discussed. The example is based on the procedure described in [18]. Additionally, various considerations for designing the input and the stability properties of the adaptive system will be discussed.

2.2.1 Parameter Estimation: An Example

Consider a first-order system described by

$$\dot{x} = ax + bu, \qquad x(0) = x_0 \tag{2.1}$$

where x is the output, u is the input and a, b are unknown constants. We also assume that the system is stable, i.e., $a < 0$ and the input u is bounded. The objective is to develop an on-line estimation algorithm for estimating the unknown parameters using the measured signals x and u.

For estimation and adaptive control problems, an effective parametrization of estimator in terms of unknown plant parameters is extremely important. A simple parametrization would be

$$x(s) = [\, a \qquad b \,] \begin{bmatrix} \dfrac{x(s)}{s} \\ \\ \dfrac{u(s)}{s} \end{bmatrix} \tag{2.2}$$

where $x(s)$ and $u(s)$ are the Laplace transforms of $x(t)$ and $u(t)$. This parametrization is not desirable due to the presence of the integrator. A similar parametrization which is implementable can be obtained by using a low pass filter for the measured signals x and u.

Let the plant be parametrized by adding and subtracting $a_m x$, where $a_m > 0, a_m \in \mathcal{R}^1$. The

parameter a_m is the low pass filter parameter whose value will be chosen later.

$$\dot{x} = -a_m x + (a + a_m)x + bu \tag{2.3a}$$

$$x = \frac{1}{s + a_m}[(a + a_m)x + bu] \tag{2.3b}$$

$$= {\theta^*}^\top \phi \tag{2.3c}$$

where ${\theta^*}^\top = [b \quad (a + a_m)]$ is the unknown parameter vector and $\phi = [\frac{1}{s+a_m}u \quad \frac{1}{s+a_m}x]^\top$ is filtered measurement. Define the estimate of x as

$$\hat{x} = \theta^\top \phi \tag{2.4}$$

where θ is the estimate of the unknown parameter vector in equation (2.3c), i.e., $\theta = [\hat{b} \quad (\hat{a} + a_m)]$. Define the estimation error as

$$\epsilon_1 = x - \hat{x} \tag{2.5}$$

The estimation error dynamics is given by

$$\dot{\epsilon}_1 = -a_m \epsilon_1 - \tilde{a}x - \tilde{b}u \tag{2.6}$$

where $\tilde{a} \triangleq \hat{a} - a$ and $\tilde{b} \triangleq \hat{b} - b$. Equation (2.6) describes the behavior of the estimator which is influenced by the parameters and their estimates. If the parameter estimates converge to the true parameter values, i.e., $\hat{a} = a, \hat{b} = b$, then $\epsilon_1 \to 0$ exponentially[1], since $a_m > 0$.

The adaptive law for updating the parameter estimates, $\hat{a}$ and $\hat{b}$, can be derived using the estimation error ϵ_1 as

$$\dot{\hat{a}} = f_1(\epsilon_1, x, \hat{x}, u), \qquad \dot{\hat{b}} = f_2(\epsilon_1, x, \hat{x}, u) \tag{2.7}$$

Notice that f_1 and f_2 are functions of the measured signals which are chosen such that the equilibrium state

$$\hat{a}_e = a, \qquad \hat{b}_e = b, \qquad \epsilon_{1e} = 0 \tag{2.8}$$

of equations (2.6) and (2.7) is uniformly stable or asymptotically stable or exponentially stable.

Let us consider a Lyapunov function candidate as a function of the three states $\epsilon_1, \tilde{a}, \tilde{b}$

$$V(\epsilon_1, \tilde{a}, \tilde{b}) = \frac{1}{2}(\epsilon_1^2 + \tilde{a}^2 + \tilde{b}^2) \tag{2.9}$$

[1]The choice of a_m determines the rate of convergence of ϵ_1, since the decay is as per $e^{-a_m t}$.

The function V is positive definite, decrescent and radially unbounded in $\mathcal{R}^3$. The time derivative of V along the trajectories of equations (2.6) and (2.7) is

$$\dot{V}(\epsilon_1, \tilde{a}, \tilde{b}) = \epsilon_1(-a_m\epsilon_1 - \tilde{a}x - \tilde{b}u) + \tilde{a}f_1 + \tilde{b}f_2 \tag{2.10a}$$

$$= -a_m\epsilon_1^2 - \tilde{a}x\epsilon_1 - \tilde{b}u\epsilon_1 + \tilde{a}f_1 + \tilde{b}f_2 \tag{2.10b}$$

If $f_1 = \epsilon_1 x, f_2 = \epsilon_1 u$, we have

$$\dot{V} = -a_m\epsilon_1^2 \leq 0. \tag{2.11}$$

The function $\dot{V}$ is negative semi-definite since for all $\tilde{a}, \tilde{b} \in \mathcal{R}$ and $\epsilon_1 = 0, \dot{V} = 0$. The parameter update law is given by

$$\dot{\hat{a}} = \epsilon_1 x, \qquad \dot{\hat{b}} = \epsilon_1 u \tag{2.12}$$

where $\hat{x}$ is generated using equation (2.4).

2.2.1.1 Analysis

Applying Theorem B.2, we conclude that V is a Lyapunov function and the equilibrium given by equation (2.8) is uniformly stable. Also $V > 0, \dot{V} \leq 0$ implies that $V \in \mathcal{L}_\infty$ which further implies that $\epsilon_1, \tilde{a},\ \tilde{b} \in \mathcal{L}_\infty$. Since $\epsilon_1 = x - \hat{x} \in \mathcal{L}_\infty$ and x is bounded, $\hat{x} \in \mathcal{L}_\infty$. Hence all the signals in the system described by equation (2.6) are bounded. Additionally,

$$||\epsilon_1||_2^2 = \int_0^\infty \epsilon_1^2(\tau)d\tau = -\frac{1}{a_m}\int_0^\infty \dot{V}d\tau = -\frac{1}{a_m}(V_\infty - V_0),$$

$$V \in \mathcal{L}_\infty \Rightarrow \exists V_\infty | \lim_{t\to\infty} V = V_\infty$$

$$\Rightarrow ||\epsilon_1||_2^2 \text{ exists} \Rightarrow \epsilon_1 \in \mathcal{L}_2$$

From equation (2.6), since $\epsilon_1, \tilde{a}, x, \tilde{b}, u \in \mathcal{L}_\infty$, $\dot{\epsilon}_1 \in \mathcal{L}_\infty$. Since $\epsilon_1 \in \mathcal{L}_2 \cap \mathcal{L}_\infty$ and $\dot{\epsilon}_1 \in \mathcal{L}_\infty$, using Lemma B.2, $\epsilon_1 \to 0$ as $t \to 0$. From equation (2.12), $\dot{\hat{a}}, \dot{\hat{b}} \to 0$ as $t \to \infty$. Now we have established that $\epsilon_1, \dot{\hat{a}}, \dot{\hat{b}} \to 0$, as $t \to \infty$ but this does not imply that $\tilde{a}, \tilde{b} \to 0$ as $t \to \infty$. From equation (2.9) it is clear that $\lim_{t\to\infty} V = V_\infty = \frac{1}{2}(\tilde{a}^2 + \tilde{b}^2)$ but this does not mean that $\tilde{a}, \tilde{b}$ have a limit. Notice that there is no restriction on the input u apart from being bounded. To guarantee parameter convergence additional conditions have to be imposed on the input u.

2.2.1.2 Sufficiently Rich Signals

In this section the properties of the input signal for parameter convergence are discussed in detail. The notion of *sufficiently rich signal* and *persistent excitation* are introduced.

The general solution for the differential equation (2.1) is

$$x(t) = e^{at}x_0 + \int_0^t e^{a(t-\tau)}bu(\tau)d\tau \tag{2.14}$$

The first part of equation (2.14) decays to zero as $t \to \infty$ since $a < 0$. Taking Laplace transform on both sides for equation (2.1) with zero initial condition we get

$$X(s) = \frac{b}{s-a}U(s) = G(s)U(s) \tag{2.15}$$

If $u = 0$, then the solution carries information about the parameter a alone, and if $x_0 = 0$, information about both the parameters a, b cannot be extracted from the input/output signals.

Similarly if $u = c,\ c \neq 0$, a constant, then

$$\begin{aligned} u(t) = c \quad &\Rightarrow U(s) = \frac{c}{s} \\ \Rightarrow X(s) = \frac{b\,c}{s(s-a)} &= \frac{-b\,c/a}{s} + \frac{b\,c/a}{s-a} \\ \Rightarrow x(t) &= \frac{-b\,c}{a} + \frac{b\,c}{a}e^{at} \end{aligned}$$

$x(t) \to -\frac{bc}{a}$ as $t \to \infty$. Hence, the input/output signals only have the information about the ratio $\frac{b}{a}$, and not about the individual values of a and b.

If $u(t) = \sin\omega_0 t$, then

$$\begin{aligned} X(s) &= \frac{\omega_0\, b}{(s^2+\omega_0^2)(s-a)} \\ \Rightarrow x(t) &= k_1 e^{at} + \mathfrak{L}^{-1}\{\frac{k_2 s + k_3}{s^2+\omega_0^2}\} \end{aligned}$$

where k_1, k_2, k_3 are constants which depend on a and b. Notice that as $a < 0$ and $t \to \infty$,

$$\begin{aligned} x(t) &= \mathfrak{L}^{-1}\{\frac{k_2 s + k_3}{s^2+\omega_0^2}\} \\ &= |G(j\omega_0)|\sin(\omega_0 t + \varrho), \quad \varrho = \angle G(j\omega_0) \\ |G(j\omega_0)| = \frac{|b|}{\sqrt{\omega_0^2 + a^2}}&, \quad \angle G(j\omega_0) = \tan^{-1}\frac{\mathrm{Im}G(j\omega_0)}{\mathrm{Re}G(j\omega_0)} \end{aligned}$$

By observing the magnitude and the phase of the output signal at steady-state, the unknown constants a and b can be determined. Hence, with a sinusoidal input the unknown parameters can be estimated. Such a signal is a *sufficiently rich signal* for this system. The property of the signal u to be sufficiently rich is called *persistent excitation* (PE). Persistent excitation is very important in identification problems where parameter convergence is of utmost importance.

For adaptive control problems where output error convergence to zero is desired, it is not critical. For more information on persistent excitation refer to [17] (pages 63 – 73), [18] (pages 177 – 180) and [22] (Chapter 6).

2.3 Adaptive Control

In this section the design of model reference adaptive control is introduced by considering a scalar tracking problem. The stability analysis and convergence properties use the mathematical preliminaries given in Appendix B.

2.3.1 Adaptive Regulation using a Reference Model: An Example

Consider a scalar plant with dynamics described by

$$\dot{x} = ax + u, \qquad x(0) = x_0 \tag{2.19}$$

where a is the unknown plant parameter. It is desired to apply a bounded control input, u, such that the closed system is stable and $x \to x_m$ as $t \to \infty$, where x_m is the output of the reference model given by

$$\dot{x}_m = -a_m x_m, \quad x_m(0) = x_{m0}, \quad a_m > 0 \tag{2.20}$$

2.3.1.1 Control Law

Let $u = -k^* x$ be the control law such that $a - k^* = -a_m$. In other words if the parameter a is known, then one can choose $k^* = a + a_m$ so that the closed-loop dynamics of equation (2.19) is same as the reference model (2.20). If $x_0 = x_{m0}$, then $x(t) = x_m(t)$ for all $t \geq 0$. And if $x_0 \neq x_{m0}$ then the transient response of the closed-loop system will differ from the reference model, at steady state $x(t) = x_m(t)$.

Because the parameter a is unknown, the feedback gain k^* cannot be calculated and hence the control law cannot be implemented. A control law based on the estimate of the unknown parameter is chosen as

$$u = -k(t)x \tag{2.21}$$

where $k(t)$ is the estimate of k^*.

2.3.1.2 Adaptive Law

An adaptive law is now developed to estimate the unknown parameter by posing the problem as an on-line estimation problem. Let us define the tracking error as $e_1 = x - x_m$. Therefore,

$$\begin{aligned}
\dot{e}_1 = \dot{x} - \dot{x}_m &= (a-k)x + a_m x_m \qquad (2.22a)\\
&= ax + a_m x_m - kx\\
&= ax + a_m x_m - kx + k^*x - k^*x\\
&= \underbrace{ax - k^*x} + a_m x_m + \underbrace{k^*x - kx}\\
&= \underbrace{-a_m x + a_m x_m} - \tilde{k}x, \quad \tilde{k} = k - k^*\\
\dot{e}_1 &= -a_m e_1 - \tilde{k}x \qquad (2.22b)\\
\Rightarrow e_1 &= \frac{1}{s+a_m}(-\tilde{k}x) = G_c(s)(-\tilde{k}x)
\end{aligned}$$

The transfer function $G_c(s)$ is SPR from Theorem B.6. Hence, SPR-Lyapunov[2] design scheme is considered.

All the signals in equation (2.22b) can be measured except $\tilde{k}$ which is a function of time. The error dynamics in equation (2.22b) is in a suitable form to choose the adaptive law for $k(t)$ such that $e_1 \to 0$ as $t \to \infty$. Let $\dot{\tilde{k}}(t) = f_1(e_1, x, u)$ where f_1 is a function to be chosen. Let

$$V(e_1, \tilde{k}) = \frac{e_1^2}{2} + \frac{\tilde{k}^2}{2\gamma} \qquad (2.23)$$

be a Lyapunov function candidate with $\gamma > 0$ for the system described by $\dot{e}_1$ and $\dot{k}$. Choosing $f_1 = \gamma e_1 x$, we get

$$\dot{V} = -a_m e_1^2 \leq 0 \qquad \text{and} \qquad \dot{k} = \gamma e_1 x, \qquad k(0) = k_0 \qquad (2.24)$$

2.3.1.3 Analysis

Because $V > 0$ and $\dot{V} \leq 0$, V is bounded i.e., $V \in \mathcal{L}_\infty \Rightarrow e_1 \in \mathcal{L}_\infty, \tilde{k} \in \mathcal{L}_\infty$ (from (2.23)). $e_1 = x - x_m \Rightarrow x \in \mathcal{L}_\infty$ (since $x_m \in \mathcal{L}_\infty$). Additionally,

$$\int_0^\infty e_1^2(\tau)d\tau = \int_0^\infty \dot{V}(\tau)d\tau = V(0) - V(\infty) \qquad \Rightarrow \dot{V} \in \mathcal{L}_1 \Rightarrow e_1 \in \mathcal{L}_2 \qquad (2.25)$$

[2] In this design the estimation error is related to the parameter by a SPR transfer function. Once in this form, the KYP (Lemma B.5) or MKY (Lemma B.6) Lemmas can be invoked to choose an appropriate Lyapunov function V such that $\dot{V} \leq 0$. Refer to chapter 4 (On-Line Parameter Estimation) in [18].

$\tilde{k} \in \mathcal{L}_\infty \Rightarrow k \in \mathcal{L}_\infty$ since, k^* is constant. From equation (2.22b) we get $\dot{e}_1 \in \mathcal{L}_\infty$. Therefore, all the signal in the closed-loop system are bounded. Because $\dot{e_1} \in \mathcal{L}_\infty$ and $e_1 \in \mathcal{L}_2 \cap \mathcal{L}_\infty$, from lemma B.2, $e_1(t) \to 0$ as $t \to \infty$. $u = -kx \Rightarrow u \in \mathcal{L}_\infty$. Hence, all the signals in the closed-loop system are bounded and the tracking error, e_1, converges to zero. It has to be noted that, even though $k \in \mathcal{L}_\infty, \dot{k} \to 0$ as $t \to \infty, \tilde{k}$ may not converge to zero. Convergence of $\tilde{k}$ to zero can be gauranteed only when $\dot{k} \in \mathcal{L}_\infty, k \in \mathcal{L}_p \cap \mathcal{L}_\infty$ where $p \in [1, \infty]$ (using lemma B.2).

2.4 Simplified Guide Adaptive Controller Design

In the rest of this chapter model reference adaptive controllers called *Guide Adaptive Controller* (GAC) for web guiding applications are developed. In this section a simplified approximation of the GAC is designed to regulate the position of the web by considering a simple lateral web dynamic model. Recall that the transfer functions for both the steering guide and the displacement guide are of relative degree $n^* = 0$ and of the order $n = 2$. By approximating the system with a reduced order model, the number of estimated parameters in the adaptive control design is reduced and the controller implementation is simpler.

The transfer function for a steering guide (between the guide position and the lateral web position) is given by

$$y_L(s) = \frac{s^2 + \beta_2 s + \beta_1}{s^2 + \beta_2 s + \beta_0} Z(s) \tag{2.26}$$

The transfer function between the voltage input and the lateral web position is given by

$$y_L(s) = \frac{k_m C_m (s^2 + \beta_2 s + \beta_1)}{s(s+a)(s^2 + \beta_2 s + \beta_0)} u_p(s) \tag{2.27}$$

where k_m and a are motor parameters and C_m is the transmission ratio between the actuator position and the guide position. Ignoring the dynamics of the web and considering only the static gain of the lateral dynamics, we get

$$y_L(s) = \frac{k_m C_m \beta_1}{s(s+a)\beta_0} = \frac{K}{s(s+a)} u_p(s) \triangleq k_p \frac{Z_p}{R_p} u_p(s). \tag{2.28}$$

The transfer function $k_p \dfrac{Z_p(s)}{R_p(s)}$ represents a general transfer function where $Z_p(s)$, $R_p(s)$ are monic polynomials and k_p is a constant. The complexity of the adaptive controller depends on the degree of the polynomials $Z_p(s)$ and $R_p(s)$. The knowledge of the sign of the constant k_p simplifies the adaptive controller design.

The dynamics in equation (2.28) in time domain is given by

$$\ddot{y}_L + a\dot{y}_L = Ku_p. \tag{2.29}$$

Define state variables $y_1 = y_L$ and $y_2 = \dot{y}_L$. The dynamics in the state space form is

$$\begin{bmatrix} \dot{y}_1 \\ \dot{y}_2 \end{bmatrix} = \begin{bmatrix} 0 & 1 \\ 0 & -a \end{bmatrix} \begin{bmatrix} y_1 \\ y_2 \end{bmatrix} + \begin{bmatrix} 0 \\ K \end{bmatrix} u_p \tag{2.30a}$$

$$= Ay + Bu_p \tag{2.30b}$$

$$y_L = [1 \quad 0]y = C^\top y \tag{2.30c}$$

Notice that since $K > 0$, $a > 0$, the system is controllable. Since the system is controllable, a suitable reference model can be chosen such that the closed-loop plant dynamics matches the reference model dynamics. A reference model with the same relative degree as the plant model is chosen to be

$$\frac{y_m}{r} = \frac{\omega_n^2}{s^2 + 2\zeta\omega_n s + \omega_n^2} = k_m \frac{Z_m}{R_m} = W_m(s) \tag{2.31}$$

The reference model in state space form is

$$\begin{bmatrix} \dot{x}_1 \\ \dot{x}_2 \end{bmatrix} = \begin{bmatrix} 0 & 1 \\ -\omega_n^2 & -2\zeta\omega_n \end{bmatrix} \begin{bmatrix} x_1 \\ x_2 \end{bmatrix} + \begin{bmatrix} 0 \\ \omega_n^2 \end{bmatrix} r \tag{2.32a}$$

$$\dot{x} = A_c x + B_c r \tag{2.32b}$$

$$y_m = [1 \quad 0]x = C_c^\top x \tag{2.32c}$$

Two different types of adaptive controllers can be designed for the simplified system given in equation (2.28), each of which has a different number of estimated parameters.

By reducing the number of estimated parameters, the controller is simple. But with very few parameters, it may not be possible to sufficiently capture the dynamic behavior of the system. Theoretical and simulation results are presented for the two adaptive controllers designed based on the reduced order lateral dynamic models. The results indicate that for lateral guiding applications the simplified adaptive controllers are able to provide good tracking performance in the presence of process variations and disturbances. Experimental results that illustrate the effect of the number of the estimated parameters on guiding performance will be discussed in the next chapter.

2.4.1 Three parameter Guide Adaptive Controller

2.4.1.1 Control Law

Our objective is to design an adaptive control law such that the closed-loop plant matches the reference model. Consider a control law with a feedback term and a feed forward term.

$$u_p = L^* y + P^* r = \begin{bmatrix} L_1^* & L_2^* & P^* \end{bmatrix} \begin{bmatrix} y_1 \\ y_2 \\ r \end{bmatrix}$$

$$= {\theta^*}^\top \omega \tag{2.33a}$$

where L_1^*, L_2^* and P^* are the parameter values which make the closed-loop system match the reference model. Substituting u_p in equation (2.30)

$$\begin{aligned} \dot{y} &= \begin{bmatrix} 0 & 1 \\ 0 & -a \end{bmatrix} y + \begin{bmatrix} 0 \\ K \end{bmatrix} \begin{bmatrix} L_1^* & L_2^* & P^* \end{bmatrix} \begin{bmatrix} y_1 \\ y_2 \\ r \end{bmatrix} \\ &= \begin{bmatrix} 0 & 1 \\ 0 & -a \end{bmatrix} y + \begin{bmatrix} 0 & 0 \\ KL_1^* & KL_2^* \end{bmatrix} y + \begin{bmatrix} 0 \\ KP^* \end{bmatrix} r \\ &= \begin{bmatrix} 0 & 1 \\ KL_1^* & KL_2^* - a \end{bmatrix} y + \begin{bmatrix} 0 \\ KP^* \end{bmatrix} r \end{aligned} \tag{2.34}$$

Comparing the closed-loop system in equation (2.34) with the desired reference model given by equation (2.32a) , the desired control parameters that match the closed-loop system with the reference model are

$$\begin{aligned} L_1^* &= -\frac{\omega_n^2}{K} \\ L_2^* &= \frac{a - 2\zeta\omega_n}{K} \\ P^* &= \frac{\omega_n^2}{K} \end{aligned}$$

2.4.1.2 Adaptive Law

Since the parameters K and a are unknown, it is not possible to find the exact values of the control parameters. The adaptive control problem is posed as an estimation problem with an objective of minimizing the estimation error. Let us estimate L_1^*, L_2^*, P^* and use the estimates ($\theta^\top = [L_1\ L_2\ P]$) in the control input.

Consider the open-loop system

$$\dot{y} = \begin{bmatrix} 0 & 1 \\ 0 & -a \end{bmatrix} y + \begin{bmatrix} 0 \\ K \end{bmatrix} u_p \tag{2.35}$$

Adding and subtracting the desired control input we get

$$\dot{y} = \begin{bmatrix} 0 & 1 \\ 0 & -a \end{bmatrix} y + \begin{bmatrix} 0 \\ K \end{bmatrix} \left[u_p + {\theta^*}^\top \omega - {\theta^*}^\top \omega \right] \tag{2.36}$$

where ${\theta^*}^\top = [L_1^* \quad L_2^* \quad P^*]$, $\omega^\top = [y_1 \quad y_2 \quad r]$

$$\dot{y} = \begin{bmatrix} 0 & 1 \\ 0 & -a \end{bmatrix} y + \begin{bmatrix} 0 \\ K \end{bmatrix} [u_p + L_1^* y_1 + L_2^* y_2 + P^* r - L_1^* y_1 - L_2^* y_2 - P^* r] \tag{2.37}$$

$$= \underbrace{\begin{bmatrix} 0 & 1 \\ 0 & -a \end{bmatrix} y + \begin{bmatrix} 0 \\ K \end{bmatrix} [L_1^* y_1 + L_2^* y_2 + P^* r]}_{} + \underbrace{\begin{bmatrix} 0 \\ K \end{bmatrix} [u_p - L_1^* y_1 - L_2^* y_2 - P^* r]}_{} \tag{2.38}$$

$$= \underbrace{\begin{bmatrix} 0 & 1 \\ -\omega_n^2 & -2\zeta\omega_n \end{bmatrix} y + \begin{bmatrix} 0 \\ \omega_n^2 \end{bmatrix} r}_{} + \underbrace{\begin{bmatrix} 0 \\ K \end{bmatrix} \left[u_p - {\theta^*}^\top \omega \right]}_{} \tag{2.39}$$

$$= \underbrace{A_c y + B_c r}_{} + \underbrace{\begin{bmatrix} 0 \\ K \end{bmatrix} \left[u_p - {\theta^*}^\top \omega \right]}_{} \tag{2.40}$$

Denote the state estimation error by $\epsilon \triangleq y - x$ and the tracking error by $e_1 \triangleq y_L - y_m$. Then,

$$\dot{\epsilon} = A_c \epsilon + B \left[u_p - {\theta^*}^\top \omega \right] = A_c \epsilon + B \tilde{\theta}^\top \omega, \quad \tilde{\theta} = \theta - \theta^* \tag{2.41}$$

$$e_1 = [1 \quad 0] \epsilon = C_c^\top \epsilon \tag{2.42}$$

Therefore,

$$e_1 = C_c^\top \left[sI - A_c \right]^{-1} \begin{bmatrix} 0 \\ K \end{bmatrix} \left[u_p - {\theta^*}^\top \omega \right] \tag{2.43}$$

Since

$$W_m(s) = C_c^\top [sI - A_c]^{-1} \begin{bmatrix} 0 \\ KP^* \end{bmatrix}, \quad \text{we have} \tag{2.44}$$

$$e_1 = W_m(s) \rho^* \tilde{\theta}^\top \omega \tag{2.45}$$

where $\rho^* = \frac{1}{P^*}$. One can think of an adaptive law based on the SPR-Lyapunov approach and hence could take advantage of the KYP (B.5) and MKY lemmas (B.6). Since the relative degree of the reference model is 2, $W_m(s)$ is not SPR and hence a modification to the system has to be made so that the error e_1 relates to the parameters through a SPR transfer function. With this modification the adaptive controller design procedure is similar to a relative degree one system (controller design for a relative degree one system is presented in Appendix C.1).

If the controller can have differentiators, one can choose a transfer function $L(s) = (s + p_0)$ such that $W_m(s)L(s)$ is SPR and follow the same procedure as in Appendix C.1. Narendra and Valavani [23] introduced a new control structure which was able to make $W_m(s)L(s)$ SPR without using differentiators in the controller. Since $W_m(s)$ has a relative degree 2, let us use the operator $P_L(\theta) \triangleq L(s)\theta L(s)^{-1}$ in equation (2.45) and follow the same modification to the control structure and the error equation as in [23] to find the adaptive control law.

The error equation changes to

$$\dot{\epsilon} = A_c\epsilon + \overline{B}\rho^*\tilde{\theta}^\top\phi, \quad \overline{B} = (s+p_0)BP^* \tag{2.46a}$$

$$e_1 = \underbrace{W_m(s)(s+p_0)}\rho^*\tilde{\theta}^\top\phi, \quad \phi = \frac{1}{s+p_0}\omega \tag{2.46b}$$

$$= W_{m1}(s)\rho^*\tilde{\theta}^\top\phi, \quad \text{where } W_{m1}(s) \text{ is SPR} \tag{2.46c}$$

$$= W_{m1}(s)\rho^*(\theta^\top\phi - {\theta^*}^\top\phi) \tag{2.46d}$$

$$= W_{m1}(s)\rho^*(L(s)^{-1}\theta^\top\omega - {\theta^*}^\top\phi) \tag{2.46e}$$

Let the estimate of tracking error be

$$\hat{e}_1 = W_{m1}(s)\rho(L(s)^{-1}u_p - \theta^\top\phi) \tag{2.47}$$

Notice that equation (2.47) is similar to equation (C.3). In order to use the procedure as in Appendix C.1, the estimation error $\epsilon_1 = e_1 - \hat{e}_1$ should be e_1, hence the controller has to be modified such that the term $(L(s)^{-1}u_p - \theta^\top\phi)$ is zero.

$$\begin{aligned} u_p &= L(s)\theta^\top\phi \\ &= (s+p_0)\theta^\top\phi \\ &= \dot{\theta}^\top\phi + \theta^\top\dot{\phi} + p_0\theta^\top\phi \\ &= \dot{\theta}^\top\phi + \theta^\top\underbrace{(\dot{\phi} + p_0\phi)} \\ &= \dot{\theta}^\top\phi + \theta^\top\omega \end{aligned} \tag{2.48a}$$

With the appropriate modifications to the estimation error dynamics and the controller, the dynamics of the system resemblems a relative degree one system. The procedure in Appendix C.1 is followed to find the adaptive law that results in a stable system with $\lim_{t\to\infty} e_1(t) = 0$. The adaptive law is

$$\dot{\theta} = -\Gamma e_1 \phi \text{sgn}(\rho^*) = -\Gamma e_1 \phi \quad \because \rho^* > 0 \tag{2.49}$$

Notice that the controller has a differentiator, but $\dot{\theta}$ can be obtained from the adaptive law given in equation (2.49). This modified structure was first introduced in [23]. For a detailed analysis of this problem (relative degree = 2) refer to chapter 5, pages 199 - 226, [22] and the article by Narendra and Valavani [23].

2.4.1.3 Simulation

In order to understand the validity of the simplified model, the GAC based on the simplified model was simulated in Simulink using the complete plant model. The lateral web dynamics block in Figure 2.7 represents the second order model for the web dynamics. The adaptive law and the control law are based on the simplified model. Figure 2.6 shows the performance of the controller with a sinusoidal reference trajectory. The top plot shows the tracking performance, the middle shows the controller output while the bottom plot shows the time history of the estimated parameters. Notice that the estimated parameters reach a steady value but these parameter values are not necessarily their true values. The parameter update stops as soon as the error reaches zero. The Simulink block diagram for this simulation is shown in Figure 2.7.

The simulation results indicate that the adaptive control scheme based on the approximate model is capable of regulating the position of the web. A sinusoidal reference with a bias was used as the output of the reference model in order to observe the transient, steady-state and tracking performance of the controller.

2.4.2 Simplified GAC with an Estimator

In consideration of the implementation of the controller in practice note that it is not possible to obtain the measurement of the lateral velocity $\dot{y}_L$ (Notice that the control input depends on ω which depends on $\dot{y}_L$). One possible way to obtain the lateral velocity $\dot{y}_L$ would be to use the finite difference approximation from the lateral position measurement y_L. One can also setup an estimator for the measurement $\dot{y}_L$ based on the previous assumption that the dynamics of

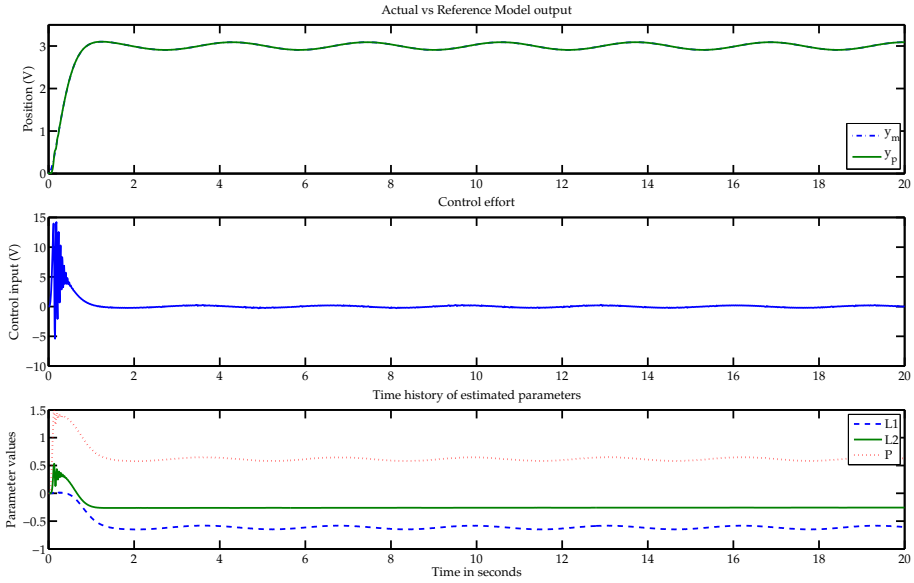

Figure 2.6: Simulation Results for 3-Parameter GAC

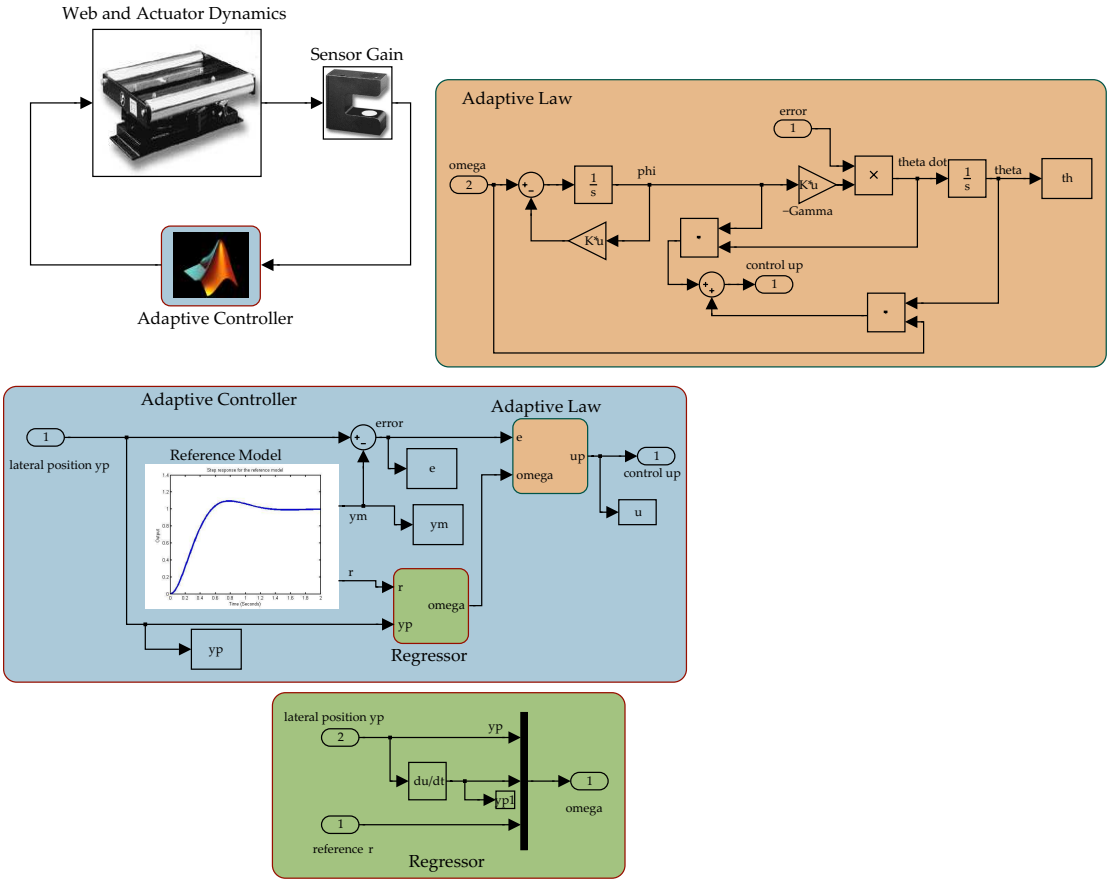

Figure 2.7: Simulink Block Diagram for 3-Parameter GAC

the web is a constant and if the motor velocity measurement is available.

The relationship between the motor velocity and the lateral velocity can be approximated as

$$\dot{y}_L = K_w \dot{\theta} = K_w v_m \tag{2.50}$$

where $\dot{y}_L$ is the lateral web velocity, K_w is a constant which is the approximated lateral web dynamics and $\dot{\theta} = v_m$ is the motor velocity. Filtering both left and right hand side of equation (2.50) by a low pass filter $F(s) = \frac{1}{\tau s+1}$ and taking the Laplace transform we get

$$sF(s)y_L = K_w F(s) v_m \tag{2.51}$$

Let an intermediate system be defined as

$$Z = {\varphi^*}^\top \phi \tag{2.52}$$

where $Z \triangleq F(s)v_m$, $\phi = sF(s)y_L$ and $\varphi^* = \frac{1}{K_w}$. Hence ϕ is obtained by filtering the lateral position measurement using the filter $\frac{s}{\tau s+1}$ and Z is obtained by filtering the motor velocity v_m by using the filter $\frac{1}{\tau s+1}$. Let e be the estimation error $y - \varphi^\top \phi$ with φ being the estimate of φ^*. Notice that this is a linear estimation problem and hence the minimum can be reached in a single step if the update is in the direction of negative gradient of the cost function. It is common to choose the cost function as $J(\varphi) = \frac{e^2}{2}$ and hence the gradient is $\bigtriangledown J(\varphi) = e\dot{e} = -e\phi$. Hence the update law for the φ is $\dot{\varphi} = \gamma e\phi$, where $\gamma > 0$ and $\varphi(0) = \varphi_0$. From the estimate of $\varphi = \frac{1}{K_w}$, we can use the equation (2.50) to find the estimated lateral velocity of the web.

2.4.2.1 Simulation

Figure 2.8 shows the simulation result for the simplified guide adaptive controller with the estimated lateral velocity. The top plot shows the tracking performance of the controller while the middle plot shows the control effort and the bottom plot shows the estimated parameters. The simulation results indicate a similar performance as observed with the previous controller. The Simulink model is presented in shown in Figure 2.9.

2.4.3 Four Parameter Guide Adaptive Controller

Notice that the adaptive controllers derived in the previous section require two measurements, the lateral position y_L and the velocity $\dot{y}_L$. It is possible to derive a model reference adaptive

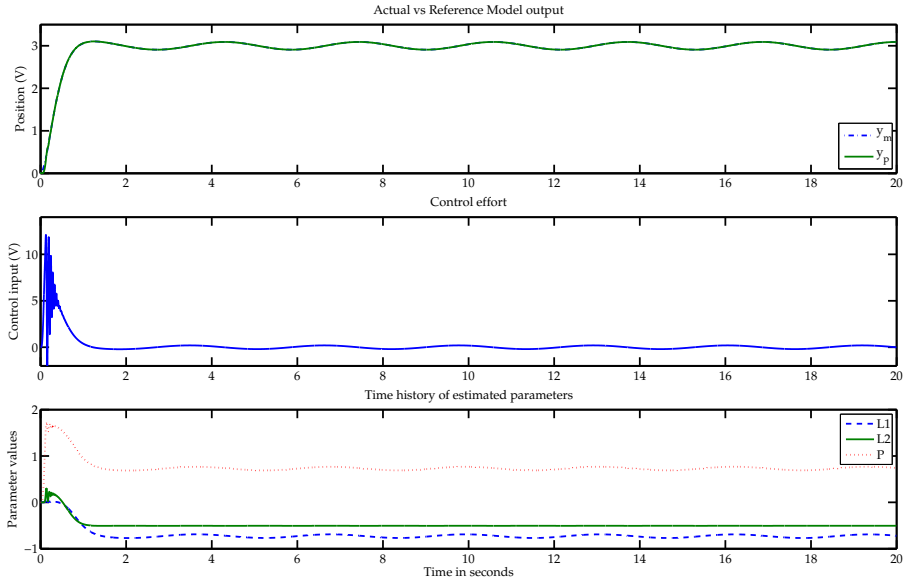

Figure 2.8: Simulation Results for 3-Parameter GAC with an Estimator

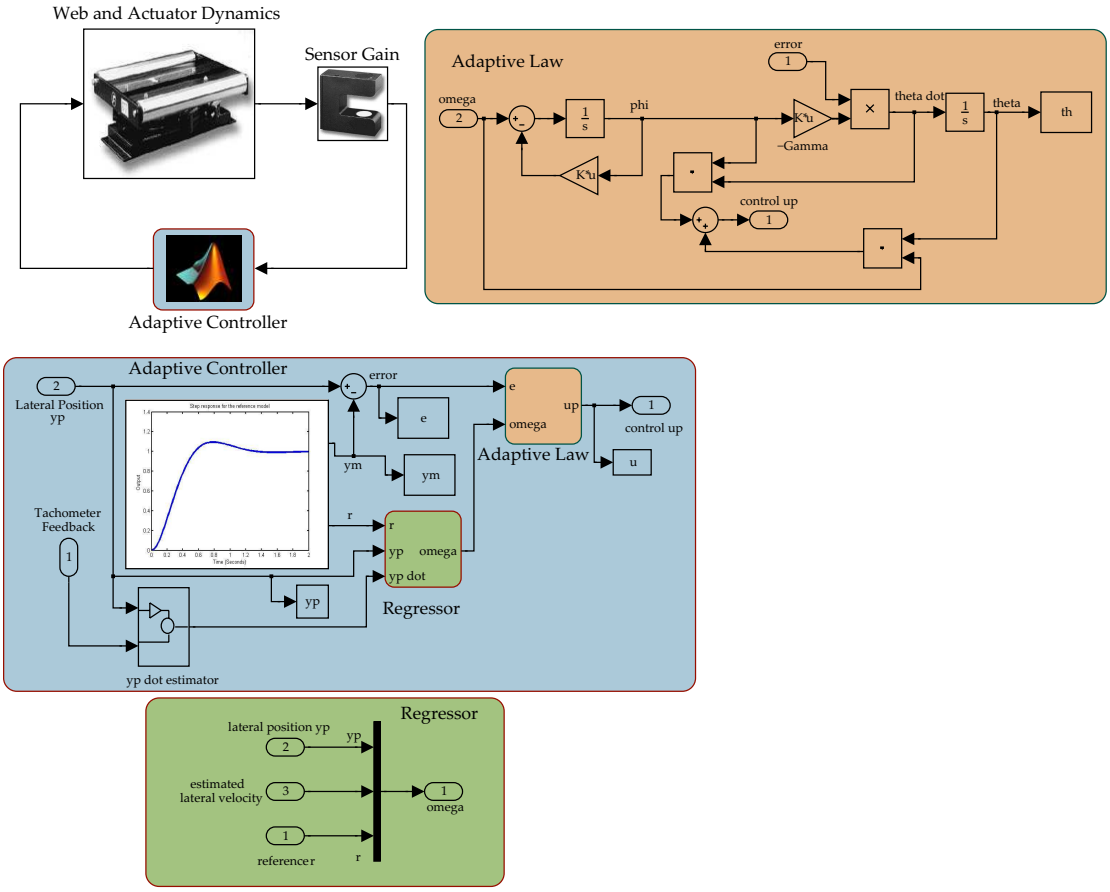

Figure 2.9: Simulink Block Diagram for 3-Parameter GAC with an Estimator

control law for the system described by equation (2.30) using one measurement, the lateral position measurement y_L. The following section describes the design process.

2.4.3.1 Control Law

Let us define the following control law for the system described by equation (2.30) so that the dynamics of the closed-loop plant matches the dynamics of the reference model given in equation (2.32a) .

$$u_p = \theta_1^* \frac{1}{\Lambda(s)} u_p + \theta_2^* \frac{1}{\Lambda(s)} y_L + \theta_3^* y_L + c_0^* r \tag{2.53}$$

where $\Lambda(s) = s + a_0$ be a Hurwitz polynomial and θ_i^*'s, c_0^* are the true parameters which make the closed-loop system dynamics match the reference model dynamics. The usefulness of parametrizing the control law in this manner will be evident later. Rewriting the control law in terms of the feedback and feedforward terms we get

$$u_p = \frac{\theta_3^* s + (\theta_2^* + a_0\theta_3^*)}{s + (a_0 - \theta_1^*)} y_L + \frac{(s + a_0)c_0^*}{s + (a_0 - \theta_1^*)} r \tag{2.54}$$

Substituting the control law given by equation (2.54) in the system described by equation (2.28) we get

$$s^2 y_L + a s y_L = K \left[\frac{\theta_3^* s}{s + (a_0 - \theta_1^*)} y_L + \frac{\theta_2^* + a_0\theta_3^*}{s + (a_0 - \theta_1^*)} y_L + \frac{(s + a_0)c_0^*}{s + (a_0 - \theta_1^*)} r \right] \tag{2.55}$$

$$\left[(s^2 + as)(s + (a_0 - \theta_1^*)) - K\theta_3^* s - K(\theta_2^* + a_0\theta_3^*) \right] y_L = K(s + a_0)c_0^* r \tag{2.56}$$

$$\frac{y_L}{r} = \frac{K(s + a_0)c_0^*}{s^3 + (a_0 - \theta_1^* + a)s^2 + \left[a(a_0 - \theta_1^*) - K\theta_3^*\right] s - K(\theta_2^* + a_0\theta_3^*)} = \frac{w_n^2}{s^2 + 2\zeta\omega_n s + \omega_n^2} \tag{2.57}$$

Notice that in order to have the closed-loop system dynamics match the reference model dynamics, there has to be a pole-zero cancellation. The cancellation will occur at $-a_0$ and hence the filter $\Lambda(s) = s + a_0$ has to be Hurwitz. If $\Lambda(s)$ is not Hurwitz, then the pole-zero cancellation will occur in the right-half plane which is not desirable.

If $Kc_0^* = \omega_n^2$ then,

$$(s + a_0)(s^2 + 2\zeta\omega_n s + \omega_n^2) = s^3 + (a_0 - \theta_1^* + a)s^2 + \left[a(a_0 - \theta_1^*) - K\theta_3^*\right] s - K(\theta_2^* + a_0\theta_3^*) \tag{2.58a}$$

Equating both we obtain the true parameters to be

$$\theta_1^* = a - 2\zeta\omega_n \tag{2.59a}$$

$$\theta_3^* = \frac{1}{K}(aa_0 - a^2 + 2\zeta\omega_n a - \omega_n^2 - 2\zeta\omega_n a_0) \tag{2.59b}$$

$$\theta_2^* = -\frac{a_0\omega_n^2}{K} - a_0\theta_3^* \tag{2.59c}$$

$$c_0^* = \frac{\omega_n^2}{K} \tag{2.59d}$$

It is not always possible to find the desired control law which can make the closed-loop system match the reference model. A few conditions on the type of the plant model and the reference model have to be made [18].

1. The polynomial $Z_p(s)$ should be Hurwitz and monic.
2. The order, n, of the plant should be known or at least an upper bound should be known.
3. The relative degree of the plant (n^*) should be known.
4. The sign of k_p should be known.
5. $Z_m(s), R_m(s)$ should be monic and Hurwitz and the order of the reference model should not be greater than the order of the plant.
6. The relative degree of the reference model should be same as that of the plant model.

From equation (2.57) it can be seen that if the zeros of the reference model are not the same as the plant zeros, then the plant zeros will be cancelled by the control in order to match the closed-loop system dynamics to the reference model dynamics. If $Z_p(s)$ is not Hurwitz, then pole-zero cancellation would occur in the right half plane which is not desirable. If $Z_p(s)$ is not monic, then the constant term of the leading coefficient can be pulled out and augmented to the gain k_p. The requirement for the sign of k_p to be known will be evident from the adaptive law derivation. Without the knowledge of the relative degree of the plant, it would not be possible to design an adaptive control law. The order of the plant is important because it is not always possible to find a parametrized control law such that the closed-loop system dynamics matches the reference model. But we can use the *Bezout Identity* to overcome the problem (refer to [22] sections 5.4.1 and 5.4.2).

In order to obtain proper parametrization of the controller parameters θ_i^*'s, both the numerator and denominator polynomials of the reference model transfer function should be Hurwitz.

In order to have the minimum number of controller parameters, it is necessary that both polynomials of the transfer function of the reference model be monic.

Since the parameters a and K are unknown it is not possible to use the control law in equation (2.54) and hence the adaptive control problem is posed as an estimation problem with the objective of minimizing the parameter estimation error. We can follow the same procedure of adding and subtracting the desired control effort, but first we need to represent the control law in the state-space form in order to simplify the analysis. We shall also define an augmented system which is useful for our analysis both in this section as well as in the next section.

$$u_p = \theta_1^* \frac{1}{s+a_0} u_p + \theta_2^* \frac{1}{s+a_0} y_L + \theta_3^* y_L + c_0^* r$$

$$u_p = {\theta^*}^\top \omega$$

where ${\theta^*}^\top = [\theta_1^*,\ \theta_2^*,\ \theta_3^*,\ c_0^*]$ and $\omega^\top = \left[\frac{1}{s+a_0}u_p,\ \frac{1}{s+a_0}y_L,\ y_L,\ r\right]$.

$$\dot{\omega}_1 = F\omega_1 + g u_p, \qquad \omega_1(0) = 0, F = -a_0 \tag{2.60a}$$

$$\dot{\omega}_2 = F\omega_2 + g y_p, \qquad \omega_2(0) = 0, g = 1 \tag{2.60b}$$

The state-space representation of the closed-loop system with the **desired control effort** can be obtained by augmenting the states y of the system described by equation (2.30) with the states of the controller in equation (2.60).

$$\dot{Y} = A_s Y + B_s c_0^* r \tag{2.61a}$$

$$y_L = C_s^\top Y \tag{2.61b}$$

where $Y = \left[y^\top,\ \omega_1,\ \omega_2\right]^\top$ and

$$\dot{y} = Ay + Bu_p = Ay + B\left[\theta_1^*\omega_1 + \theta_2^*\omega_2 + \theta_3^* y_L + c_0^* r\right] \tag{2.62a}$$

$$\dot{\omega}_1 = F\omega_1 + g u_p = F\omega_1 + g\left[\theta_1^*\omega_1 + \theta_2^*\omega_2 + \theta_3^* y_L + c_0^* r\right] \tag{2.62b}$$

$$\dot{\omega}_2 = F\omega_2 + g y_p = F\omega_2 + gC^\top y \tag{2.62c}$$

$$\therefore \quad \dot{Y} = \begin{bmatrix} A + B\theta_3^* C^\top & B\theta_1^* & B\theta_2^* \\ g\theta_3^* C^\top & F + g\theta_1^* & g\theta_2^* \\ gC^\top & 0 & F \end{bmatrix} Y + c_0^* \begin{bmatrix} B \\ g \\ 0 \end{bmatrix} r \tag{2.63a}$$

$$y_L = [C^\top \ \ 0 \ \ 0]Y \tag{2.63b}$$

From equation (2.57)

$$\frac{y_L(s)}{r(s)} = \frac{K(s+a_0)c_0^*}{s^3 + (a_0 - \theta_1^* + a)s^2 + [a(a_0 - \theta_1^*) - K\theta_3^*]\, s - K(\theta_2^* + a_0\theta_3^*)} = W_m(s) \tag{2.64}$$

and from equation (2.61)

$$\frac{y_L(s)}{r(s)} = C_s^\top (sI - A_s)^{-1} B_s c_0^* = W_m(s) = \frac{y_m}{r} \tag{2.65}$$

The reference model can be described by the following state space representation.

$$\dot{Y}_m = A_s Y_m + B_s c_0^* r \tag{2.66a}$$

$$y_m = C_s^\top Y_m \tag{2.66b}$$

Similarly, the augmented closed-loop system with the **control** u_p can be obtained as

$$\dot{Y}_c = A_0 Y_c + B_s u_p \tag{2.67a}$$

$$y_L = C_s^\top Y_c \tag{2.67b}$$

where $Y_c = \left[y^\top,\ \omega_1,\ \omega_2\right]^\top$.

$$\dot{y} = Ay + Bu_p \tag{2.68a}$$

$$\dot{\omega}_1 = F\omega_1 + gu_p \tag{2.68b}$$

$$\dot{\omega}_2 = F\omega_2 + gy_p = F\omega_2 + gC^\top y \tag{2.68c}$$

Therefore,

$$\dot{Y}_c = \begin{bmatrix} A & 0 & 0 \\ 0 & F & 0 \\ gC^\top & 0 & F \end{bmatrix} Y_c + \begin{bmatrix} B \\ g \\ 0 \end{bmatrix} u_p \tag{2.69a}$$

$$y_L = [C^\top \ \ 0 \ \ 0] Y_c \tag{2.69b}$$

2.4.3.2 Adaptive Law

Our objective now is to obtain an estimate of θ^* so that the closed-loop system described in equation (2.69) matches the reference model in equation (2.66). Adding and subtracting the

desired control effort ${\theta^*}^\top\omega$ we get

$$\dot{Y}_c = A_0 Y_c + B_s u_p + B_s {\theta^*}^\top\omega - B_s {\theta^*}^\top\omega \tag{2.70a}$$

$$= \underbrace{A_0 Y_c + B_s {\theta^*}^\top\omega} + B_s(u_p - {\theta^*}^\top\omega) \tag{2.70b}$$

$$= A_s Y_c + B_s c_0^* r + B_s(u_p - {\theta^*}^\top\omega) \tag{2.70c}$$

$$y_L = C_s^\top Y_c \tag{2.70d}$$

Let $\epsilon = Y_c - Y_m$ be the state estimation error and $e_1 = y_L - y_m$ be the tracking error. Hence the error equations can be obtained from equations (2.70) and (2.66) as

$$\dot{\epsilon} = A_s\epsilon + B_s(u_p - {\theta^*}^\top\omega), \quad \epsilon(0) = \epsilon_0 \tag{2.71a}$$

$$e_1 = C_s^\top\epsilon \tag{2.71b}$$

Notice that

$$\frac{e_1}{u_p - {\theta^*}^\top\omega} = C_s^\top(sI - A_s)^{-1}B_s \tag{2.72}$$

and

$$W_m(s) = C_s^\top(sI - A_s)^{-1}B_s c_0^* \tag{2.73}$$

$$\Rightarrow e_1 = W_m(s)\rho^*(u_p - {\theta^*}^\top\omega), \quad \rho^* = \frac{1}{c_0^*} \tag{2.74}$$

The error equation is similar to the form seen in equation (C.5) and the same procedure can be continued if $W_m(s)$ is SPR. Since the relative degree of the reference model is 2, $W_m(s)$ is not SPR and hence we shall use the operator $P_L(\theta)$ as before and the modified error equation is

$$\dot{\epsilon} = A_s\epsilon + \overline{B_c}\rho^*\tilde{\theta}^\top\phi \tag{2.75a}$$

$$e_1 = C_s^\top\epsilon \tag{2.75b}$$

which is similar to the error equation (2.46). The same procedure is followed and the adaptive law and control law which result in a stable system with $e_1(t) \to 0$ as $t \to \infty$ are given by

$$\dot{\theta} = -\Gamma e_1\phi\text{sgn}(\rho^*) = -\Gamma e_1\phi \tag{2.76a}$$

$$u_p = \theta^\top\omega + \dot{\theta}^\top\phi \tag{2.76b}$$

2.4.3.3 Simulation

Figure 2.10 shows the performance of the adaptive controller. The plant used in this simulation is the complete plant model instead of the simplified plant. The top plot shows the tracking performance, the middle plot shows the control input, while the bottom plot shows the estimated

parameters. The Simulink block diagram for the simulation is shown in Figure 2.12. Similar to the previous controller the adaptive controller with four parameters is capable of regulating the lateral position of the web. By observing the control effort for the two controllers one can notice that the controller with four parameters exhibits a better transient response behavior. This can be attributed to the fact that the controller with three parameters has no knowledge of the control effort generated. The estimated parameters settle to a steady state value after the plant starts tracking the sinusoidal reference. A common disturbance which helps in characterizing the transient response is a pulse disturbance. The performance of the controller with a pulse disturbance is shown in Figure 2.11 and the plots indicate that the controller is capable of rejecting the pulse disturbances.

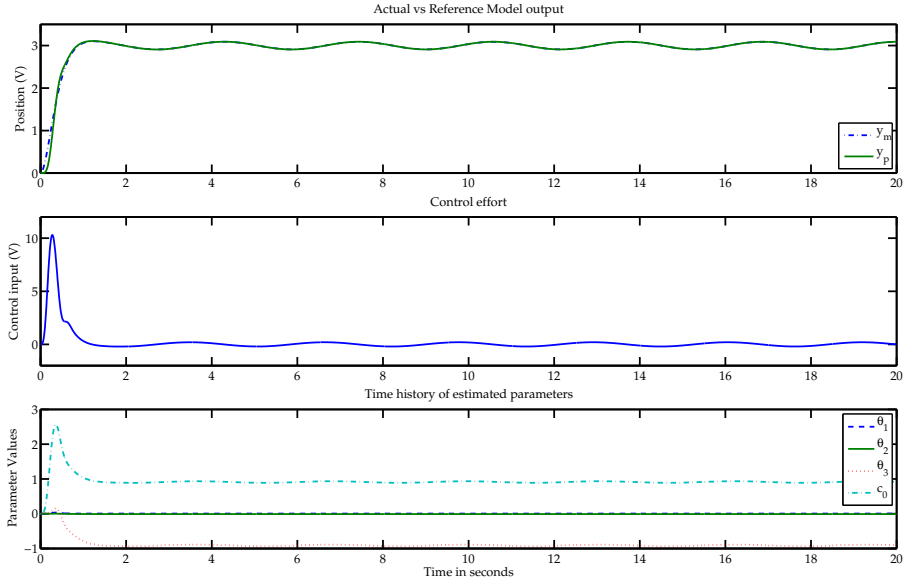

Figure 2.10: Simulation Results for 4-Parameter GAC

2.5 Guide Adaptive Controller

In the previous section a simplified guide adaptive controller was designed based on the assumption that the dynamics of the web is a constant. Here in this section we shall consider the complete dynamics of the web and develop a guide adaptive controller. The transfer function for a steering guide is given by equation (2.27) and its state space form is

$$\dot{y} = Ay + Bu_p, \quad y_L = C^\top y \tag{2.77}$$

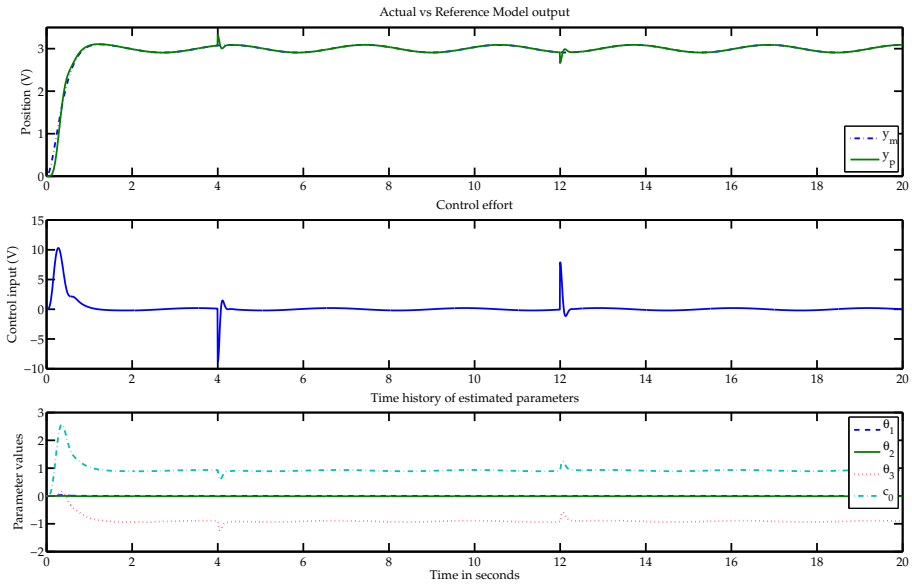

Figure 2.11: Simulation Results for 4-Parameter GAC with a Pulse Disturbance

Consider the reference model in equation (2.32a) and the objective is to design a control law such that the closed-loop system matches the reference model. So far our first step in designing an adaptive controller has been to find the desired control input which can ensure that the closed-loop system matches the reference model. Then we would pose the problem as an estimation problem and use the estimated parameters in the control law. In a general model reference adaptive control problems with relative degree $n^* = 1$, it is simple to choose a parametrized control law which can algebraically render the closed-loop system to have the same roots as the reference model. But in a general adaptive control problem with relative degree $n^* \geq 2$, finding the desired control is not simple. In the previous section, we were able to choose a desired control ($\theta^{*\top}\omega$) which resulted in a closed-loop system that matched the reference model. As discussed in [22] (section 5.4.1 and 5.4.2), *Bezout Identity* can be used to show that it is always possible to find a parameter vector θ^* so that the following control law [18] will result in a closed-loop system whose dynamics is same as the reference model dynamics:

$$u_p = \theta_1^{*\top}\frac{\alpha(s)}{\Lambda(s)}u_p + \theta_2^{*\top}\frac{\alpha(s)}{\Lambda(s)}y_L + \theta_3^* y_L + c_0^* r \tag{2.78}$$

where $\alpha(s) = [s^2\ s\ 1]^\top$, $\Lambda(s)$ is an arbitrary monic Hurwitz polynomial of degree 3 which has to be chosen. Similar to the procedure in the previous section (section (2.60) on page 35) we can

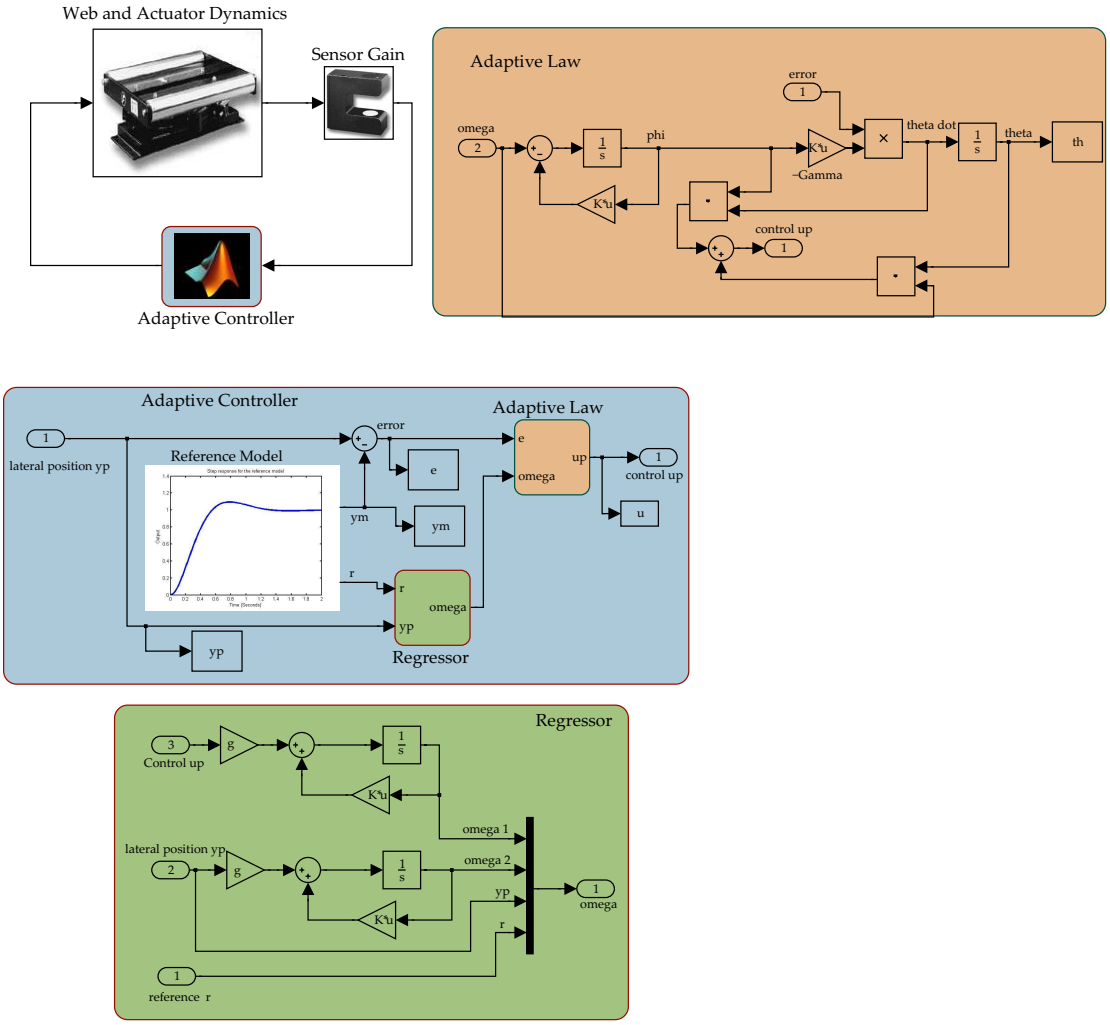

Figure 2.12: Simulink Block Diagram for 4-Parameter GAC

represent the control law in the state-space form as

$$\dot{\omega}_1 = F\omega_1 + gu_p, \qquad \omega_1(0) = 0 \tag{2.79a}$$

$$\dot{\omega}_2 = F\omega_2 + gy_p, \qquad \omega_2(0) = 0 \tag{2.79b}$$

$$u_p = \theta^{*\top}\omega \tag{2.79c}$$

where $\omega_1, \omega_2, \theta_1, \theta_2 \in \mathcal{R}^3$, $\theta^* = [\theta_1^{*\top}\ \theta_2^{*\top}\ \theta_3^*\ c_0^*]$ and $\omega = [\omega_1^\top\ \omega_2^\top\ y_L\ r]$. The matrix F and g are realized as

$$F = \begin{bmatrix} -\lambda_2 & -\lambda_1 & -\lambda_0 \\ 1 & 0 & 0 \\ 0 & 1 & 0 \end{bmatrix}, \quad g = \begin{bmatrix} 1 \\ 0 \\ 0 \end{bmatrix} \tag{2.80}$$

where $\Lambda(s) = s^3 + \lambda_2 s^2 + \lambda_1 s + \lambda_0$.

The adaptive control design is similar to the design in the previous section but with more estimation parameters which are a result of considering the complete web lateral dynamic model. Notice that in equation (2.59) we have shown the existence of the true parameters with the desired control given by equation (2.53). Similarly, it is possible to show the existence of the true parameters for the adaptive controller with the desired control given in equation (2.78). Same procedure as in the previous section can be followed to obtain the adaptive law and control law (refer to chapter 6 in [18] for a comprehensive formulation).

2.5.1 Control Law

$$u_p = \theta^\top\omega + \dot{\theta}^\top\phi \tag{2.81a}$$

$$\phi = \frac{1}{s+p_0}\omega \tag{2.81b}$$

$$\omega = [\omega_1^\top\ \omega_2^\top\ y_L\ r] \tag{2.81c}$$

$$\dot{\omega}_1 = F\omega_1 + gu_p, \qquad \omega_1(0) = 0 \tag{2.81d}$$

$$\dot{\omega}_2 = F\omega_2 + gy_p, \qquad \omega_2(0) = 0 \tag{2.81e}$$

2.5.2 Adaptive Law

$$\dot{\theta} = -\Gamma e_1\phi, \quad e_1 = y_L - y_m \tag{2.82}$$

2.5.3 Analysis

It has been shown in [18] that the above adaptive law along with the control law results in a stable closed-loop system with $e_1(t) \rightarrow 0$ as $t \rightarrow \infty$. The proof is similar to the one described in section C.1.0.1. The chosen Lyapunov-like function is

$$V(\tilde{\theta}, \epsilon) = \frac{\epsilon^\top P_c \epsilon}{2} + \frac{\tilde{\theta}^\top \Gamma^{-1} \tilde{\theta} |\rho^*|}{2}$$

and with the above control law and adaptive law the time derivative of V is given by

$$\dot{V} = -\frac{\epsilon^\top q q^\top \epsilon}{2} - \frac{\epsilon^\top \nu_c L_c^\top \epsilon}{2}$$

where q is a vector and $\nu_c > 0$ is a scalar and L_c is a positive definite matrix.

Because $V > 0$ and $\dot{V} \leq 0$, V is bounded or $V \in \mathcal{L}_\infty \Rightarrow \epsilon, \theta, \tilde{\theta} \in \mathcal{L}_\infty$. With $\epsilon \in \mathcal{L}_\infty$ we get $Y_c, Y_m \in \mathcal{L}_\infty$. In addition to proving that $u = \theta^\top \omega \in \mathcal{L}_\infty$, we need to prove that $u = \theta^\top \omega + \dot{\theta}^\top \phi \in \mathcal{L}_\infty$. Since ϕ is a filtered version of ω and F being a stable filter, it is clear that $u \in \mathcal{L}_\infty$.

2.5.4 Simulation

Figures 2.13 and 2.14 show the performance of guide adaptive controller. The top plot in each figure shows the tracking performance, the middle plot shows the controller output while the bottom plot shows the estimated parameters. In Figure 2.14 in addition to the sinusoidal reference, a pulse disturbance of 0.25 V amplitude is introduced at two time instants, 4 and 12 seconds. The controller is capable of rejecting the pulse disturbance. The Simulink block diagram for the GAC is shown in Figure 2.15.

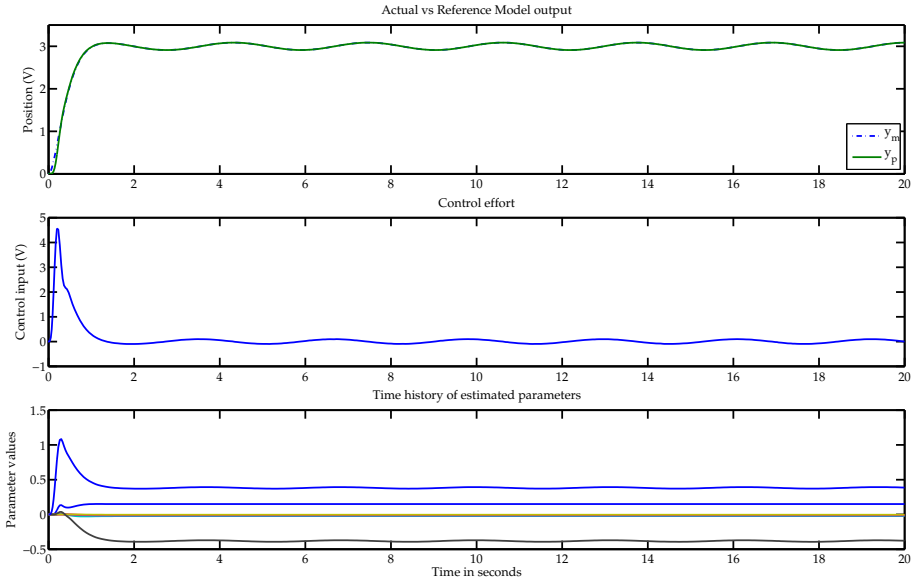

Figure 2.13: Simulation Results for Guide Adaptie Controller

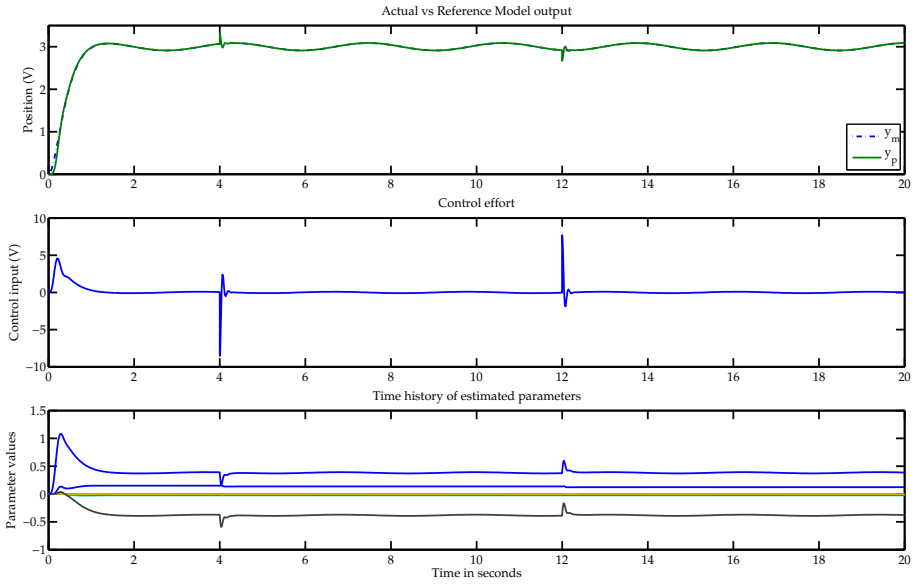

Figure 2.14: Simulation Results for Guide Adaptie Controller with a Pulse Disturbance

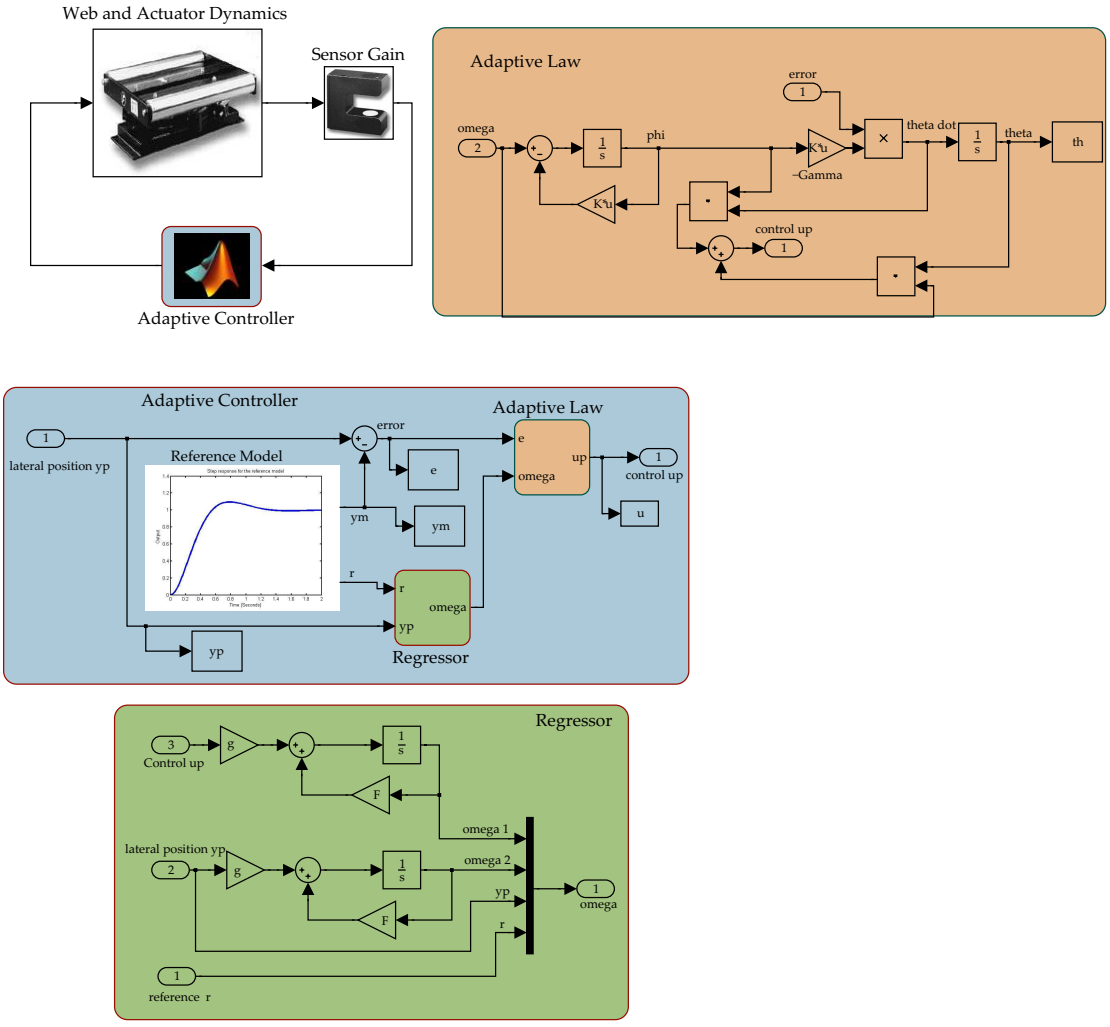

Figure 2.15: Simulink Block Diagram for Guide Adaptie Controller

Chapter 3

Experimental Results

In the previous chapter the design and analysis of model reference adaptive control strategies suitable for web guiding were presented. Three different guide adaptive controllers were developed based on the number of estimated parameters in the control law. Two adaptive controllers were designed based on a simplified model for the lateral web dynamics and one was based on the complete model. In this chapter the controller designs are implemented on an experimental web platform containing two intermediate web guides and their performance under different operating conditions are evaluated. Guidelines for implementation of the adaptive algorithms are given and discussed.

3.1 Experimental Platform

The experimental web handling platform used for implementing the designed controllers is shown in Figure 3.1. A line schematic of the platform is shown in Figure 3.2. The platform is an *endless web line* with several idle rollers and one driven roller (Master Speed Roller). The platform does not have an unwind or a rewind section; the web runs in a loop around the rollers. The transport velocity of the web is set by the speed of the driven roller. In order to provide traction between the driven roller and the web, a nip roller is used on the driven roller. The nip roller applies pressure at the contact surface to maintain web traction on the driven roller during the start-up of the line.

The platform is equipped with a passive dancer and an active dancer which can be used to control the tension of the web in the platform [24, 25]. In an active dancer, the dancer roller position is controller by an actuator. The tension in the web line can be increased or decreased by varying the position of the dancer roller. In a passive dancer mechanism the dancer roller is

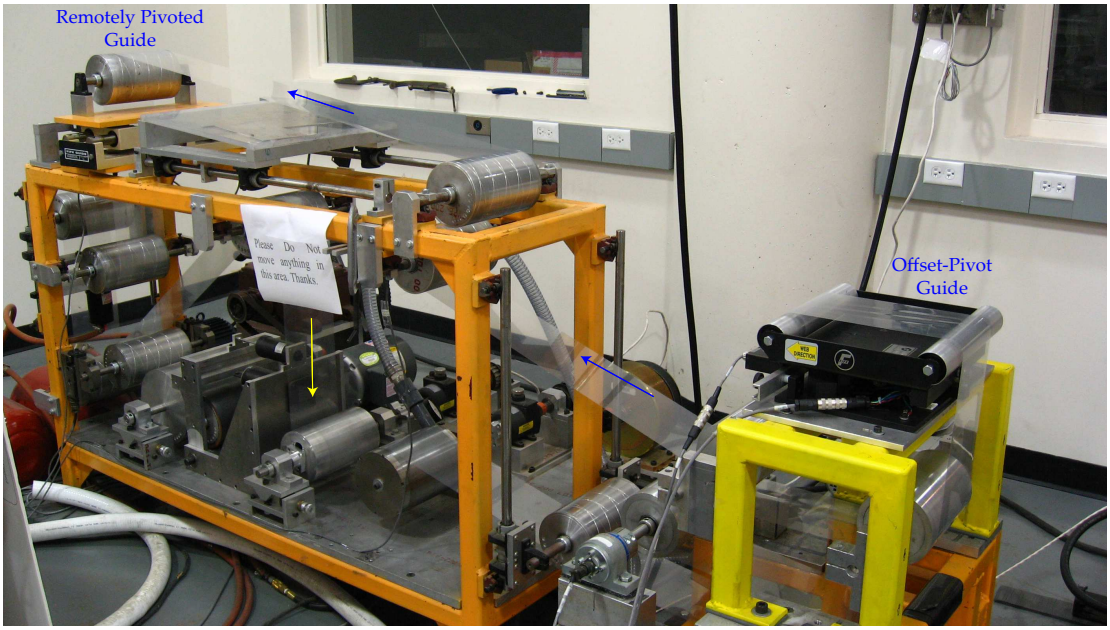

Figure 3.1: Experimental Web Handling Platform

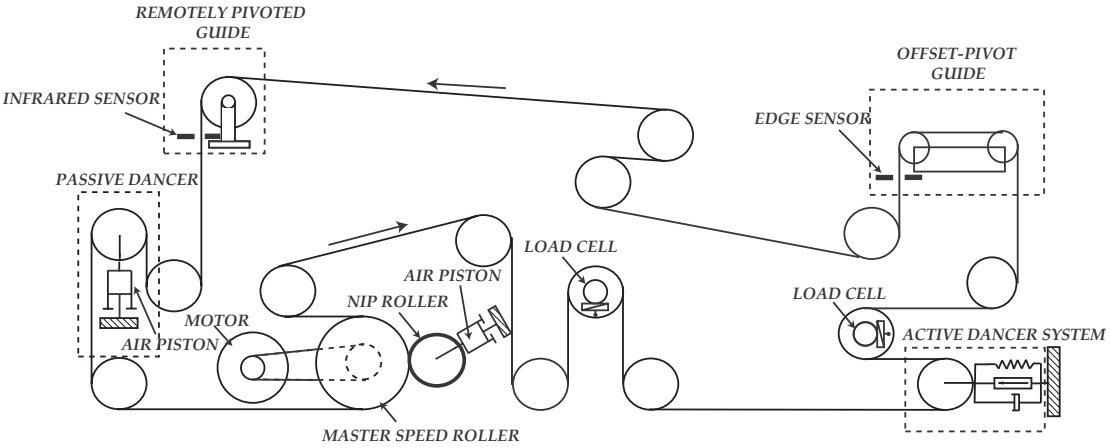

Figure 3.2: Line Schematic of the Experimental Web Handling Platform

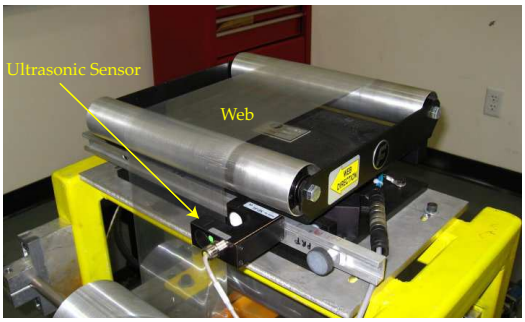

Figure 3.3: offset pivot Guide

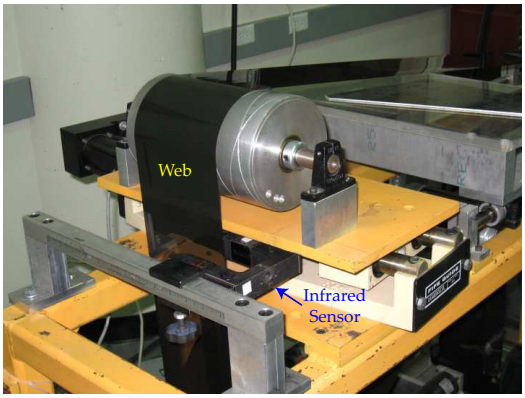

Figure 3.4: Remotely Pivoted Guide

free to move about a pivot or on a linear slide [25]. The dancer roller in a passive dancer is not actuated but floats due to the pressure from an air cylinder.

There are two web guides in the platform; an offset pivot guide and a remotely pivoted guide. The offset pivot guide is a Fife Narrow web guide and the remotely pivoted guide is a Fife Kamberoller guide. The offset pivot guide is equipped with an ultrasonic sensor and the remotely pivoted guide is equipped with an infrared sensor.

The actuators (servo motors) and the sensors of each guide mechanism are connected to a dSPACE DS1103 real-time board through Fife controller hardware. The Kamberoller guide and its infrared sensor is connected to the real-time hardware through a Fife A9 analog controller. Electrical provisions are made such that the guide can be controlled either with the A9 controller or with the dSPACE hardware. The offset pivot guide is connected to the dSPACE hardware through a Fife DP-01 controller. The offset pivot guide can only be controlled using the dSPACE hardware.

The feedback signals from the sensors and the control signals to the actuators are processed by the dSPACE hardware. The DS1103 hardware has eight A/D converters for a total of 20 A/D channels, of which 16 channels are multiplexed by four converters. The digital output from the real-time hardware is converted into analog output by 8 D/A converters. The input and output range of the dSPACE board is $\pm$ 10 V. The dSPACE board is driven by a PowerPC CPU running at 400 MHz. The real-time control software is written in C using dSPACE RTLib real-time libraries. The control software is driven by interrupts which occur every sampling period. At each sampling time the following operations are performed by the real-time software:

1. the sensor feedback signals are read;

2. the control algorithm is executed and the required control effort is calculated; and

3. the control effort is then supplied to the actuators.

The dSPACE board is installed inside a host computer running Microsoft Windows 2000 operating system. The dSPACE ControlDesk software is utilized to communicate between the real-time hardware and the host computer. The real-time hardware is capable of buffering the data using its internal memory. Trace variables can be setup so that the buffered data in the real-time control hardware can be stored/displayed in the host computer. These trace variables can also be used to change the variable values in the real-time control software while executing in real-time.

3.2 Experimental Procedure

Experiments were carried out to observe the guiding performance of the designed adaptive controllers for process variations and disturbances. The experimental results presented in this thesis cover only the Kamberoller guide. Experiments were also conducted on the offset pivot guide and similar results were observed.

The Kamberoller is located four spans downstream of the offset pivot guide. Any arbitrary disturbance can be created using the offset pivot guide and the Kamberoller can be used to reject the disturbance. On the contrary, since the web has to travel 13 spans from the Kamberoller to the offset pivot guide, the lateral disturbances generated at the Kamberoller do not propagate to the offset pivot guide. The Kamberoller guide is connected to the dSPACE hardware through the Fife A9 controller. Electrical modifications to the A9 controller were made so that either the A9 controller or the controller implemented on the dSPACE hardware can be used to control the Kamberoller guide. This setup provides a convenient way to compare the two controllers. Such an arrangement is not available with the offset pivot guide.

The adaptive control schemes were compared with an A9 analog controller (PI controller). The A9 controller is the only industrial controller in the experimental platform which can be directly compared with the adaptive control schemes. Modifications to the existing setup are required in order to incorporate other industrial controllers in the experimental platform.

The following sections present the process variations and the disturbances that were created for controller evaluation.

3.2.1 Process Variations

The guiding performance of the developed adaptive control schemes were evaluated with different process parameters. Two main process parameters that affect the coefficients of the web lateral dynamic model are the web span parameter K and the longitudinal velocity of the web v. The parameter K is affected by the properties of the web material. Two different web materials with distinct physical characteristics were used; an optically opaque magnetic film like material (Figure 3.5) and an optically transparent polyethylene polymer web (Figure 3.6). The webs used were of different dimensions. The experiments were conducted with different web transport velocities and with different tensions in the web line.

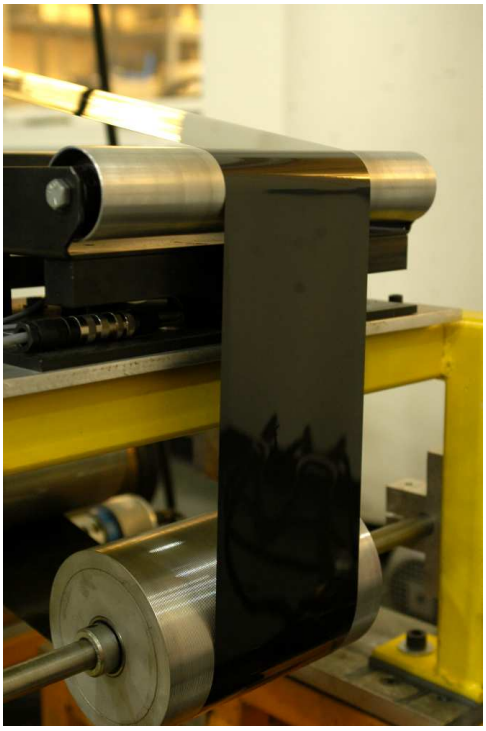

Figure 3.5: Opaque Web

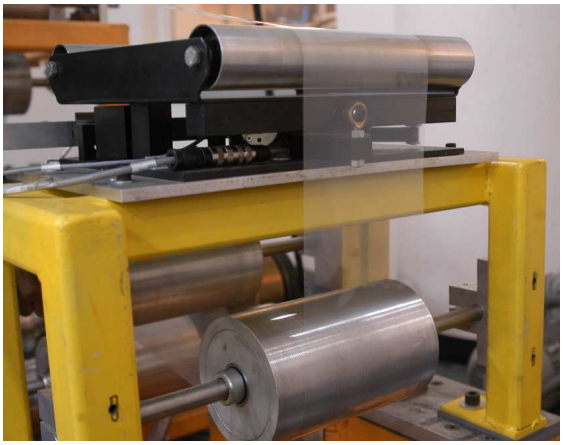

Figure 3.6: Transparent Web

Whenever the web material is changed from opaque to transparent web, the gain of the infrared sensor changes. The full scale voltage range changes from 0 - 6 V (opaque) to approximately 5 - 6 V (transparent) as illustrated in Figure 3.7. One of the drawbacks of the existing controllers is their inability to cope with sensor gain variations. Due to sensor gain variations the *guide-point* also changes. The guide-point is the physical reference position of the web inside the sensing window. Notice from Figure 3.7, the minimum voltage output from the sensor

is 5 V for a transparent web. This is due to the fact that the maximum signal attenuation with the transparent web is only 1 V.

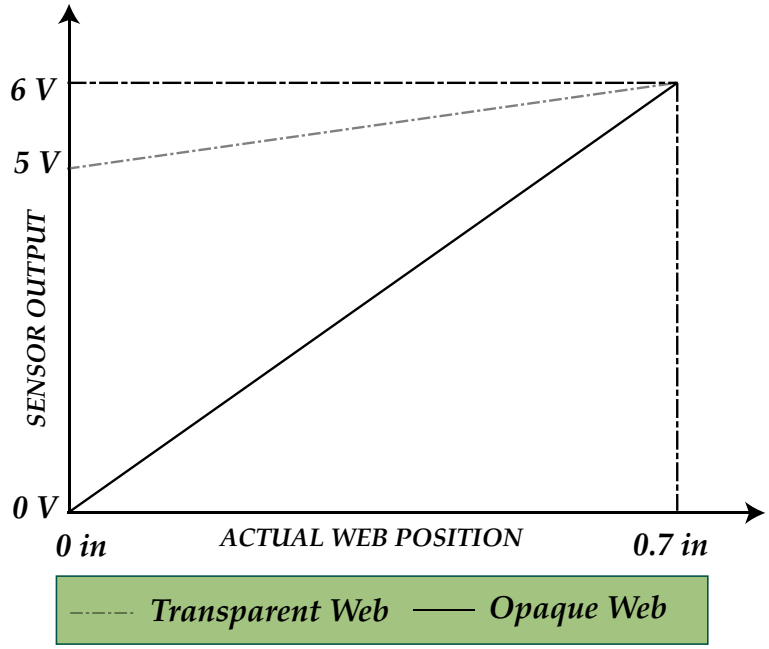

Figure 3.7: The Effect of Opacity on Sensor Gain for an Infrared Sensor

Experiments were conducted with the two web materials to evaluate the performance of the controllers for sensor gain variations. All the parameters of the controllers including the gain matrix and the filter parameters remained constant with both webs. Similarly the PI controller gains remained constant with both webs. Since the guide-point changes with the opacity of the web material, different guide-points were used with the two webs. For example, the guide-point for the opaque was 3 V while the guide-point with the transparent web was 5.4 V. Both guide-points correspond to the same physical position of the web. A new technique for automatic guide-point detection called offset-adaptation is presented in Appendix A.

3.2.2 Disturbances

Some common lateral disturbances in industrial lines are the result of misaligned rollers, telescoped unwind rolls, splicing, improper web edges, wrinkled web, etc. To mimic these disturbances in the experimental web platform, sinusoidal, step and pulse disturbances were created by the offset pivot guide and with changes to the web edge.

A common disturbance observed in an industrial web line is due to misaligned rollers.

It is seldom possible to have exact alignment for all the rollers in a web line. The angular misalignment of a series of rollers may produce lateral disturbances which can be periodic. Telescoping of rolls may produce periodic disturbances when unwound. In order to simulate a periodic disturbance, the offset pivot guide in the web line is used. The offset pivot guide, which is located before the Kamberoller in the web line (refer Figure 3.2), was made to follow a sinusoidal reference. As the sinusoid propagates, a periodic disturbance is created at the Kamberoller.

In order to characterize the transient response, the performance of the controller with a pulse disturbance was evaluated in the experiments. The pulse disturbance was generated by adding a small strip of web material about one feet long and 0.2 inches wide to the edge of the web. Since the strip is of constant length, the duration of the pulse is dependent on the transport velocity of the web. As the web transport velocity increases, the pulse width reduces and tends to an impulse.

In order to observe the performance characteristics such as the percentage overshoot and settling time, step-reference-change experiments were conducted. The guide-point or the lateral position reference was changed and the performance of the controllers for this change was evaluated.

The sensor signals from both the infrared sensor and the ultrasonic sensor were noisy. In industrial controllers, analog or digital signal conditioning are carried out on the raw signal to filter the noise. The error signal for the adaptive controllers were unfiltered in order to observe the performance of the controllers with noisy measurements.

3.3 Three Parameter Guide Adaptive Controller

The performance of the three parameter guide adaptive controller under different operating conditions and disturbances are presented in this section. The three parameter GAC requires an additional measurement, i.e., the lateral web velocity. While implementing the controller using the real-time hardware, the lateral velocity measurement was approximated by the finite difference of the lateral position.

Recall that the control law and the adaptive law for the three parameter GAC is given by

Control Law

$$u_p = \dot{\theta}^\top \phi + \theta^\top \omega$$

Adaptive Law

$$\dot{\theta} = -\Gamma e_1 \phi$$

where $\theta^\top = [L_1\ L_2\ P]$, $\omega^\top = [y_L\ \dot{y}_L\ r]$, $e_1 = y_L - y_m$ and $\phi = \dfrac{1}{s+p_0}\omega$.

3.3.1 Experiments with opaque web

Figures 3.8 to 3.11 show a representative sample of experimental results with the three parameter adaptive controller with the opaque web. In Figure 3.8 the top plot shows the sinusoidal disturbance observed by the Kamberoller when the guide is not actuated. The middle plot shows the performance of the PI controller. And the bottom plot shows the performance of the adaptive control scheme. A significant amount of the sinusoidal disturbance generated at the offset pivot guide has propagated to the Kamberoller. The three parameter guide adaptive controller is able to significantly attenuate the disturbance when compared to the PI controller. The guide-point for the two experiments were not the same. In subsequent experiments the guide-points for the adaptive scheme and the PI controller were matched to maintain consistency.

In Figure 3.9 the performance of the adaptive controller with sine disturbance is shown in the top plot, the control effort is shown in the middle plot, and the parameter estimates are shown in the bottom plot. The control effort generated is well within the actuator limits which is $\pm$ 10 V. Even though the parameters may not converge to their true values, it is important to observe the evolution of the estimated parameters. Notice that the last two parameters (L_2 and P) vary sinusoidally while the first parameter (L_1) slowly increases. It was experimentally observed that L_1 reaches a steady-state value while the other two parameters vary about zero sinusoidally. These observations are useful in improving the robustness properties of the adaptive controller. One such algorithm which can increase the robustness of the adaptive controller is *parameter projection*. For more information on parameter projection refer to page 565 in [18] and page 328 in [17].

The top plot in Figure 3.10 shows the performance of the PI controller with a pulse disturbance while the bottom plot shows the performance of the three parameter GAC. The adaptive controller is able to provide a faster response with better guiding performance. Similar performance is also seen at different transport speeds.

The performance of the adaptive controller for step-reference-change is shown in the Figure

3.11. The adaptive controller is capable of following the reference model accurately. The transient response characteristics of the guiding system is similar to the reference model transient response characteristics.

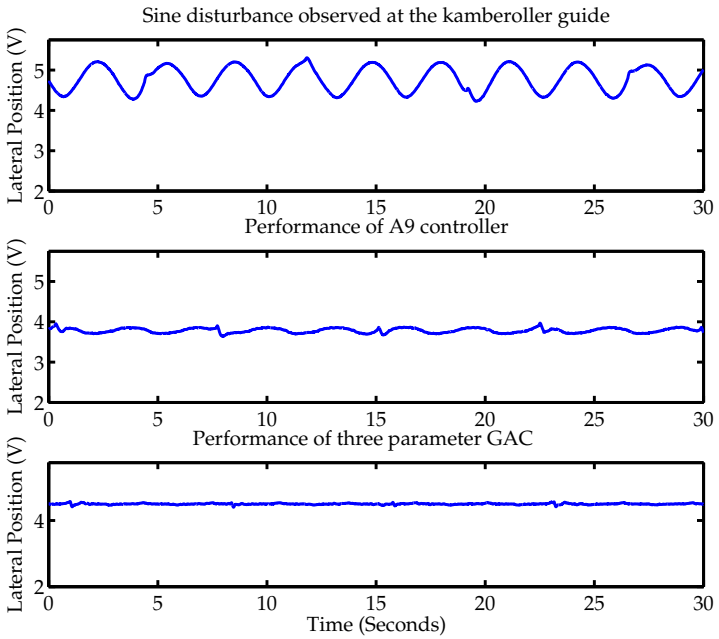

Figure 3.8: Performance Comparison: 3 Parameter, Sine Disturbance, 300 fpm, Opaque Web

3.3.2 Experiments with transparent web

Figures 3.12 to 3.14 show the performance of the three parameter guide adaptive controller with the transparent web. Figure 3.12 compares the performance of the PI controller and the adaptive controller. The top plot shows the disturbance observed at the Kamberoller when the guide is not actuated. The middle plot shows the performance of the PI controller. Comparing the top and the middle plots, no disturbance attenuation is observed. The PI controller is not able to cope with the sensor gain change. The adaptive controller on the other hand is able to attenuate the sinusoidal disturbance. Notice that a small streak is observed in all the three plots. This streak is observed when the joint passes the sensor window. The web opacity variation at the joint is significant to cause a sudden jump in the sensor output which causes the streak.

In Figure 3.13 the top plot shows the adaptive controller performance, the middle plot shows the control effort generated and the bottom plot shows the time history of the estimated parameters. Similar to the experiments with the opaque web, the last two parameters vary

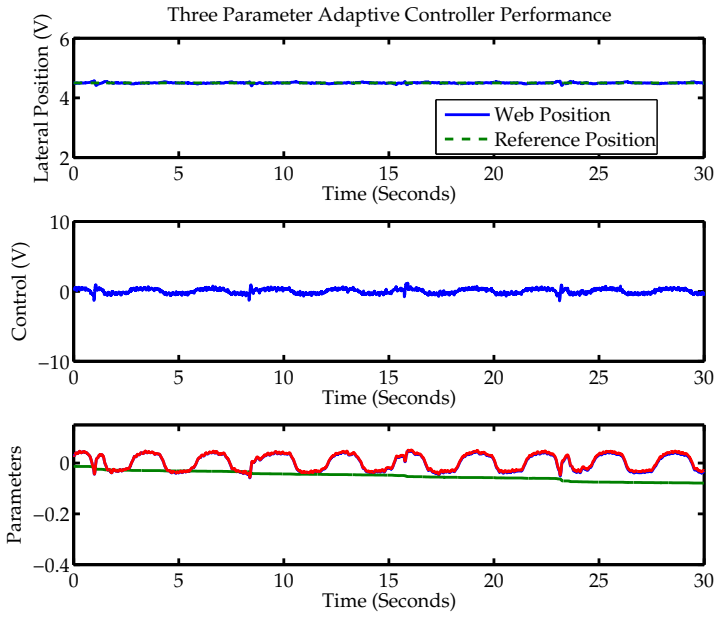

Figure 3.9: Adaptive Controller: 3-Parameter, Sine Disturbance, 300 fpm, Opaque Web

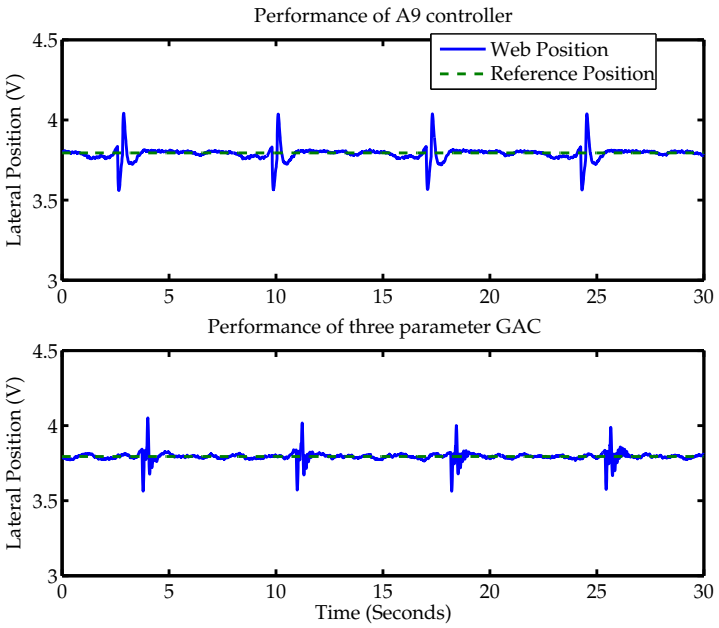

Figure 3.10: Performance Comparison: 3-Parameter, Pulse Disturbance, 300 fpm, Opaque Web

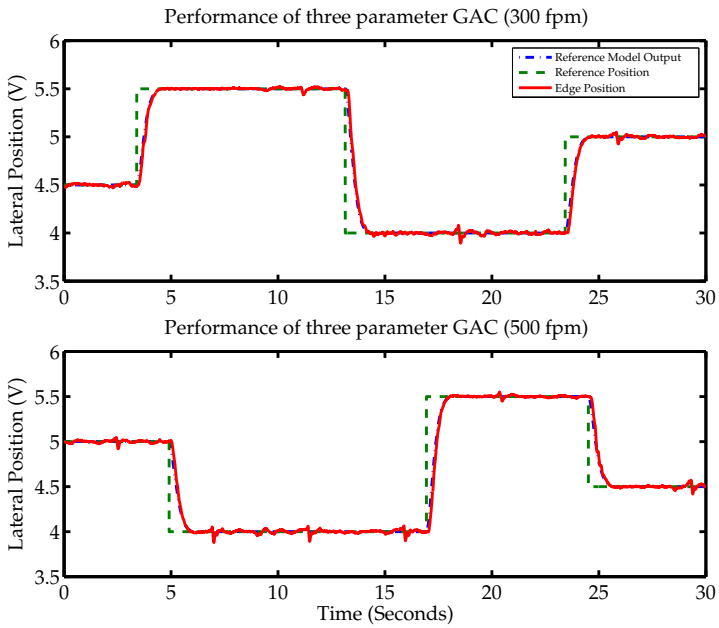

Figure 3.11: Adaptive Controller: 3-Parameter, 300 and 500 fpm, Step Reference Changes, Opaque Web

sinusoidally. The sinusoidal variation is centered around zero while the parameter L_1 slowly increases and reaches a steady state value.

In Figure 3.14 the performance of the PI controller and the adaptive controller for a pulse disturbance is shown. The top plot shows the performance of the PI controller while the bottom plot shows the performance of the adaptive controller. Even though the results look similar, a careful examination would reveal that the PI controller is non-responsive to the pulse disturbance. Due to the change in the sensor gain the PI controller is not capable of providing good guiding performance. In fact the response observed using the PI controller is exactly the same as the response when the Kamberoller is unactuated.

To clearly visualize the performance of the adaptive controller it is necessary to examine the typical response for a pulse disturbance. The pulse disturbance is formed by a series of two steps. The first step has a positive magnitude and the second has the same magnitude but a negative sign. As soon as the first step passes the sensor, an error in lateral position is created. The controller tries to regulate the position by bringing the web back to its reference position. Therefore as soon as the pulse disturbance enters the sensor a sudden dip is observed and the guide is actuated to bring the web back to its reference position. The second step creates a

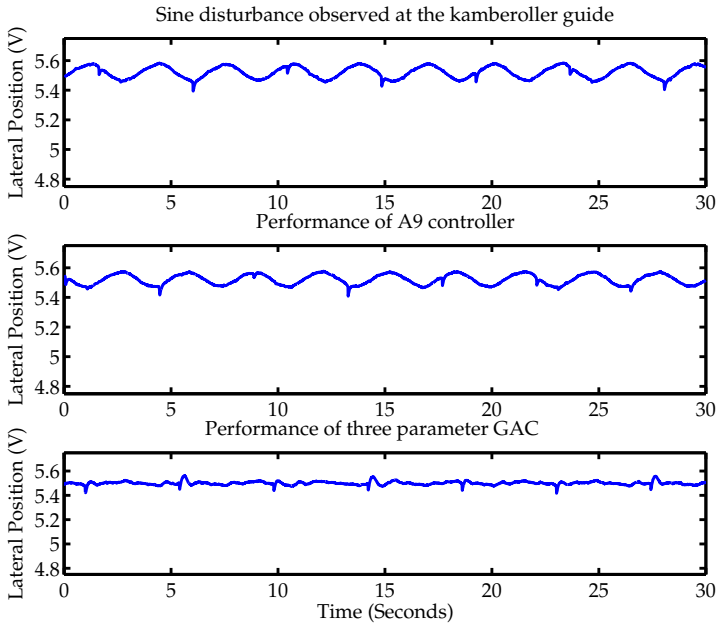

Figure 3.12: Performance Comparison: 3-Parameter, 500 fpm, Sine Disturbance, Transparent Web

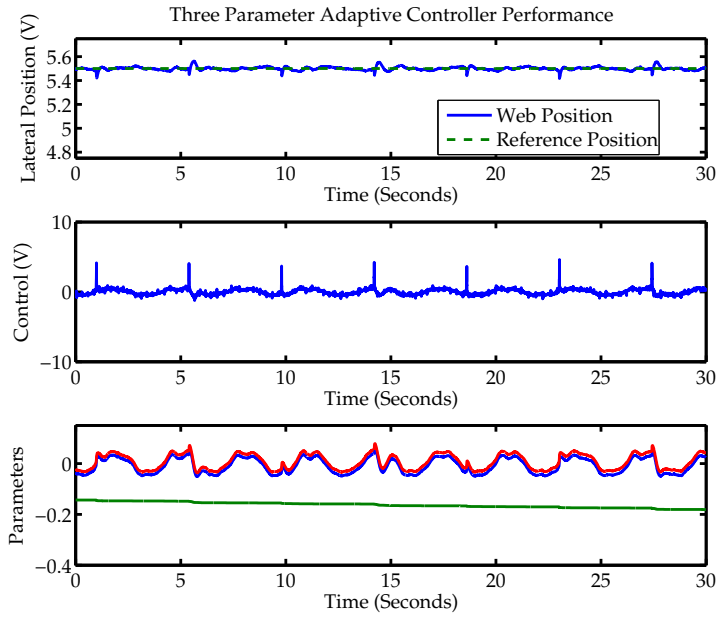

Figure 3.13: Adaptive Controller: 3-Parameters, 500fpm, Sine Disturbance, Transparent Web

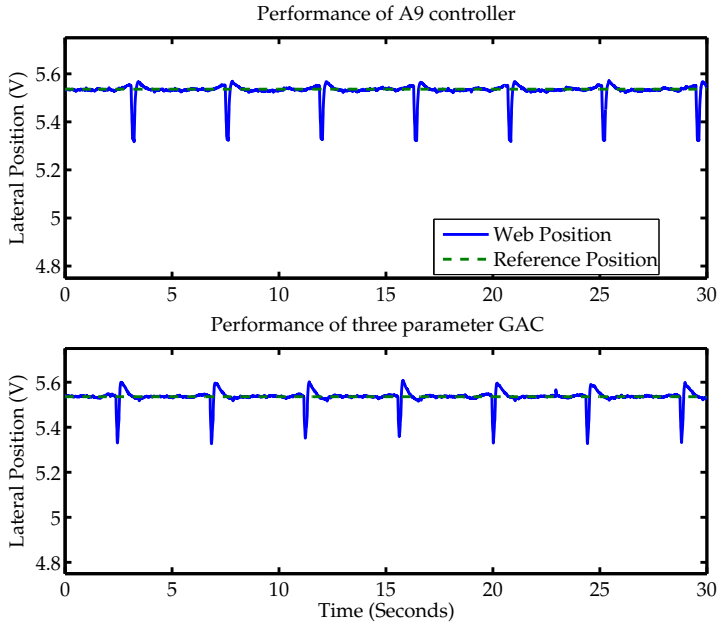

Figure 3.14: Performance Comparison: 3-Parameter, 500 fpm, Pulse Disturbance, Transparent Web

similar error but in the opposite direction, i.e., it creates a positive error. Therefore, when the pulse disturbance leaves the sensor, a spike is observed and the controller tries to regulate the web edge back to its reference. If the guide is unactuated the lateral position of the web is unchanged as the pulse passes the sensor. The complete pulse is observed in the sensor output.

Observing the plots in Figure 3.14, we can notice that the PI controller is unable to regulate the lateral position in the presence of a pulse disturbance. While the adaptive controller is capable of providing good guiding performance in the presence of the pulse disturbance. Additional experimental results for the three parameter adaptive controller are presented in Appendix D section D.1.

From the experimental results it is evident that the three parameter adaptive controller is suitable for web guiding. The controller is capable of compensating for the common disturbances and process variations. The adaptive algorithm is able to adapt to the process variations and is capable of providing the appropriate control effort to regulate the lateral edge position. The adaptive controller is also able to provide good guiding performance in the presence of measurement noise.

3.4 Four Parameter Guide Adaptive Controller

The same set of experiments with the two types of web materials were carried out with the four parameter guide adaptive controller. In this controller implementation only one measurement is needed, the lateral web position. The performance of the four parameter adaptive controller was similar to the three parameter adaptive controller. The adaptive controller provides good guiding perfromance in the presence of the common disturbances and process variations. A complete set of the experimental results is presented in Appendix D.2.

Figure 3.15 shows the guiding performance of the adaptive controller at different guide-points for a sinusoidal disturbance. Interestingly, at different guide-points the performance of the same controller is different. When the guide-point is around 3 V clear indication of the sinusoidal disturbance is observed. Additionally, the Kamberoller guide was positioned at different guide-points and the magnitude of the sinusoidal disturbance was observed. The magnitude was higher at 3 V compare to a guide-point of 5 V. This may be attributed to sensor nonlinearity. The slope of the sensor may not be linear along its entire window length.

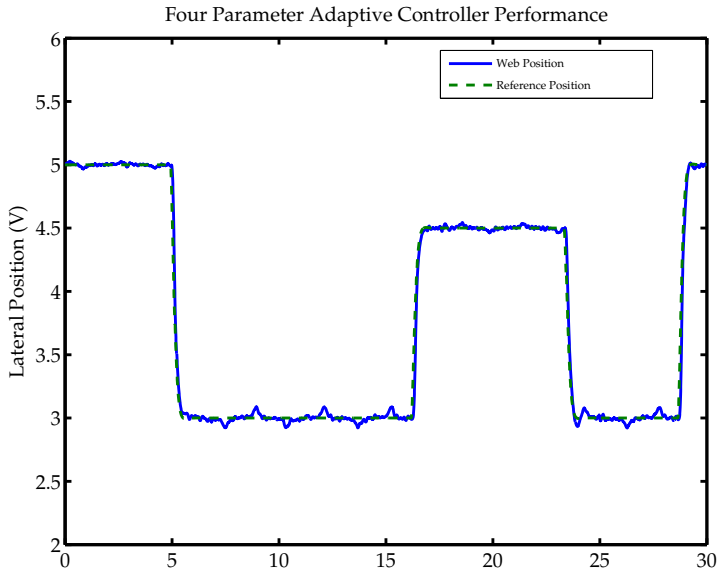

Figure 3.15: Adaptive Controller: 4-Paramater, 300 fpm, Sine Disturbance, Opaque Web

3.5 Guide Adaptive Controller

The guide adaptive controller (with eight parameters) has a similar implementation as the four parameter GAC: it is a SISO system with eight parameters. Figure 3.16 shows a representative sample of the performance of the eight parameter adaptive controller and the PI controller. A complete set of the experimental results is presented in Appendix D.3. The experimental results indicate that the controller provides good guiding perfromance in the presence of the common disturbances and process variations.

While implementing the adaptive controller on the real-time hardware no assumption on the values of the parameters were made. The initial values for all the parameters were set to zero. The plots in Figure 3.17 shows the performance of the adaptive controller as soon as it is started. The plots in Figure 3.18 show the performance of the adaptive controller after the adaptation is continued for a long time. Observe the bottom plots in Figures 3.17 and 3.18. The plots show the evolution of the estimated parameters. As the time progresses the estimated parameters reach steady state values. The guiding performance of the controller is unaffected during the evolution of the parameters. This clearly indicates that the variables associated with the system are bounded. Similar results were found with all the adaptive control schemes, and with all the disturbances that were discussed previously.

Recall that the control law and the adaptive law for an eight parameter adaptive controller is given by:

Control Law

$$u_p = \theta^\top \omega + \dot{\theta}^\top \phi \tag{3.1a}$$

$$\phi = \frac{1}{s + p_0}\omega \tag{3.1b}$$

$$\omega = [\omega_1^\top \ \omega_2^\top \ y_L \ r] \tag{3.1c}$$

$$\dot{\omega}_1 = F\omega_1 + g u_p, \qquad \omega_1(0) = 0 \tag{3.1d}$$

$$\dot{\omega}_2 = F\omega_2 + g y_p, \qquad \omega_2(0) = 0 \tag{3.1e}$$

Adaptive Law

$$\dot{\theta} = -\Gamma e_1 \phi, \quad e_1 = y_L - y_m \tag{3.2}$$

Notice that the control law not only depends on the actual value of the parameter vector θ, but also depends on the rate of change ($\dot{\theta}$) of the parameter vector. This is one of the reasons why the adaptive controller provides good guiding performance even when the parameters

does not reach a steady-state value. Once the parameters reach a steady-state value then the control will only be dependent on the parameter vector θ and the regressor vector ω.

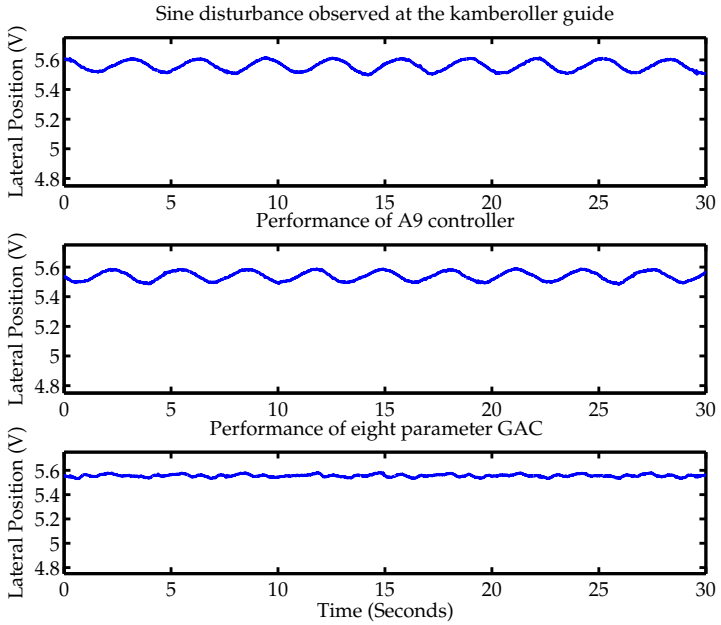

Figure 3.16: Performance Comparison: 8-Parameter, 300 fpm, Sine Disturbance, Transparent Web

3.6 Systematic Procedure for Adaptive Controller Implementation

The theory developed in the previous chapter does not impose any constraint on the value of design parameters. Most of the design parameters have to be positive in the case of scalars and positive definite in the case of matrices. When implementing the adaptive controller, it is important to consider the actuator rate constraints, the bandwidth of the actuator, etc., and the design parameters cannot be chosen arbitrarily. This section presents a systematic procedure for choosing various design parameters in the adaptive control schemes presented in the previous chapters.

1. Choose a suitable reference model: In a model reference adaptive controller design, the first step is to choose a reference model. The choice of the reference model is based on common performance characteristics like the settling time and the percentage overshoot.

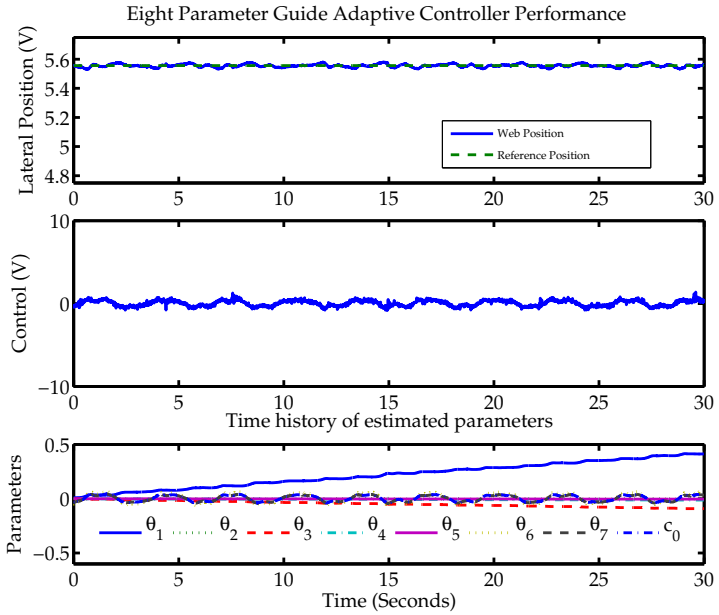

Figure 3.17: Adaptive Controller: 8-Parameter, 300 fpm, Sine Disturbance, Transparent Web

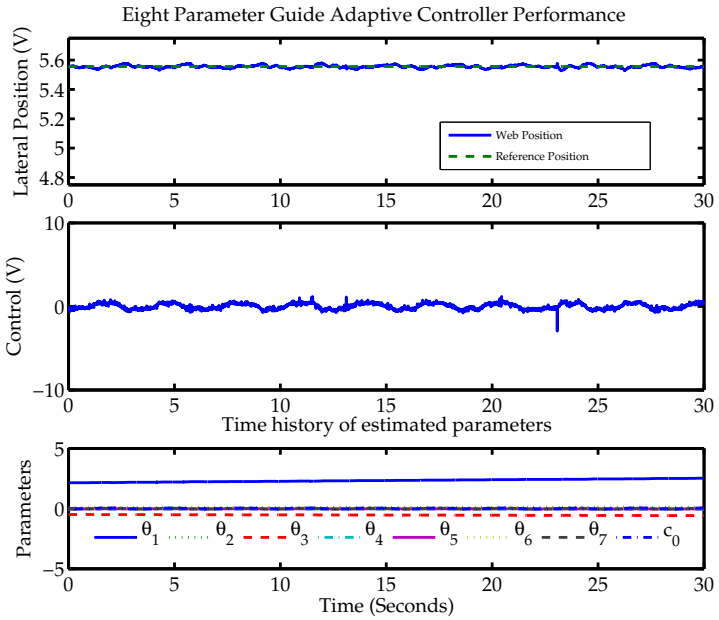

Figure 3.18: Adaptive Controller: 8-Parameter, 300 fpm, Sine Disturbance, Steady-State, Transparent Web

Choose a model which is well damped. The settling time can be chosen based on the performance requirements and the actuator rate constraints.

2. Perform computer simulations: Computer simulations are important because they provide a good starting point for practical implementation. Some basic information about the evolution of the estimated parameters, the gain matrices and the control effort generated can be obtained from the computer simulations.

3. Choose the polynomial $\Lambda(s)$: This polynomial is chosen only in the four parameter and the eight parameter case. A simple choice would be

$$\Lambda(s) = (s + a_0)^n \tag{3.3}$$

where $n = 1$ for the four parameter case and $n = 3$ for the eight parameter case. Notice that the polynomial $\Lambda(s)$ filters the control input signal u_p and the lateral position signal y_L (refer equations (2.53) and (2.78)). This polynomial can be chosen based on the bandwidth of the motor. The polynomial is chosen such that the filtered versions of u_p and y_L have the same bandwidth as the actuator.

4. Choose the parameter p_0: Based on the necessary and sufficient conditions derived in section C.2, p_0 is chosen according to the constraint $0 < p_0 < 2\zeta\omega_n$. This parameter sets the bandwidth of the filter $L(s)^{-1}$ which is defined as

$$L(s)^{-1} = \frac{1}{s + p_0}$$

Recall that this filter is added to satisfy the SPR condition. The filter $L(s)^{-1}$ filters all the regressor signals. Large values for the parameter p_0 will significantly attenuate the magnitude of the regressor vector. This may lead to poor guiding performance due to very slow adaptation. Figure 3.19 shows the performance of the adaptive controller with different values of the parameter p_0. The value of the parameter p_0 is decreased after 15 seconds and the guiding performance improves with the decrease. Small values for the parameter p_0 may help in quick adaptation but may also cause the system to be sensitive (equations (2.76b) and (3.1a)).

5. Choose gains based on simulation: The initial choice of the gains can be based on the simulation results. A positive definite diagonal matrix can be chosen as the gain matrix. As a starting point all the diagonal elements may have the same value.

6. Observe the evolution of parameters: Observing the way in which the parameters adapt is important in the design parameter selection process. The experiments with pulse disturbance help in selecting the adaptation gains. The control effort supplied to the actuator is directly related to the magnitude and the rate at which the estimated parameters vary ((2.76b) and (3.1a)). When the parameters vary quickly, the magnitude of the control effort tends to increase. This may not be desirable in most cases.

7. Set a bound on the parameter estimates: Simple bounding of parameters improves the robustness of the controller. In order to set a bound, knowledge of the estimated parameters is required. Conservative bounds can be set based on the experiments with pulse disturbance.

8. Observe the control effort: The control effort supplied to the actuator can help us in choosing some parameters such as p_0. If the parameter p_0 is very small, then the guiding system may be sensitive. This can be clearly observed even without a pulse disturbance experiment. When the parameter p_0 is small, noisy measurement may cause a *ringing effect* (the guide may vibrate with a very high frequency about the guide-point). The parameter p_0 may be increased to reduce this effect.

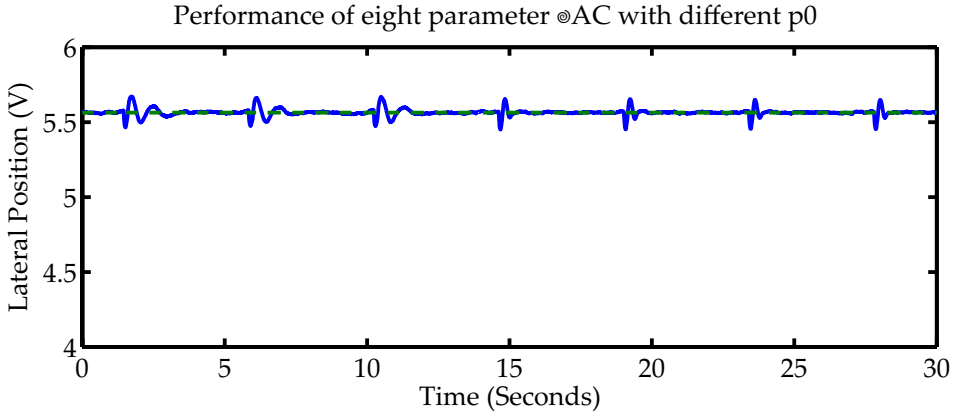

Figure 3.19: Performance Comparison: 8-Parameter, 500 fpm, Pulse Disturbance, Effect of p_0, Transparent Web

Based on the observations from the experiments some guidelines for practical implementation are as follows:

- The estimated parameters reach a steady-state value after some time. How fast the parameters reach the steady-state value is dependent on the adaptation gains. Once the steady-state value is reached there is no significant change in the estimated parameters. Therefore, adaptation can be stopped or the estimated parameters can be frozen. Once the parameters are frozen, the controller behaves like a fixed gain controller.

- When changes in the process parameters are made, adaptation can be continued. This can be implemented by continuously monitoring the error variable. Once the error variable exceeds a predefined limit, the adaptation of the parameters can be continued.

- Instead of stopping all the parameters, the estimated parameters can be selectively frozen. All the parameters except the last two parameters can be frozen.

- The decision on when to stop the adaptation can be made based on the adaptive law. Notice that the adaptive law is given by:

$$\dot{\theta} = -\Gamma e_1 \phi, \quad e_1 = y_L - y_m \tag{3.4}$$

  When the parameters reach a steady-state value, the vector $\dot{\theta}$ would be zero. Whenever all the elements of the vector $\dot{\theta}$ are close to zero, then the adaptation can be stopped.

Chapter 4

Friction Compensation in Web Guides

Friction is a type of phenomena that is found in almost all servo-mechanisms. Friction is inevitable in mechanisms with relative motion between parts which are in contact with each other. Although friction is essential in some mechanisms, such as braking, it is usually not desired in high precision motion control systems. Typically friction may cause steady-state errors in position regulation and tracking and may lead to limit cycle behavior. Hence it is important to consider the effect of friction when designing and implementing a closed-loop control system. In this chapter we consider static friction models and analyze compensation techniques which are specific to web guides.

4.1 Static Models

Early modeling of friction involved static models of friction which are simply a function of relative velocity between contacting surfaces. Static friction takes into account only a few properties of friction with the main idea being that the friction force opposes motion and the magnitude of friction is independent of the surface area of contact. A brief discussion of some well known static friction models are given below.

Coulomb investigated Da Vinci's friction model and proposed the model in 1785 [26]. Coulomb friction in dynamic systems is modeled as a piecewise continuous function which is positive for positive velocities and negative for negative velocities. Coulomb friction is given by

$$F = F_c \text{sgn}(v) \tag{4.1}$$

where F is the friction force, F_c is the Coulomb friction coefficient, sgn$(.)$ denotes the sign function, and v is the relative velocity between contacting surfaces.

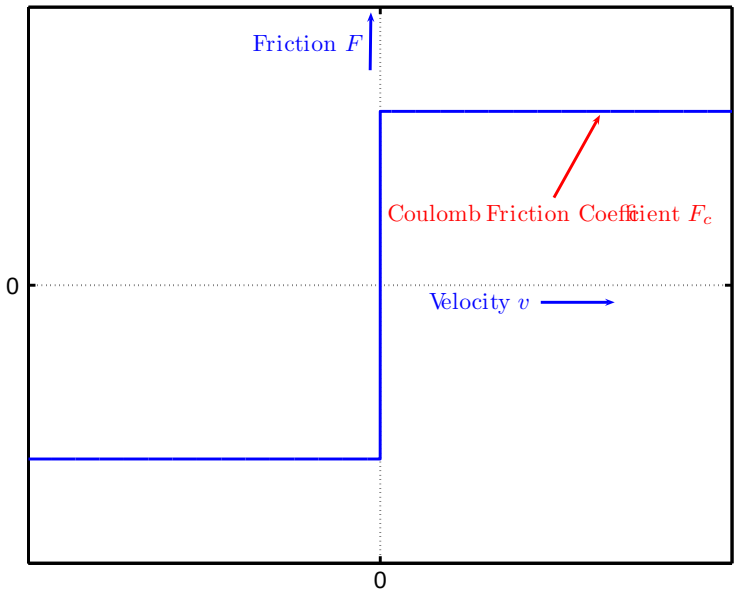

Figure 4.1: Static Friction Model with Coulomb Friction Effect

Morin (1833) [26] introduced the idea of static friction in which the friction forces opposes the direction of motion when the relative velocity is zero. The equation describing the model is given by

$$F = F_s \text{sgn}(F_t) \tag{4.2}$$

where F_s is the static friction (stiction) coefficient and F_t is the applied tangential force.

Reynolds (1886) introduced the following viscous friction model for fluids where the friction force is a linear function of the relative velocity:

$$F = F_v v \tag{4.3}$$

where F_v is viscous friction coefficient.

Common models of static friction considered in engineering analyses are a combination of the above basic models. Coulomb + viscous friction, as the name suggests, is a combination of Coulomb and viscous friction models and is given by

$$F = F_c \text{sgn}(v) + F_v v \tag{4.4}$$

The viscous friction is included to consider the influence of lubrication between contacting surfaces.

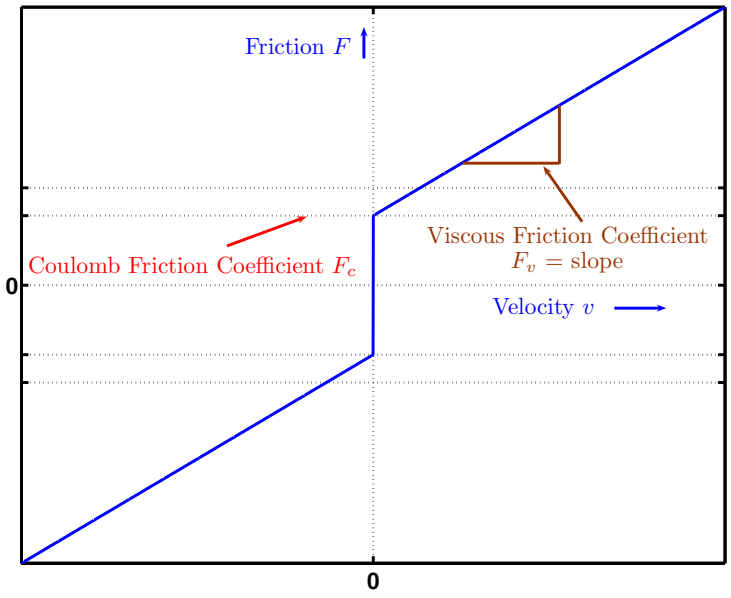

Figure 4.2: Static Friction Model with Coulomb and Viscous Effects

Further, if static friction is included to consider the force required to initiate the motion, the model that is generally used in engineering analyses is given by

$$F = \begin{cases} F_c \text{sgn}(v) + F_v v & \text{for } v \neq 0 \\ F_s \text{sgn}(F_t) & \text{for } v = 0 \end{cases} \tag{4.5}$$

Stribeck in 1902 observed a different phenomenon at low velocities. He observed that the friction decreased as velocities increased for low velocities. The velocity decrease was continuous, contrary to the model given by a combination of Coulomb, viscous and static friction. This phenomenon is called the Stribeck effect.

The model that includes Stribeck effect in place of stiction is given by

$$F = F_v v + F_c \text{sgn}(v) + (F_s - F_c) e^{(\frac{v}{v_s})^2} \text{sgn}(v) \tag{4.6}$$

where v_s is the Stribeck velocity constant. Figure 4.4 shows the model that includes the Stribeck effect.

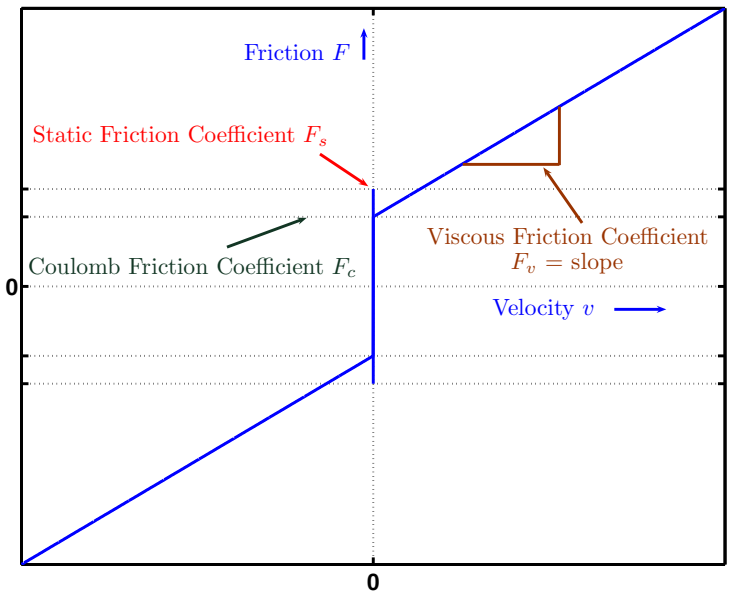

Figure 4.3: Static Friction Model with Coulomb, Viscous and Stiction Effects

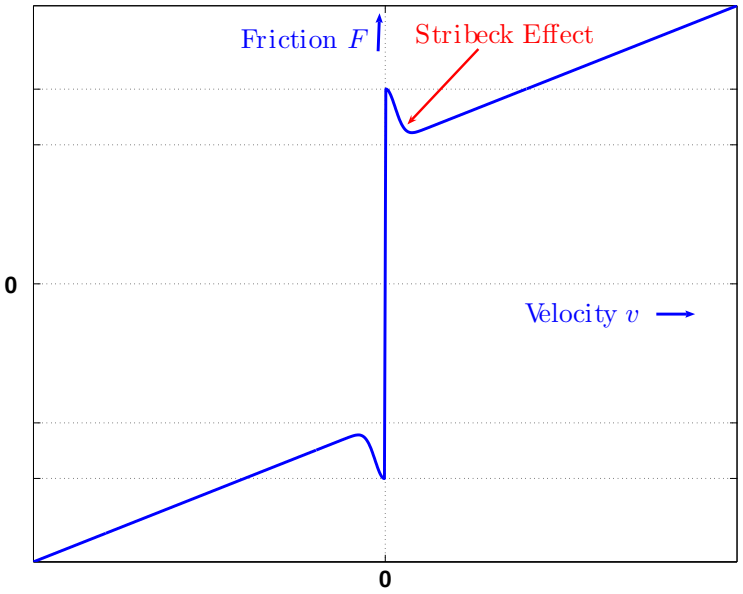

Figure 4.4: Static Friction Model with Stribeck Effect

4.2 Friction Compensation Based on Static Models

To compensate for stiction, in some applications, it is typical to add high frequency, low amplitude signals (dither) to the control signal. The main drawback of using a dither signal is the need for accurate prediction of stiction coefficient, and further the dither signal does not compensate for viscous and Stribeck effects.

For nonlinear systems with friction, it is common to use control laws that employ feedback linearization to achieve desired closed-loop characteristics. With an accurate friction model and an estimate of its coefficients, it is common to compensate for friction by adding the estimated friction to the control signal. The friction force is estimated using velocity feedback and friction coefficient estimates, and the estimated friction force $\hat{F}$ is added to the control signal. The friction coefficients are generally estimated by using least mean-square (LMS) estimation or by using recursive least-square (RLS) algorithms.

Friedland and Park [27] proposed a simple estimator for Coulomb friction coefficient, which is an adaptive estimator with asymptotic convergence. This estimate of Coulomb friction coefficient is used to estimate the friction force and is added to the control signal to compensate for friction. A simple block diagram of such a compensation is given in Figure 4.5. But this method imposes the constraint that the velocity should be bounded away from zero.

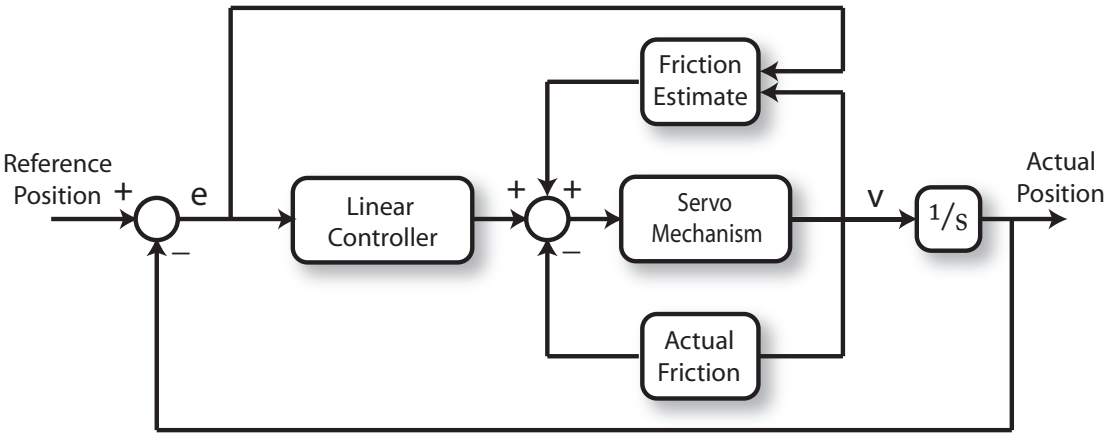

Figure 4.5: Friction Compensation using Estimated Friction

Gilbart and Winston [28] used an adaptive compensation technique for optical tracking telescopes based on the Coulomb friction model using Lyapunov based model reference adaptive controller. Zhu [29] implemented adaptive static and dynamic friction compensation techniques on a planar robot manipulator. Extensive experiments were conducted to validate the

proposed adaptive controllers; it was shown that the adaptive controllers with friction compensation had superior tracking error performance when compared to the adaptive controllers without friction compensation.

In all of the above mentioned methods, a reference velocity trajectory is tracked with friction compensation or a position reference (assumed to be differentiable twice) is tracked. Most of the existing friction compensation methods does not deal with position regulation. Adaptive friction compensation techniques for position regulation which are applicable for web guiding is discussed in the subsequent sections.

4.2.1 Friction Compensation for Web Guides Based on a Static Model

A simple compensation technique that is used frequently is based on feedback linearization in which the control input compensates for friction by directly adding the friction torque to it. The friction can be identified off-line based on a friction model. Friction torque is added to the control based on the identified friction parameters.

Consider a static friction model based on Coulomb and viscous friction as

$$F = F_c \text{sgn}(\dot{\theta}) + F_v \dot{\theta} \tag{4.7}$$

The dynamics of a DC motor actuator for a web guide is given by

$$J\ddot{\theta} + F = T \tag{4.8a}$$

$$L\frac{di}{dt} + Ri = U_p - K_e\dot{\theta} \tag{4.8b}$$

where T is the torque to the motor, J is the rotor inertia, L is the inductance of the coil, R is the resistance of the coil, U_p is the voltage input to the motor, i is the motor current and K_e is the back *e.m.f* (electro-motive force) constant. Neglecting electrical characteristics, substituting $T = K_t i$, and taking the Laplace transform we get

$$\Theta(s) = \frac{K_m}{s(s+a_m)}U_p(s) - \frac{1/J}{s(s+a_m)}F(s)$$

where $K_m = \dfrac{K_t}{JR}$ and $a_m = \dfrac{K_t K_e}{JR}$. If viscous friction is considered then the system reduces to

$$\frac{\Theta(s)}{U_p(s)} = \frac{K_m}{s(s+a_m+K_j F_v)} \tag{4.9}$$

where $K_j = \frac{1}{J}$. Clearly the system dynamics changes with the type of friction model considered. Let us first consider friction given by equation (4.7). A straight-forward compensation

would involve adding friction estimate $\hat{F}$ to the control torque and can be given as

$$T = T_{lin} + \hat{F} \tag{4.10}$$

where T_{lin} is the control input for the linear system when friction is neglected. With a perfect estimation of $\hat{F}$ the nonlinear friction term is compensated and hence linear control law can be obtained using well established control techniques. An offline estimate of $\hat{F}$ can be given by

$$\hat{F} = \hat{F}_c \text{sgn}(\dot{\theta}) + \hat{F}_v \dot{\theta} \tag{4.11}$$

where $\hat{F}_c$ and $\hat{F}_v$ are estimates of Coulomb and viscous friction which are identified offline using common identification techniques. The following section details the procedure for identifying the friction parameters for a web guide mechanism.

4.2.2 Friction Parameters Identification

4.2.2.1 Motor Parameters

Parameters	Value	Units
Max. Operating Speed	6000	rpm
Torque Sensitivity (K_t)	7.54	oz-in/amp
Back EMF constant (K_e)	5.58	V/Krpm
D.C. Resistance (R)	0.977	Ohms
Inductance L	1.5	mH
Rotor Inertia	0.0045	oz-in-sec^2
Tachometer Voltage Sensitivity	14.2	(V/Krpm)

Table 4.1: Kamberoller Guide Motor Parameters

4.2.2.2 Identification of Coulomb and Viscous Friction Coefficients

The friction parameters can be identified using common estimation techniques such as a Least Square Estimation. To avoid the Stribeck effect, the identification is carried out at velocities greater than the Stribeck velocity. The dynamics of an inertia load with a static friction model is given by

$$J\ddot{\theta} = T - F_c \text{sgn}(\dot{\theta}) - F_v \dot{\theta} \tag{4.12}$$

which can be parametrized as

$$T = \begin{bmatrix} \ddot{\theta} & \dot{\theta} & \text{sgn}(\dot{\theta}) \end{bmatrix} \begin{bmatrix} J \\ F_v \\ F_c \end{bmatrix} = \varphi_u^\top \phi \tag{4.13}$$

Applying a low-pass filter ($F(s) = \frac{1}{\tau s+1}$) to each signal in equation (4.13) we get

$$y = \varphi^\top \phi \tag{4.14}$$

where y is the filtered version torque T and φ is the filtered version of the regressor φ_u.

Hence from the *normal equation* for least square estimation, the vector ϕ is obtained as

$$\phi = (\psi\psi^\top)^{-1}\psi Y \tag{4.15}$$

where

$$\psi = [\varphi(1), \ldots, \varphi(n)], \quad Y = [y(1), \ldots, y(n)]^\top \tag{4.16}$$

and n is the total number of data points.

Hence the estimates of F_v and F_c can be obtained from input-output data set of the web guide. Sinusoidal inputs were given to the guide at various amplitude and frequency. Using the least-square-estimator the parameters F_v and F_c were estimated and they were found to be $F_v = 0.0167705$ N-m-s/rad and $F_c = 0.030709$ N-m. The filter was assumed to have the following transfer function $\frac{1}{0.001\tau s+1}$ and the Stribeck velocity was assumed to be 0.1 rad/sec. Table 4.2 shows the estimates for different input-output pairs. A representative sample of the experimental results is given in Figure 4.6. Figure 4.6 shows the tachometer output for a sinusoidal input voltage to the guide motor. The input voltage was applied with a frequency of 2π rad/sec and amplitudes of 4.8 and 12 volts. In Figure 4.7 the friction effect when the velocity crosses zero is clearly observed.

4.2.2.3 Stiction Coefficient

Stiction can be identified by finding the torque at which the guide starts to move, when a ramp input is given to the guide. The slope of the ramp is small, i.e., the control input is incremented in small steps and the torque at which the guide starts to move is the stiction coefficient F_s. As the guide starts to move the motor velocity is very small, therefore the current in the motor coil can be approximated as $\frac{U_p}{R}$ and hence $Fs = K_t\frac{U_p}{R}$. F_s was found to be 0.325968 N-m. A representative sample of the experimental results is shown in Figure 4.8.

Exp No.	Amplitude (Volts)	Frequency (rad/sec)	F_v (Nm/rad/s)	F_c (Nm)
1	$4.8, 12$	2π	0.016259	0.032497
2	7.2	2π	0.016459	0.030559
3	4.8	4π	0.016595	0.028851
4	4.8	4π	0.016585	0.029035
5	6	2π	0.016742	0.031159
6	3	4π	0.017302	0.031879
7	3	2.75π	0.017451	0.030985

Table 4.2: Coulomb and Viscous Friction Estimates

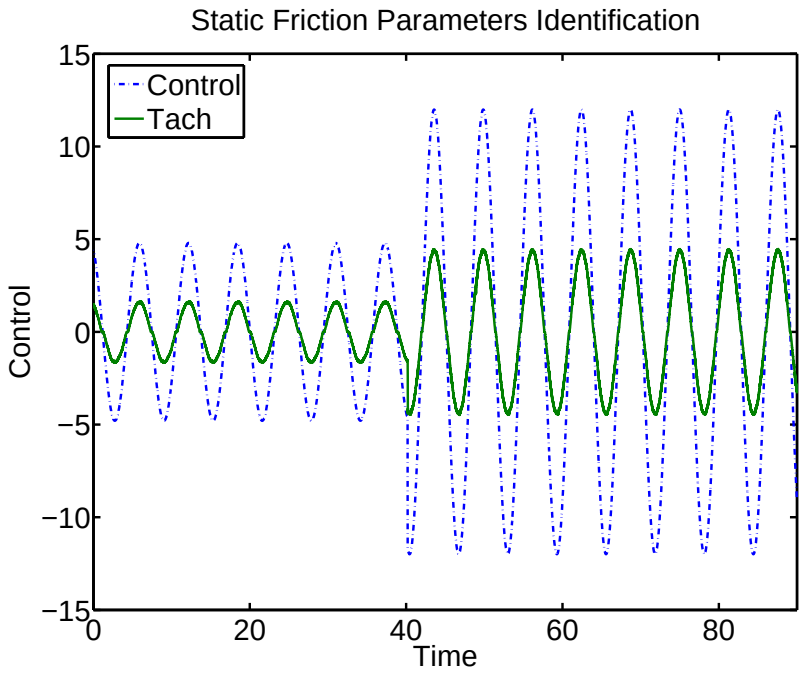

Figure 4.6: Velocity Output for a Sinusoidal Input Voltage

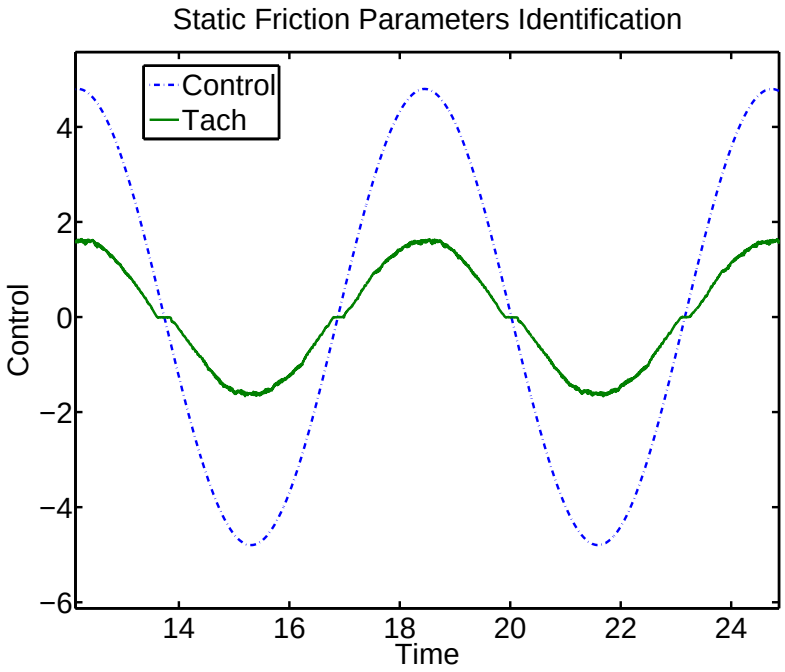

Figure 4.7: Zero Velocity Crossing Friction Effect

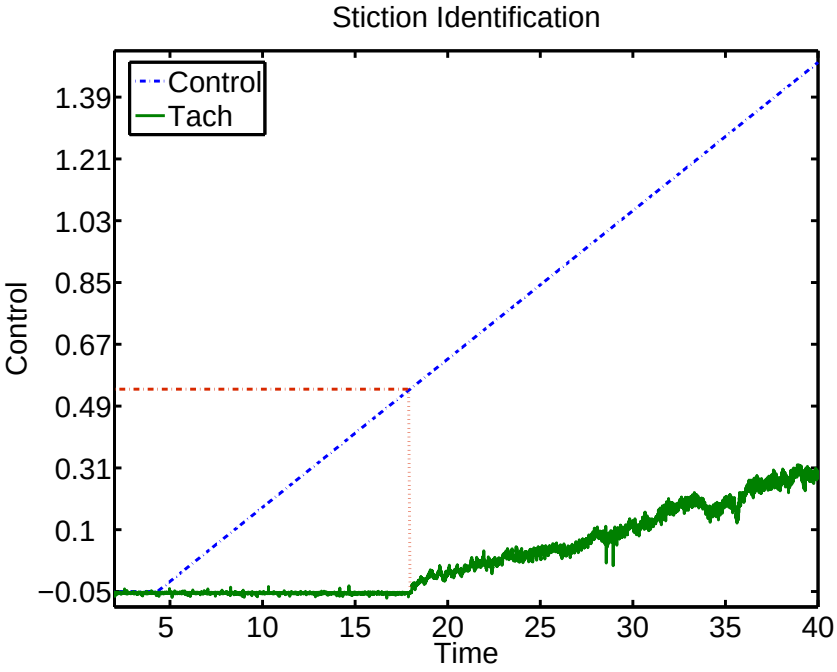

Figure 4.8: Estimation of Stiction Using a Ramp Input

4.2.2.4 Stribeck Velocity

The static friction model with the Stribeck effect is given by

$$F = F_v\dot{\theta} + F_c\text{sgn}(\dot{\theta}) + (F_s - F_c)e^{(\frac{\dot{\theta}}{v_s})^2}\text{sgn}(\dot{\theta}) \tag{4.17}$$

where v_s is the Stribeck velocity. When the guide moves at sufficiently low velocities, friction is given by

$$F = F_c\text{sgn}(\dot{\theta}) + (F_s - F_c)e^{(\frac{\dot{\theta}}{v_s})^2}\text{sgn}(\dot{\theta}) \tag{4.18}$$

and substituting F in equation (4.8a) we get

$$J\ddot{\theta} = T - F_c\text{sgn}(\dot{\theta}) - (F_s - F_c)e^{\left(\frac{\dot{\theta}}{v_s}\right)^2} \tag{4.19}$$

Equation (4.19) can be simplified as

$$\left[(T - J\ddot{(\theta)})\text{sgn}(\dot{\theta}) - F_c\right] = (F_s - F_c)e^{\left(\frac{\dot{\theta}}{v_s}\right)^2} \tag{4.20}$$

and further as

$$\dot{\theta}^2 = \ln\left(\frac{F_s - F_c}{[T - J\ddot{\theta}]\text{sgn}(\dot{\theta}) - F_c}\right)v_s^2 \tag{4.21}$$

Therefore, from the previously estimated values of F_c and F_v and from the response of the system for a given sinusoidal input, Stribeck velocity is estimated using

$$y = \varphi^\top\phi \tag{4.22}$$

where

$$y = \dot{\theta}^2, \quad \phi = v_s^2, \quad \varphi = \ln\gamma \tag{4.23}$$

Only values of $\gamma \geq 1$ yield real solutions and hence only those values are considered for estimation. The representative sample of experimental results is shown in Figure 4.9. Stribeck velocity was observed to be negligible for the web guide.

It is not possible to identify all the friction parameters each time and compensate by adding the extra control input. It is known that friction parameters vary based on normal forces, change in temperature and vary over time due to change in lubricating conditions. Hence, an adaptive friction compensator is required to effectively compensate for friction. The following section will discuss an adaptive scheme to compensate for friction in web guides. The identification carried out in this section is used as a basis for validating the results from the adaptive controller.

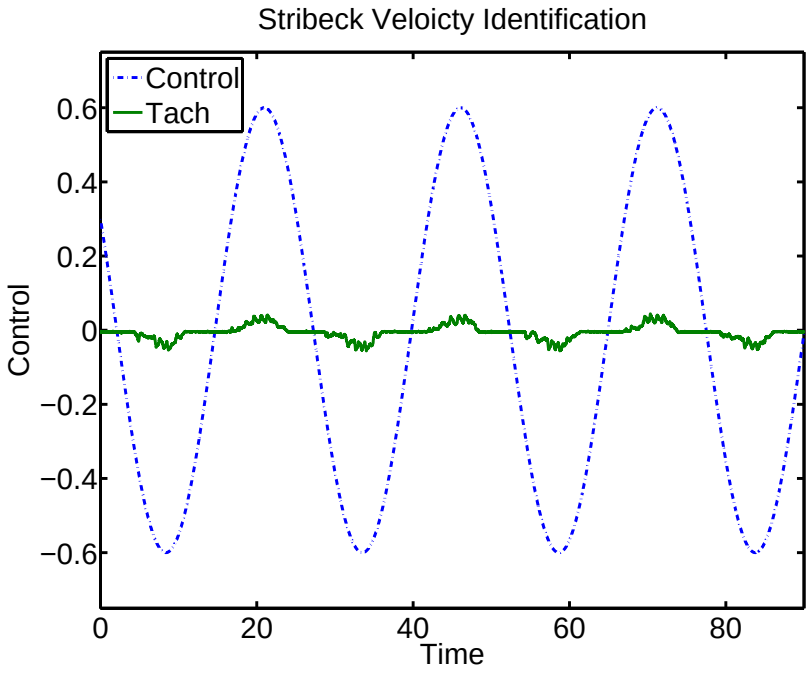

Figure 4.9: Stribeck Velocity Identification

4.3 Adaptive Static Friction Compensation for Web Guides

Offline friction parameter identification and compensation is not suitable for web guiding applications. Friction parameters are known to change and hence an adaptive friction compensation is suitable. In this section, static friction model with Coulomb and viscous effects is considered; Coulomb and viscous friction coefficients are unknown. An adaptive static friction compensation technique is developed in this section. The dynamics of the system with friction

is given by

$$J\ddot{\theta} + C\dot{\theta} + F = \alpha u, \quad \text{where } \alpha = \frac{K_t}{R} \tag{4.24a}$$

$$\frac{J}{\alpha}\ddot{\theta} + \frac{C}{\alpha}\dot{\theta} + \frac{1}{\alpha}F = u \tag{4.24b}$$

$$\beta_1\ddot{\theta} + \beta_2\dot{\theta} + \frac{1}{\alpha}[F_v\dot{\theta} + F_c\text{sgn}(\dot{\theta})] = u \tag{4.24c}$$

$$\beta_1\ddot{\theta} + \beta_2\dot{\theta} + \frac{1}{\alpha}F_v\dot{\theta} + \frac{1}{\alpha}F_c\text{sgn}(\dot{\theta}) = u \tag{4.24d}$$

$$\beta_1\ddot{\theta} + \underbrace{(\beta_2 + \frac{1}{\alpha}F_v)}\dot{\theta} + \frac{1}{\alpha}F_c\text{sgn}(\dot{\theta}) = u \tag{4.24e}$$

$$\beta_1\ddot{\theta} + \beta_2\dot{\theta} + \beta_3\text{sgn}\dot{\theta} = u \tag{4.24f}$$

$$\text{where } \beta_2 = \beta_2 + \frac{1}{\alpha}F_v \text{ and } \beta_3 = \frac{1}{\alpha}F_c$$

Representing the system in equation (4.24f) in the state space form with state variables $x_1 = \theta$ and $x_2 = \beta_1\dot{\theta}$ yields,

$$\begin{bmatrix} \dot{x}_1 \\ \dot{x}_2 \end{bmatrix} = \begin{bmatrix} 0 & \alpha_1 \\ 0 & -\alpha_2 \end{bmatrix} \begin{bmatrix} x_1 \\ x_2 \end{bmatrix} + \begin{bmatrix} 0 \\ 1 \end{bmatrix} u - \begin{bmatrix} 0 \\ \alpha_3\text{sgn}(x_2) \end{bmatrix} \tag{4.25}$$

where

$$\alpha_1 = \frac{1}{\beta_1}, \quad \alpha_2 = \frac{\beta_2}{\beta_1}, \quad \alpha_3 = \beta_3$$

The equilibrium for equation (4.25) is $x_1 = 0$ and $x_2 = 0$. If the coefficients α_1, α_2 and α_3 are known, then one can choose the control law to be

$$u = \alpha_3\text{sgn}(x_2) - \alpha_1 x_1 \tag{4.27}$$

Then the closed loop system is given by

$$\begin{bmatrix} \dot{x}_1 \\ \dot{x}_2 \end{bmatrix} = \begin{bmatrix} 0 & \alpha_1 \\ -\alpha_1 & -\alpha_2 \end{bmatrix} \begin{bmatrix} x_1 \\ x_2 \end{bmatrix} \tag{4.28}$$

Consider a Lyapunov function candidate which is a function of states as

$$V(X) = \frac{1}{2}X^\top X, \qquad X = \begin{bmatrix} x_1 \\ x_2 \end{bmatrix} \tag{4.29}$$

Taking the time derivative of the Lyapunov function candidate along the trajectories of equation (4.28) we get

$$\dot{V}(X) = \dot{X}^\top X = \begin{bmatrix} \dot{x_1} & \dot{x_2} \end{bmatrix} \begin{bmatrix} x_1 \\ x_2 \end{bmatrix} \tag{4.30a}$$

$$= \alpha_1 x_1 x_2 - \alpha_1 x_1 x_2 - \alpha_2 x_2^2 \tag{4.30b}$$

$$= -\alpha_2 x_2^2 \tag{4.30c}$$

$$\Rightarrow \dot{V}(X) \leq 0 \tag{4.30d}$$

Since α_1, α_2 and α_3 are unknown, let us consider the control to be

$$u = -\hat{\alpha_1} x_1 + \hat{\alpha_3} \text{sgn}(x_2) \tag{4.31}$$

Only two unknowns are needed for control and hence the parameters, their estimates, estimation error are defined as follows.

$$\Theta = \begin{bmatrix} \alpha_1 \\ \alpha_3 \end{bmatrix}, \quad \hat{\Theta} = \begin{bmatrix} \hat{\alpha}_1 \\ \hat{\alpha}_3 \end{bmatrix}, \quad \tilde{\Theta} = \begin{bmatrix} \tilde{\alpha}_1 \\ \tilde{\alpha}_3 \end{bmatrix} = \begin{bmatrix} \alpha_1 - \hat{\alpha}_1 \\ \alpha_3 - \hat{\alpha}_3 \end{bmatrix} \text{ and } \dot{\tilde{\Theta}} = \begin{bmatrix} -\dot{\hat{\alpha}}_1 \\ -\dot{\hat{\alpha}}_3 \end{bmatrix} \tag{4.32}$$

The closed loop control system is given by

$$\begin{bmatrix} \dot{x}_1 \\ \dot{x}_2 \end{bmatrix} = \begin{bmatrix} 0 & \alpha_1 \\ -\hat{\alpha}_1 & -\alpha_2 \end{bmatrix} \begin{bmatrix} x_1 \\ x_2 \end{bmatrix} - \begin{bmatrix} 0 \\ \alpha_3 - \hat{\alpha}_3 \end{bmatrix} \text{sgn}(x_2) \tag{4.33}$$

i.e.,

$$\dot{x}_1 = \alpha_1 x_2 \tag{4.34a}$$

$$\dot{x}_2 = -\alpha_2 x_2 - \hat{\alpha}_1 x_1 - \tilde{\alpha}_3 \text{sgn}(x_2) \tag{4.34b}$$

Consider a Lyapunov function candidate

$$V(X, \tilde{\Theta}) = \frac{1}{2} X^\top X + \frac{1}{2\gamma} \tilde{\Theta}^\top \tilde{\Theta}, \quad \gamma > 0 \tag{4.35}$$

The time derivative of V along the trajectories of equation (4.33) is given by

$$\dot{V}(X,\tilde{\Theta}) = \dot{X}^\top X + \frac{1}{\gamma}\dot{\tilde{\Theta}}^\top\tilde{\Theta} \tag{4.36a}$$

$$= \begin{bmatrix} \dot{x}_1 & \dot{x}_2 \end{bmatrix}\begin{bmatrix} x_1 \\ x_2 \end{bmatrix} + \frac{1}{\gamma}\dot{\tilde{\Theta}}^\top\tilde{\Theta} \tag{4.36b}$$

$$= \alpha_1 x_1 x_2 - \hat{\alpha}_1 x_1 x_2 - \alpha_2 x_2^2 - \tilde{\alpha}_3 x_2 \text{sgn}(x_2) + \frac{1}{\gamma}\dot{\tilde{\Theta}}^\top\tilde{\Theta} \tag{4.36c}$$

$$= -\alpha_2 x_2^2 + \underbrace{(\alpha_1 - \hat{\alpha}_1)}\, x_1 x_2 - \tilde{\alpha}_3 x_2 \text{sgn}(x_2) + \frac{1}{\gamma}\dot{\tilde{\Theta}}^\top\tilde{\Theta} \tag{4.36d}$$

$$= -\alpha_2 x_2^2 + \tilde{\alpha}_1 x_1 x_2 - \tilde{\alpha}_3 x_2 \text{sgn}(x_2) + \frac{1}{\gamma}\dot{\tilde{\Theta}}^\top\tilde{\Theta} \tag{4.36e}$$

$$= -\alpha_2 x_2^2 + \begin{bmatrix} x_1 x_2 & -x_2 \text{sgn}(x_2) \end{bmatrix}\begin{bmatrix} \tilde{\alpha}_1 \\ \tilde{\alpha}_3 \end{bmatrix} + \frac{1}{\gamma}\dot{\tilde{\Theta}}^\top\tilde{\Theta} \tag{4.36f}$$

$$= -\alpha_2 x_2^2 + \begin{bmatrix} x_1 x_2 & -x_2 \text{sgn}(x_2) \end{bmatrix}\tilde{\Theta} + \frac{1}{\gamma}\dot{\tilde{\Theta}}^\top\tilde{\Theta} \tag{4.36g}$$

$$= -\alpha_2 x_2^2 + \begin{bmatrix} x_1 x_2 - \frac{1}{\gamma}\dot{\hat{\alpha}}_1 & -x_2 \text{sgn}(x_2) - \frac{1}{\gamma}\dot{\hat{\alpha}}_3 \end{bmatrix}\tilde{\Theta} \tag{4.36h}$$

Hence for a stable system each element in the second term is equated to zero, which yields the adaptive control law.

$$\dot{\hat{\alpha}}_1 = \gamma x_1 x_2, \qquad \dot{\hat{\alpha}}_3 = -\gamma x_2 \text{sgn}(x_2) \qquad \text{and} \qquad \hat{\alpha_1}(0) \neq 0, \qquad \hat{\alpha_3}(0) \neq 0 \tag{4.37}$$

The above adaptive law results in $\dot{V}(X,\tilde{\Theta}) \leq -\alpha_2 x_2^2$. To prove asymptotic stability, let us consider the invariant set $\Omega = \{x_1, x_2 | x_2 = 0, x_1 \neq 0\}$. When x_2 is zero and x_1 is non-zero, then x_2 will move away from zero since $\dot{x}_2 = -\tilde{\alpha}_1 x_1$. Hence the solutions in the invariant set will not stay inside the set and will always reach the only equilibrium that is $x_1 = x_2 = 0$. Hence the system is globally asymptotically stable.

A Simulink block diagram of the nonlinear adaptive friction compensation is given in Figure 4.10. The plant considered in the Simulink model had the friction modeled as viscous and Coulomb friction, whose coefficients were the identified values from the previous section. The response of the system with position and velocity initial conditions are given in Figures 4.11 and 4.13.

This method regulates the states (angular velocity and angular position) to zero. Position regulation can be achieved by a simple coordinate transformation. Consider the following

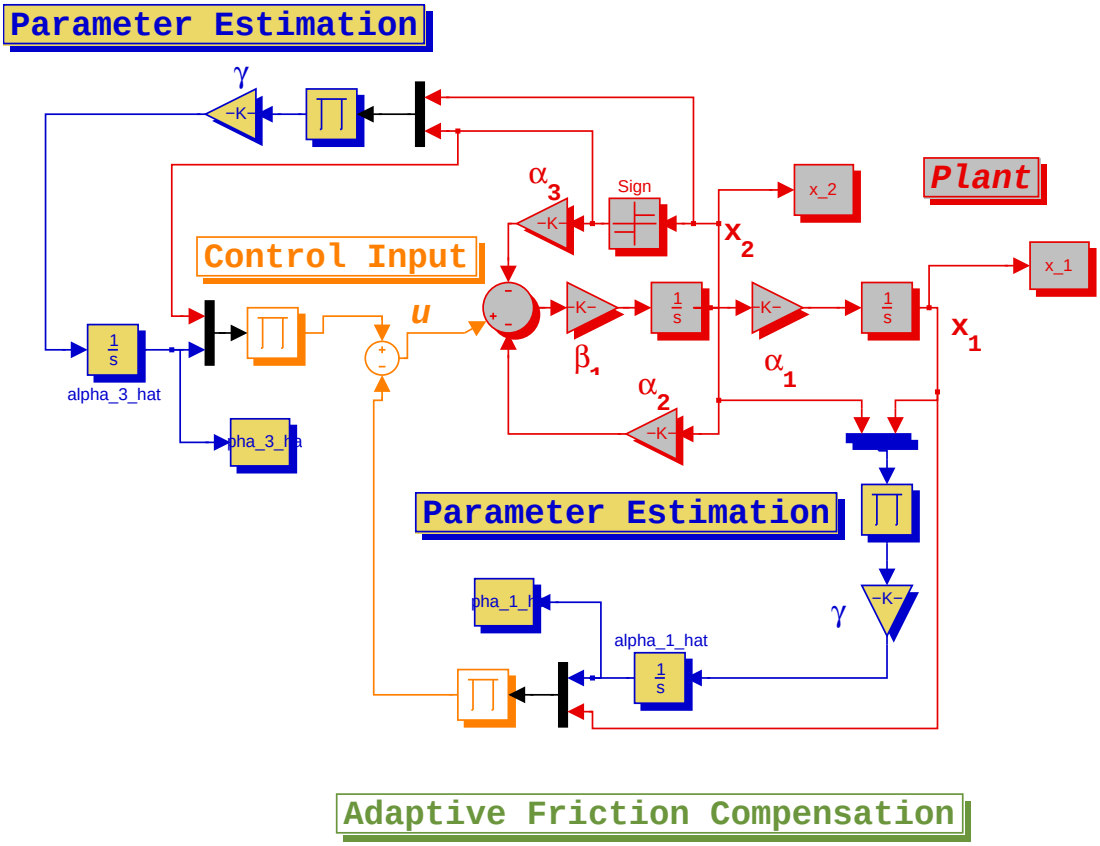

Figure 4.10: Simulink Block Diagram: Adaptive Friction Compensation

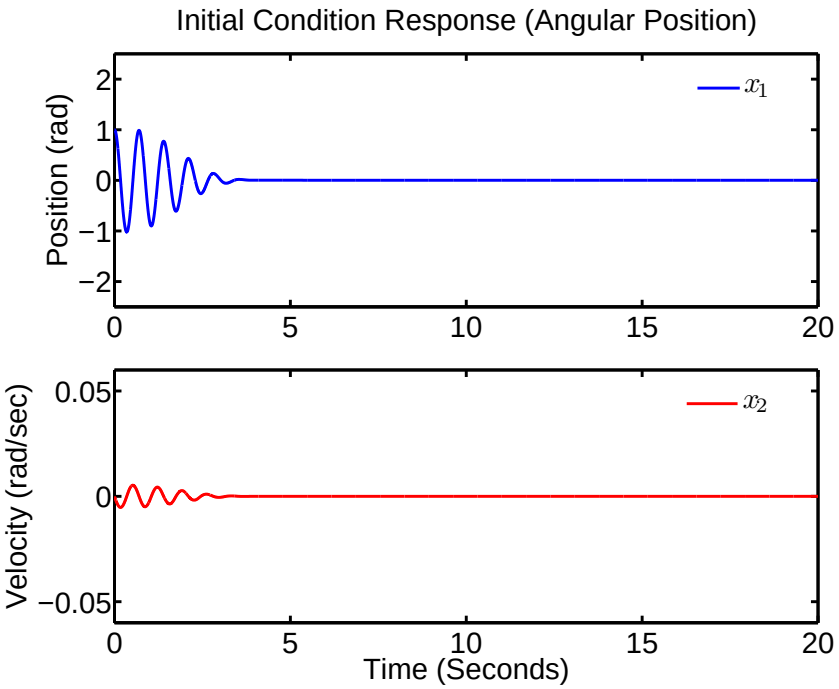

Figure 4.11: Initial Condition Response (Angular Position)

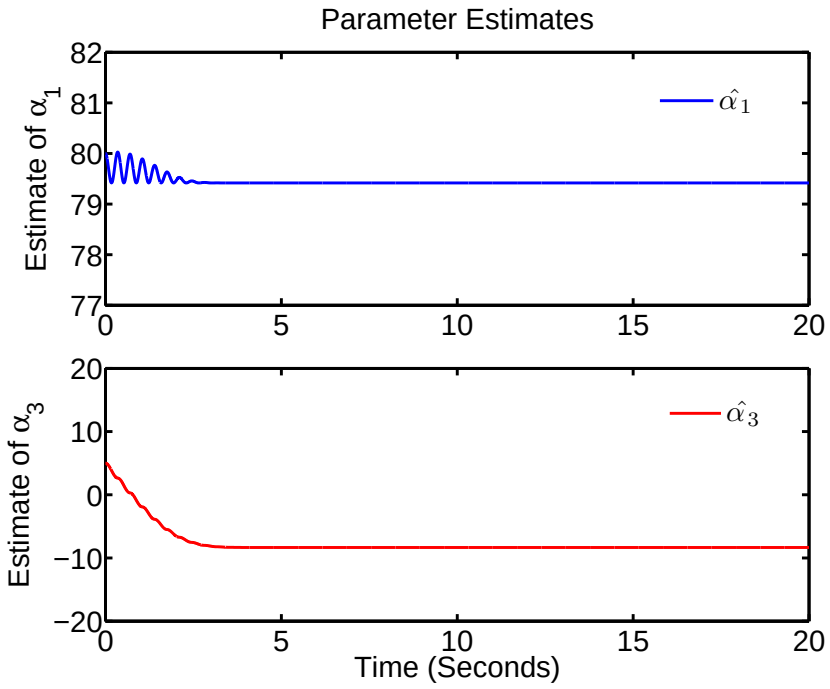

Figure 4.12: Parameter Estimated with Initial Condition Response (Angular Position)

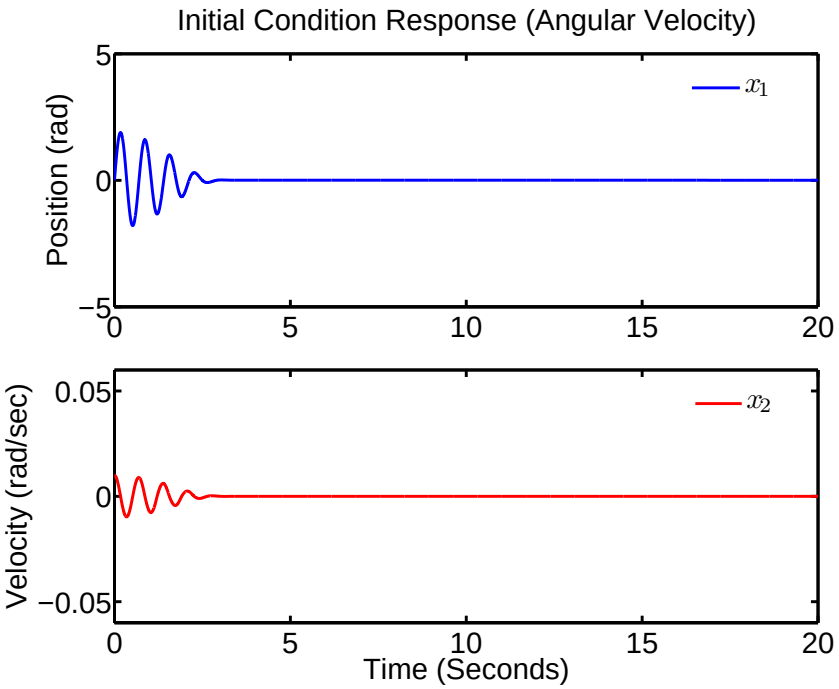

Figure 4.13: Initial Condition Response Angular Velocity

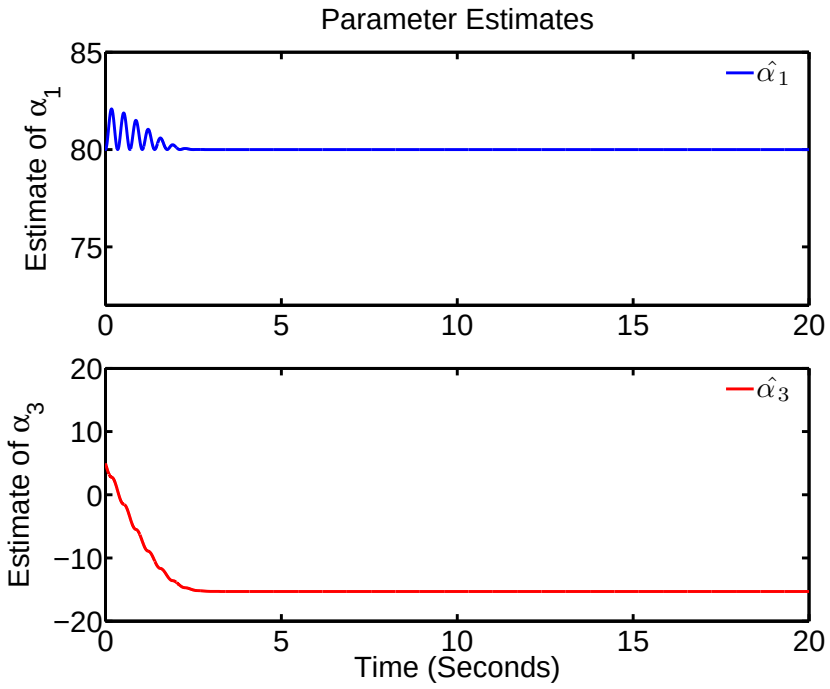

Figure 4.14: Parameter Estimated with Initial Condition Response (Angular Velocity)

coordinate transformation:

$$\tilde{x}_1 = \theta - \theta_{des}, \quad \text{where } \theta_{des} \text{ is the desired position} \tag{4.38a}$$

$$\tilde{x}_2 = \beta_1 \dot{\theta} \tag{4.38b}$$

$$\Rightarrow \dot{\tilde{x}}_1 = \dot{\theta} = \alpha_1 \tilde{x}_2 \tag{4.38c}$$

$$\Rightarrow \dot{\tilde{x}}_2 = \beta_1 \ddot{\theta} = u - \frac{\beta_2}{\beta_1}\tilde{x}_2 - \beta_3 \text{sgn}(\tilde{x}_2) \tag{4.38d}$$

$$= u - \alpha_2 \tilde{x}_2 - \alpha_3 \text{sgn}(\tilde{x}_2) \tag{4.38e}$$

By choosing a similar Lyapunov function candidate as given in equation (4.35), where X is replaced by $\tilde{X}$ a similar adaptive law is obtained, which is given by

$$\dot{\hat{\alpha}_1} = \gamma \tilde{x_1} \tilde{x_2}, \quad \dot{\hat{\alpha}_3} = -\gamma \tilde{x_2} \text{sgn}(\tilde{x_2}) \quad \text{and} \quad \hat{\alpha_1}(0) \neq 0, \quad \hat{\alpha_3}(0) \neq 0 \tag{4.39}$$

The modified Simulink model is shown in Figure 4.15. Figure 4.16 shows a representative

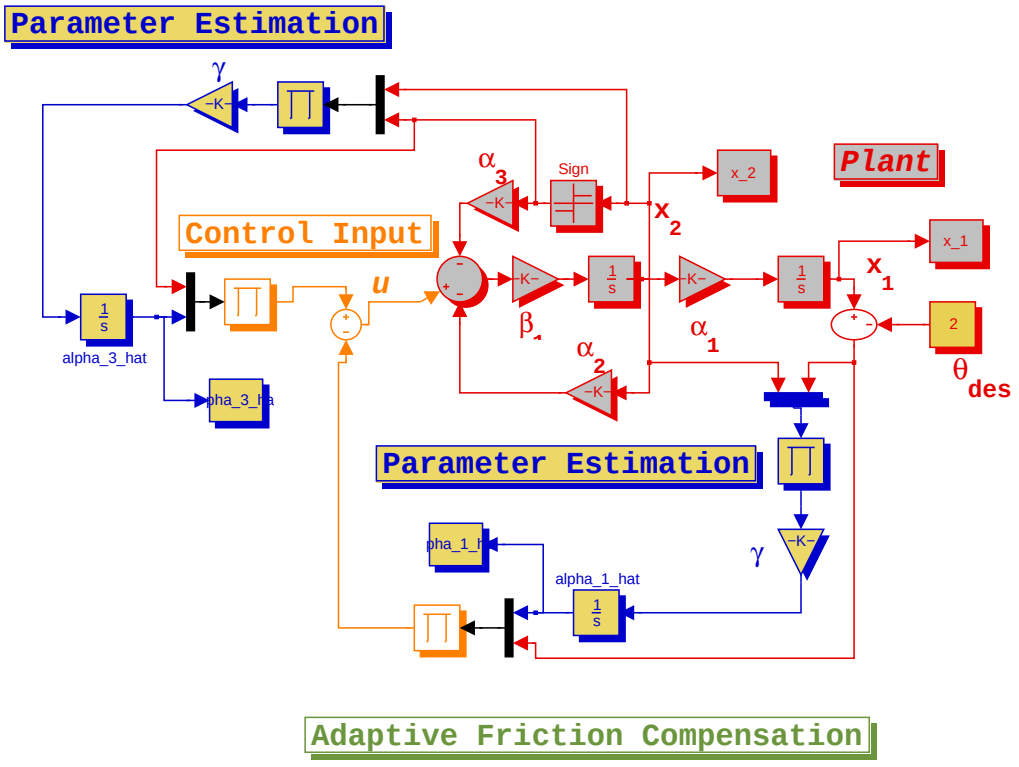

Figure 4.15: Simulink Block Diagram: Position Regulation

sample of simulation results for position regulation with zero initial conditions.

The adaptive friction compensation is the inner loop for the controller which compensates for the uncertain nonlinearities, while the outer loop is involved in compensating for the re-

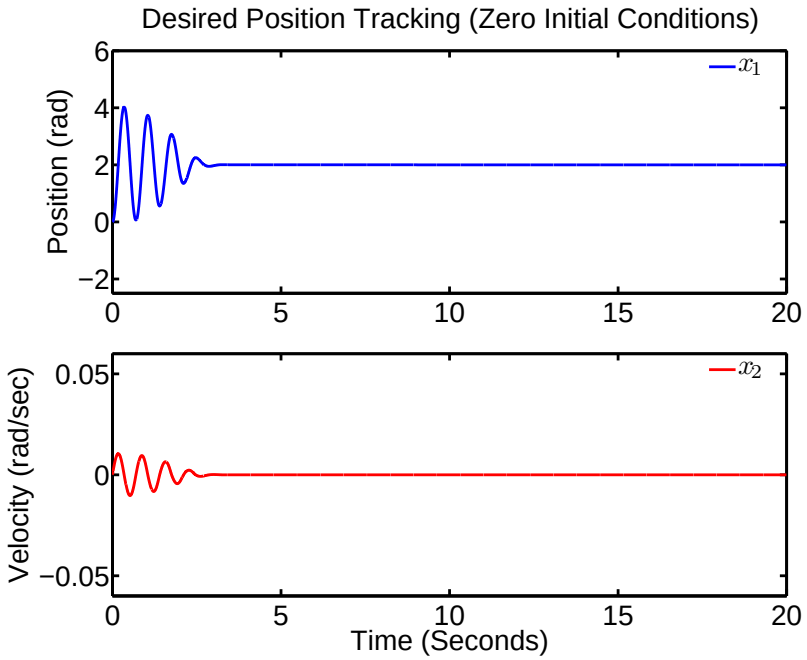

Figure 4.16: Adaptive Static Friction Compensation with Position regulation. $\theta_{des} = 2$, $\theta(0) = 0$ and $\dot{\theta(0)} = 0$

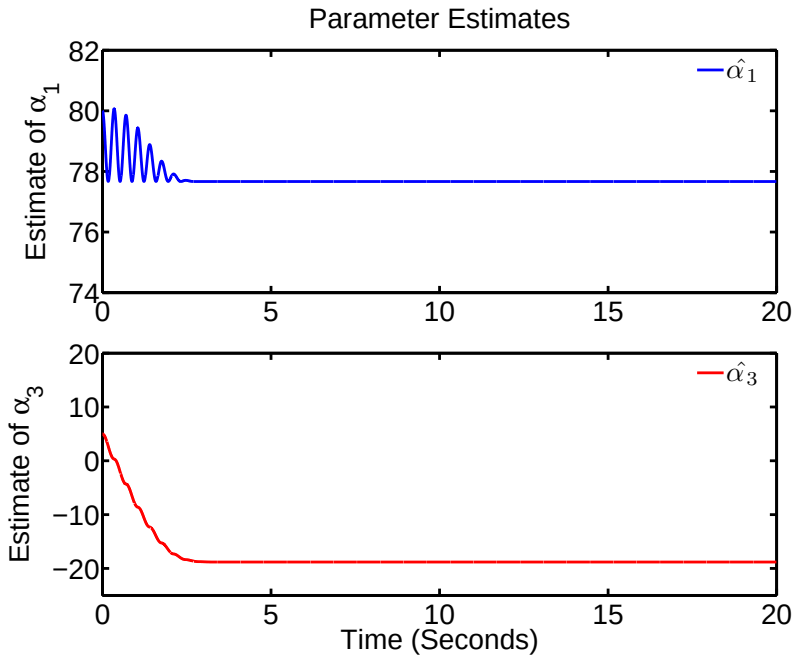

Figure 4.17: Parameter Estimates for Adaptive Static Friction Compensation with Position Regulation. $\theta_{des} = 2$, $\theta(0) = 0$ and $\dot{\theta(0)} = 0$

sulting linear system. Figure 4.18 shows a strategy for implementing model reference adaptive controller along with adaptive friction compensation for web guides. This controller is capable of compensating both uncertain parameters of the plant as well as the uncertain nonlinearities due to friction.

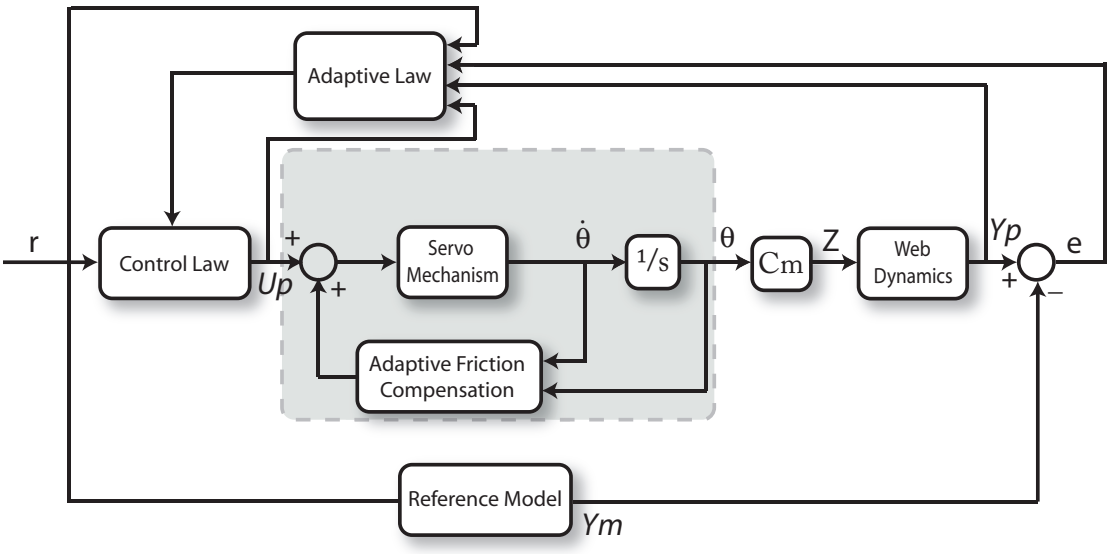

Figure 4.18: Model Reference Adaptive Control with Adaptive Friction Compensation

4.4 Adaptive Friction Compensation with Web Dynamics

The adaptive friction compensation scheme developed in the previous section requires the angular position measurement. Even though an actuator with a position encoder is available, it is currently not possible to include the actuator in the experimental platform. In this section an adaptive friction compensation scheme which does not require the motor angular position feedback is presented. In contrast to the friction compensation technique in the previous section, the controller in this section has only one loop. The adaptive controller presented in this section compensates for both the friction coefficient uncertainty and the web dynamics uncertainty simultaneously.

The simplified web dynamics with the actuator dynamics is given by

$$\frac{y_L}{u_p} = \frac{k_m C_m \beta_1}{s(s+a)\beta_0} \tag{4.40}$$

Let y_{plat} be the position of the platform or the guide, θ_L be the angular position of the motor

and C_m the transmission ratio. The system can be divided into the following:

- Motor Dynamics
$$\frac{\theta_L}{u_p} = \frac{k_m}{s(s+a)}$$
- Transmission Ratio
$$\frac{y_{plat}}{\theta_L} = C_m$$
- Web Dynamics
$$\frac{y_L}{y_{plat}} = \frac{\beta_1}{\beta_0} = \beta = \frac{1}{\alpha}$$

Friction does not affect the web dynamics and hence one can include the friction force in the following dynamics.

$$\frac{y_{plat}}{u_p} = \frac{k_m C_m}{s(s+a)}$$

Re-writing

$$\ddot{y}_{plat} + a\dot{y}_{plat} + F = k_m C_m u_p \tag{4.41}$$

$$\alpha\ddot{y}_L + a\alpha\dot{y}_{plat} + F = k_m C_m u_p \tag{4.42}$$

Equation (4.42) can be represented in the state variable form as follows:

$$x_1 = y_L, \quad \dot{x}_1 = \dot{y}_L = \frac{x_2}{\alpha} \tag{4.43a}$$

$$x_2 = \alpha\dot{y}_L = \dot{y}_{plat}, \quad \dot{x}_2 = \alpha\ddot{y}_L = k_m C_m u_p - F - a\alpha\dot{y}_L \tag{4.43b}$$

$$= Ku_p - F - ax_2 \quad K = k_m C_m \tag{4.43c}$$

$$= Ku_p - [F_v x_2 + F_c \text{sgn}(x_2)] - ax_2 \tag{4.43d}$$

$$\begin{bmatrix} \dot{x}_1 \\ \dot{x}_2 \end{bmatrix} = \begin{bmatrix} 0 & 1/\alpha \\ 0 & -(a+F_v) \end{bmatrix} \begin{bmatrix} x_1 \\ x_2 \end{bmatrix} + \begin{bmatrix} 0 \\ K \end{bmatrix} u_p - \begin{bmatrix} 0 \\ F_c \text{sgn}(x_2) \end{bmatrix} \tag{4.44}$$

If all the constants are known, then we can choose $u_p = \frac{1}{K}\left[-\alpha_1 x_1 - \alpha_2 x_2 + F_c \text{sgn}(x_2)\right]$ which results in the following closed loop system.

$$\begin{bmatrix} \dot{x}_1 \\ \dot{x}_2 \end{bmatrix} = \begin{bmatrix} 0 & 1/\alpha \\ -\alpha_1 & -(\alpha_2 + a + F_v) \end{bmatrix} \begin{bmatrix} x_1 \\ x_2 \end{bmatrix} \tag{4.45}$$

The constants α_1, α_2 can be chosen such that the desired closed-loop pole location is met. Let us consider that the constants α, a, F_v and F_c as unknown and setup the adaptive control problem

as an estimation problem. Notice that in order to cancel the signum term, it is necessary that we assume $K = k_m C_m$ is known. This is a valid assumption since it is possible to know the motor parameters while it is difficult to know the parameters in the web dynamics. If $u = \frac{1}{K}\left[-\alpha_1 x_1 - \alpha_2 x_2 + \hat{F}_c \text{sgn}(x_2)\right]$ then the closed-loop system is

$$\begin{bmatrix} \dot{x}_1 \\ \dot{x}_2 \end{bmatrix} = \begin{bmatrix} 0 & 1/\alpha \\ -\alpha_1 & -(\alpha_2 + a + F_v) \end{bmatrix} \begin{bmatrix} x_1 \\ x_2 \end{bmatrix} + \begin{bmatrix} 0 \\ \hat{F}_c \text{sgn}(x_2) - F_c \text{sgn}(x_2) \end{bmatrix} \tag{4.46}$$

$$\dot{x}_1 = \frac{1}{\alpha} x_1 \tag{4.47a}$$

$$\dot{x}_2 = -\alpha_1 x_1 - (\alpha_2 + a + F_v) x_2 + \tilde{F}_c \text{sgn}(x_2) \tag{4.47b}$$

where $\tilde{F}_c \triangleq \hat{F}_c - F_c$. Notice that the closed-loop system has one equilibrium that is $x_1 = x_2 = 0$. Let us setup a Lyapunov function candidate and find an adaptive law that would make the system asymptotically stable. Consider the following Lyapunov function candidate

$$V(X, \Theta) = \frac{1}{2} X^\top X + \frac{1}{2\gamma} \tilde{\Theta}^\top \tilde{\Theta}, \quad \tilde{\Theta} \triangleq \hat{F}_c - F_c \tag{4.48}$$

Then,

$$\begin{aligned} \dot{V} &= \dot{X}^\top X + \frac{1}{\gamma} \dot{\Theta}^\top \Theta \\ &= \frac{1}{\alpha} x_1 x_2 - \alpha_1 x_1 x_2 - (\alpha_2 + a + F_v) x_2^2 + \tilde{F}_c \text{sgn}(x_2) x_2 + \frac{1}{\gamma} \dot{\tilde{\Theta}}^\top \tilde{\Theta} \\ &= \frac{1}{\alpha} x_1 x_2 - \alpha_1 x_1 x_2 - (\alpha_2 + a + F_v) x_2^2 + \tilde{F}_c \text{sgn}(x_2) x_2 + \frac{1}{\gamma} \dot{\hat{F}}_c^\top \tilde{\Theta} \\ &= \frac{1}{\alpha} x_1 x_2 - \alpha_1 x_1 x_2 - (\alpha_2 + a + F_v) x_2^2 + \left[sgn(x_2) x_2 + \frac{1}{\gamma} \dot{\hat{F}}_c \right] \tilde{\Theta} \end{aligned}$$

If $\dot{\hat{F}}_c = -\gamma x_2 \text{sgn}(x_2)$ then

$$\dot{V} = -(\alpha_2 + a + F_v) x_2^2 - (\alpha_1 - \frac{1}{\alpha}) x_1 x_2$$

If we know α we can set $\frac{1}{\alpha} = \alpha_1$ so that

$$\dot{V} = -(\alpha_2 + a + F_v) x_2^2 \leq 0$$

We can prove that the equilibrium (the system) is asymptotically stable by considering the invariant set $\Omega = \{x_1, x_2 | x_2 = 0\}$. When $x_2 = 0$ and $x_1 \neq 0$, the solution does not stay inside

the invariant set and will always move towards the equilibrium, as long as $\alpha_1 > 0$. But since we do not know α we shall setup a different Lyapunov function candidate by modifying the system.

$$\Theta = \begin{bmatrix} \beta \\ F_c \end{bmatrix}, \hat{\Theta} = \begin{bmatrix} \hat{\beta} \\ \hat{F}_c \end{bmatrix}, \tilde{\Theta} = \begin{bmatrix} \tilde{\beta} \\ \tilde{F}_c \end{bmatrix}, \dot{\tilde{\Theta}} = \begin{bmatrix} \dot{\tilde{\beta}} \\ \dot{\tilde{F}}_c \end{bmatrix}, \beta \triangleq \frac{1}{\alpha}$$

The open-loop system can then be represented as

$$\begin{bmatrix} \dot{x}_1 \\ \dot{x}_2 \end{bmatrix} = \begin{bmatrix} 0 & \beta \\ 0 & -(a + F_v) \end{bmatrix} \begin{bmatrix} x_1 \\ x_2 \end{bmatrix} + \begin{bmatrix} 0 \\ K \end{bmatrix} u_p - \begin{bmatrix} 0 \\ F_c \text{sgn}(x_2) \end{bmatrix} \tag{4.50}$$

Let the desired control input be $u = \frac{1}{K}\left[-\beta x_1 - \alpha_2 x_2 + F_c \text{sgn}(x_2)\right]$ and since we do not know β and F_c let us use their estimates in the control law $u = \frac{1}{K}\left[-\hat{\beta} x_1 - \alpha_2 x_2 + \hat{F}_c \text{sgn}(x_2)\right]$, then the closed-loop system is given by

$$\begin{bmatrix} \dot{x}_1 \\ \dot{x}_2 \end{bmatrix} = \begin{bmatrix} 0 & \beta \\ -\hat{\beta} & -(\alpha_2 + a + F_v) \end{bmatrix} \begin{bmatrix} x_1 \\ x_2 \end{bmatrix} + \begin{bmatrix} 0 \\ \hat{F}_c \text{sgn}(x_2) - F_c \text{sgn}(x_2) \end{bmatrix} \tag{4.51}$$

Let the Lyapunov function candidate be

$$V(X, \Theta) = \frac{1}{2} X^\top X + \frac{1}{2} \tilde{\Theta}^\top \Gamma^{-1} \tilde{\Theta}, \quad \Gamma = \text{diag}(\gamma_1, \gamma_2) > 0 \tag{4.52}$$

Then

$$\begin{aligned} \dot{V} &= \dot{X}^\top X + \dot{\tilde{\Theta}}^\top \Gamma^{-1} \tilde{\Theta} \\ &= \beta x_1 x_2 - \hat{\beta} x_1 x_2 - (\alpha_2 + a + F_v) x_2^2 + \tilde{F}_c x_2 \text{sgn}(x_2) + \left[\dot{\tilde{\beta}},\ \dot{\tilde{F}}_c\right] \Gamma^{-1} \tilde{\Theta} \\ &= -(\alpha_2 + a + F_v) x_2^2 + \left[-x_1 x_2,\ x_2 \text{sgn}(x_2)\right] \tilde{\Theta} + \left[\dot{\tilde{\beta}},\ \dot{\tilde{F}}_c\right] \Gamma^{-1} \tilde{\Theta} \\ &= -(\alpha_2 + a + F_v) x_2^2 + \left[\frac{1}{\gamma_1} \dot{\tilde{\beta}} - x_1 x_2,\ \ \frac{1}{\gamma_2} \dot{\tilde{F}}_c + x_2 \text{sgn}(x_2)\right] \tilde{\Theta} \end{aligned}$$

If we set $\dot{\tilde{\beta}} = \gamma_1 x_1 x_2$ and $\dot{\tilde{F}}_c = -\gamma_2 x_2 \text{sgn}(x_2)$, then

$$\dot{V} = -(\alpha_2 + a + F_v) x_2^2 \leq 0 \tag{4.54}$$

Hence the equilibrium (the system) is asymptotically stable in the large as long as $\hat{\beta} \neq 0$. One can obtain a similar transformation of the equilibrium as in the previous section (page 83) so that regulation to a non-zero point can be achieved.

Analysis

If $\tilde{\Theta} = 0$, then the system reduces to

$$\begin{bmatrix} \dot{x}_1 \\ \dot{x}_2 \end{bmatrix} = \begin{bmatrix} 0 & \beta \\ -\beta & -\underbrace{(\alpha_2 + a + F_v)}_{} \end{bmatrix} \begin{bmatrix} x_1 \\ x_2 \end{bmatrix} = \begin{bmatrix} 0 & \beta \\ -\beta & -\zeta \end{bmatrix} \begin{bmatrix} x_1 \\ x_2 \end{bmatrix}$$

whose eigenvalues are

$$e_{1,2} = -\frac{1}{2}\beta_1 \pm \frac{1}{2}\sqrt{\zeta^2 - 4\beta^2}$$

Hence the closed-loop system is exponentially stable since $\zeta = \alpha_2 + a + F_v > 0$. The constant α_2 is a design parameter which we can be choose. Convergence of the estimated parameters is possible only if the input is sufficiently rich.

Theoretically the system is asymptotically stable in the large, but while implementing in Simulink or on an experimental web platform, the system may not behave as expected. Let us look at the adaptive law.

$$\dot{\hat{\beta}} = \gamma_1 x_1 x_2, \quad \dot{\hat{F}}_c = -\gamma_2 x_2 \text{sgn}(x_2) = -\gamma |x_2|$$

Hence as long as x_2 is non-zero, the adaptive law for $\hat{F}_c$ will always reduce the value of $\hat{F}_c$, which might not be suitable unless a theoretical bound is set on the parameter.

4.5 Adaptive Friction Compensation using RLS Algorithm

This section details the procedure for indirect friction compensation using recursive least squares (RLS) algorithm. The friction parameters are identified on-line using the RLS algorithm and the friction is compensated by feedback linearization. The friction compensation can be implemented as an inner loop as shown in Figure 4.18.

Recursive least squares is one of the simplest algorithm for parameter estimation and is based on one of the oldest algorithms for estimation of parameters (developed by Gauss in late 18th century). Notice that for static friction compensation the unknown friction parameters appear in a linear form

$$J\ddot{\theta} = T - F_c \text{sgn}(\dot{\theta}) - F_v \dot{\theta} \tag{4.55}$$

and hence the minimum can be reached in a single step. We can used the same Least Square Estimation algorithm as described in section 4.2.2.2 on page 71 but in a recursive form. Chapter 13 in [30] presents a detailed description of the RLS algorithm along with modified forms of

the algorithm and also the convergence and initialization issues. In [31] an adaptive friction compensation for DC-motor drives was presented along with experimental results. The same algorithm can be utilized for friction compensation in web guides. Another application of the RLS algorithm along with experimental results is presented in [32].

Applying a low pass filter $F(s) = \dfrac{1}{\tau s + 1}$ to the system in equation (4.55) we obtain the following linear parametrized equation.

$$y = \varphi^\top \phi$$

where,

$$y \triangleq F(s)T,\ \phi = \begin{bmatrix} J \\ F_v \\ F_c \end{bmatrix}, \quad \varphi = \begin{bmatrix} sF(s)\{\dot{\tilde{\theta}}\} \\ F(s)\{\dot{\tilde{\theta}}\} \\ F(s)\{\text{sgn}(\dot{\tilde{\theta}})\} \end{bmatrix} \quad \text{and} \quad \dot{\tilde{\theta}} = F_1(s)\dot{\theta}, \quad F_1(s) = \frac{1}{\tau_1 s + 1} \tag{4.56}$$

$\dot{\tilde{\theta}}$ is a filtered version of $\dot{\theta}$ and the low pass filter $F_1(s)$ is designed such that the measurement noise is filtered. Let us define the error equation as

$$\epsilon = y - \varphi^\top \hat{\phi}$$

The objective of the RLS algorithm is to minimize the sum of the squared error. The analytical solution for the problem in non-recursive form is given by

$$\hat{\dot{\phi}} = (\Phi^\top \Phi)^{-1} \Phi^\top Y$$

when $\Phi^\top \Phi$ is invertible.

$$\Phi[t] = \begin{bmatrix} \varphi^\top[1] \\ \varphi^\top[2] \\ \vdots \\ \varphi^\top[t] \end{bmatrix}, \quad Y[t] = \begin{bmatrix} y[1] \\ y[2] \\ \vdots \\ y[n] \end{bmatrix}$$

In the recursive form the parameter vector $\hat{\phi}$ is obtained as [17]

$$\hat{\phi}(t) = \hat{\phi}(t-1) + K(t)\left[y(t) - \varphi^\top(t)\hat{\phi}(t-1)\right]$$

$$K(t) = P(t-1)\varphi(t)\left[I + \varphi^\top P(t-1)\varphi(t)\right]^{-1}$$

$$P(t) = \left[I - K(t)\varphi^\top(t)\right] P(t-1)$$

$t-$ sample number

The algorithm can be initialized as [30]

$$P(0) = \delta^{-1} I, \qquad \delta = \text{small positive constant}$$
$$\hat{\phi}(0) = 0$$

The initialization procedure is referred to as *soft-constrained initialization*. Based on the practical experience with the RLS algorithm, it is recommended that δ is chosen such that it is smaller than $0.01\sigma_{\varphi}^2$, where σ_{φ}^2 is the variance of φ [30]. For large lengths, the exact value of the initialization constant δ does not have any significant effect on the convergence of the parameters [30]. Refer to lesson 4 in [33] for more information on how and why the algorithm is initialized as above and some useful comments about different forms of RLS algorithms.

4.5.1 Implementation

- Initialize $P(0) = \delta^{-1} I_{3\text{x}3}$ and $\phi(0) = [0 \;\; 0 \;\; 0]^\top$.
- Repeat the following indefinitely
  - Compute the correction vector, $K(t)_{3\text{x}1} = P(t-1)_{3\text{x}3}\varphi_{3\text{x}1}^\top \left(\dfrac{1}{1 + \varphi^\top(t) P(t-1) \varphi(t)} \right)$
  - Update the estimates as $\hat{\phi}(t) = \hat{\phi}(t-1) + K(t) \left[y(t) - \varphi^\top(t) \hat{\phi}(t-1) \right]$ based on the error between the actual and the predicted output.
  - Update the covariance matrix $P(t) = \left[I_{3\text{x}3} - K(t)\varphi^\top(t) \right] P(t-1)$
- At each sampling time we obtain the estimates $\hat{J}, \hat{F}_c$ and $\hat{F}_v$. Using these estimates compute the fiction force $\hat{F} = \hat{F}_v \dot{\hat{\theta}} + \hat{F}_c \text{sgn}(\dot{\hat{\theta}})$ and add it to the control input.

4.5.2 Experimental Results

Friction compensation using the recursive least squares algorithm computes the additional control effort needed to compensate for friction. The RLS implementation can be used along with any existing web guiding algorithm. Experiments were conducted to observe the performance of the adaptive controllers with friction compensation using the RLS algorithm. Figures 4.19 to 4.21 show a representative sample of experiments with the transparent web. The top plots show the performance of the adaptive controller without fiction compensation and the bottom plots shows the performance of the adaptive controller with friction compensation. The plots on the left shows the time history of the lateral position while the plots on the right show the

histogram of error. Experimental results show that the adaptive controller with friction compensation exhibits a slightly better performance in all the three cases.

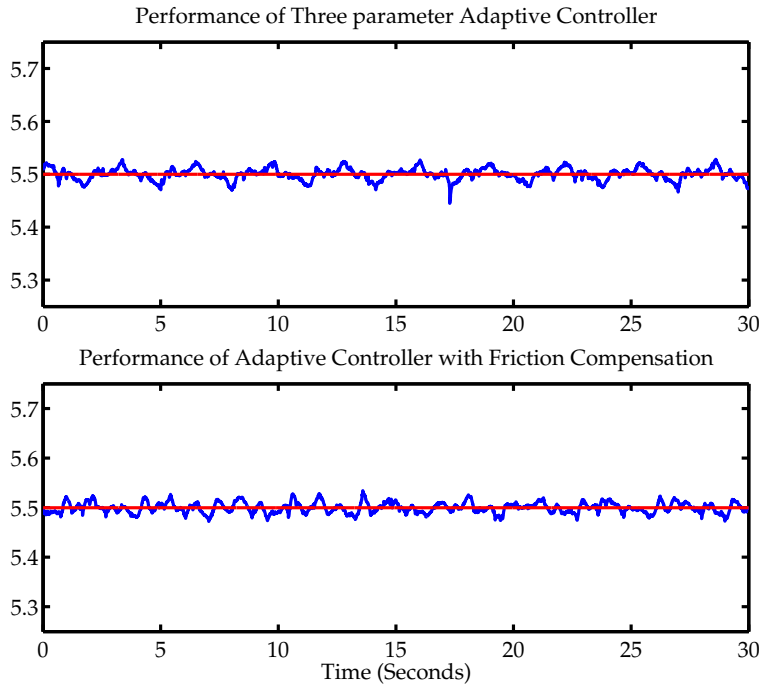

Figure 4.19: Performance Comparision: 3-Parameter, with and without Friction Compensation

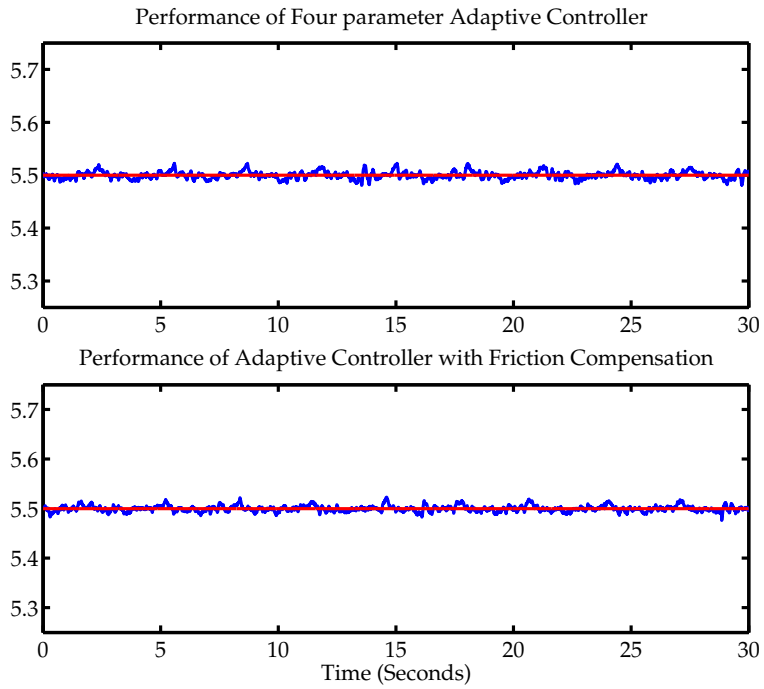

Figure 4.20: Performance Comparision: 4-Parameter, with and without Friction Compensation

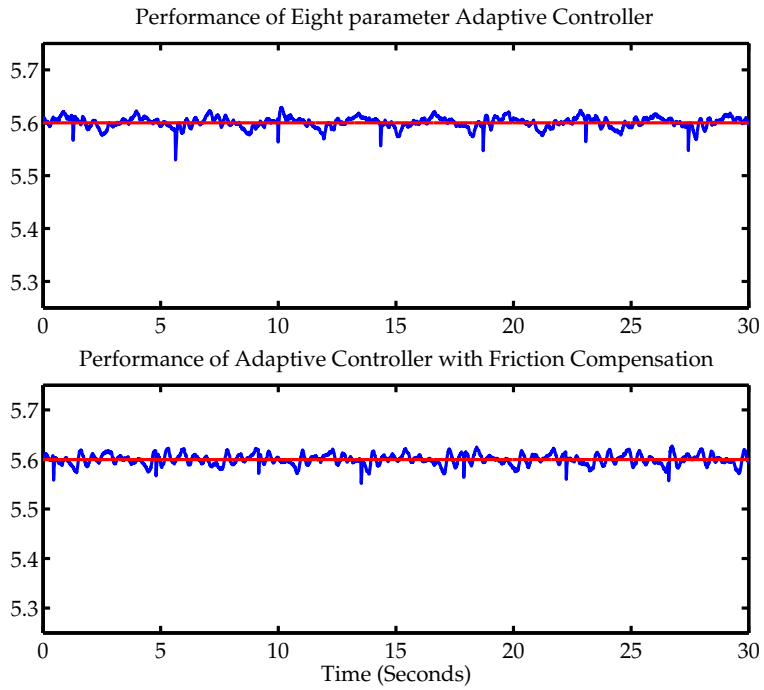

Figure 4.21: Performance Comparision: 8-Parameter, with and without Friction Compensation

Chapter 5

Histogram : A New Performance Metric for Web Guiding

In web guiding, lateral regulation error as a function of time is predominantly used to evaluate the performance of the lateral control system. In this chapter a new visual performance metric for guiding application is introduced. Several properties of the performance metric helps us to clearly understand the performance of the lateral control system.

Plots comparing the regulation error for two controllers are shown in Figures 5.1 and 5.2. From the plots in Figure 5.1 one can easily distinguish the guiding performance of the two data sets. Whereas, from the plots in Figure 5.2, a visual inspection does not help in comparing the guiding performance. Although the regulation error gives a visual quantitative indication of web guiding performance for some situations, it is not clear how well a web position is regulated in many cases.

Another performance measure one could consider is the simultaneous comparison of the regulation error and the control effort supplied to the actuator. When the regulation error appears the same, as in Figure 5.2, one can compare the control effort to choose a better controller. This performance measure is suitable for guiding control system manufacturers to compare different control structures and control algorithms. We are interested in a performance metric which could be used by the operator to tune the gains of a controller. In most industrial lines the operator cannot change the control algorithm or the controller structure; only the gains of the controller can be tuned.

An alternate performance measure is the two norm of the error. This serves as an accurate measure if the error signal is not noisy. If the error signal is noisy, then the two norm of the error is not a clear indicator of lateral performance. For example, the unexpected peaks observed in

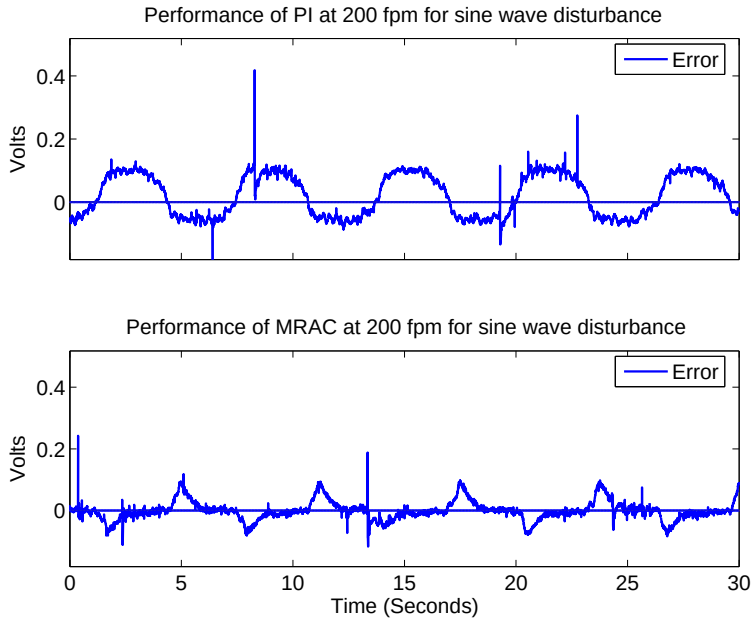

Figure 5.1: Performance Comparison Based on Regulation Error: Clear Distinction

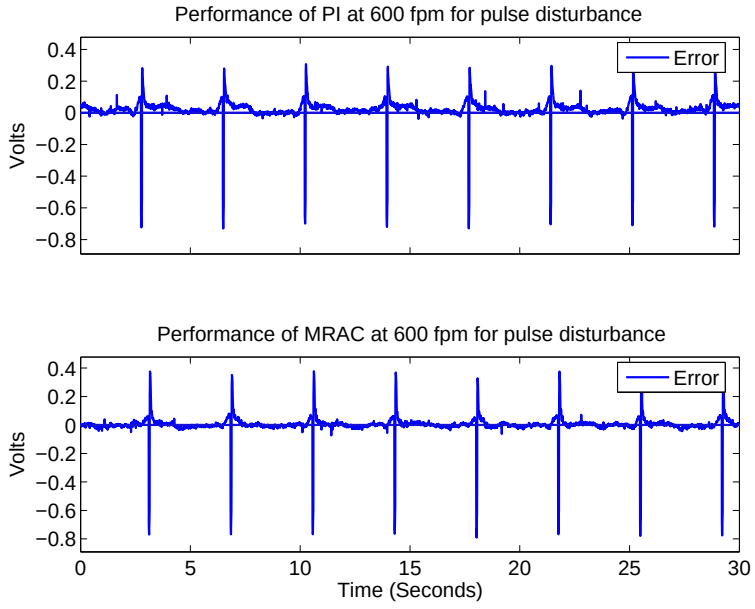

Figure 5.2: Performance Comparison Based on Regulation Error: Difficult to Compare

Figure 5.1 are mainly due to noisy measurements and not due to the guiding performance. In this case taking two norm of error would result in inaccurate performance comparison. One measure that is expected to clearly indicate the guiding performance uses *histograms*. This method provides several important characteristics of the guiding performance and is discussed in detail in the next section.

5.1 Histograms

A better way of measuring performance based on the error distribution is by using the histograms. The purpose of a histogram is to visually encapsulate the distribution of a data set. The following characteristics can be observed from a histogram:

- center of the data;
- spread of the data;
- skewness of the data;
- presence of multiple modes in the data; and
- presence of outliers.

A histogram of error is a frequency distribution of error. A histogram is divided into *'n'* equally spaced bins of error; frequency of occurrence of error within each bin is plotted as a function of error range. Figures 5.3 and 5.4 show the histogram for experimental data shown in Figures 5.1 and 5.2, respectively. The horizontal axis shows the error and the vertical axis shows the frequency of occurrence of error. In this section we concentrate on studying various types of histograms and their importance in web guiding applications.

5.1.1 Normally Distributed Histograms

Figure 5.5 shows a normally distributed histogram. This is the most common shape of the histogram observed in engineering practice and in nature. The key characteristics of this distribution is the bell-shaped curve which is symmetric about the center. The axis of symmetry is usually the mean of the distribution and the frequency of occurrence gradually decreases towards the tail[1] of the distribution.

[1]The extreme regions of a distribution are commonly referred to as the tail of the distribution.

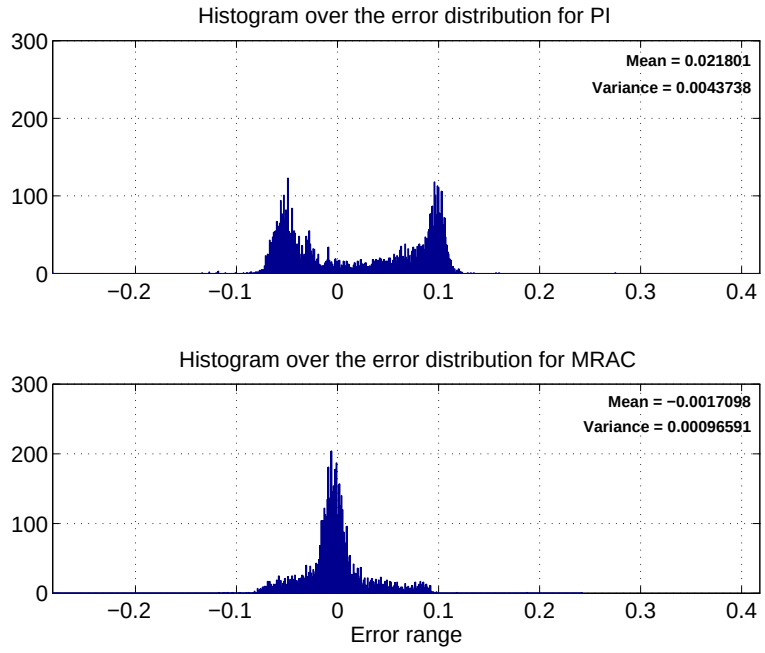

Figure 5.3: Performance Comparison using Histograms:

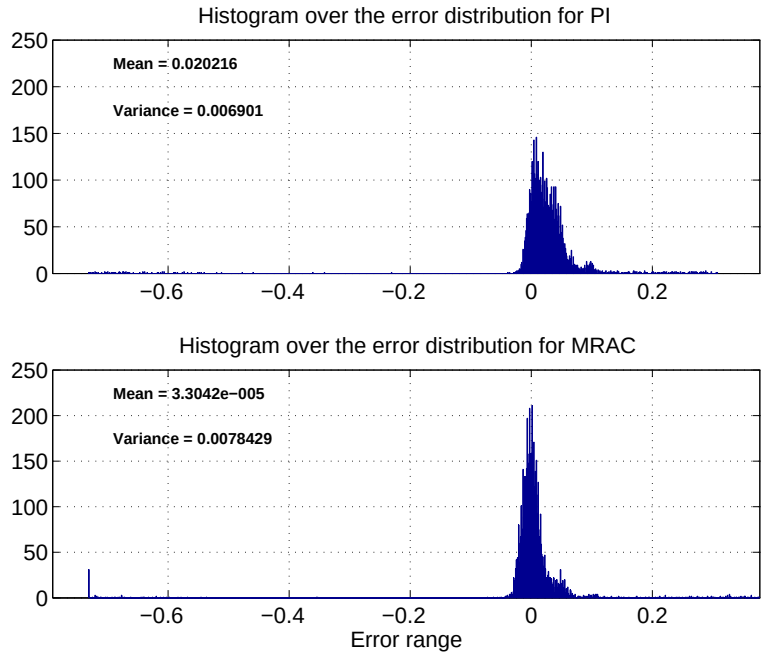

Figure 5.4: Performance Comparison using Histograms:

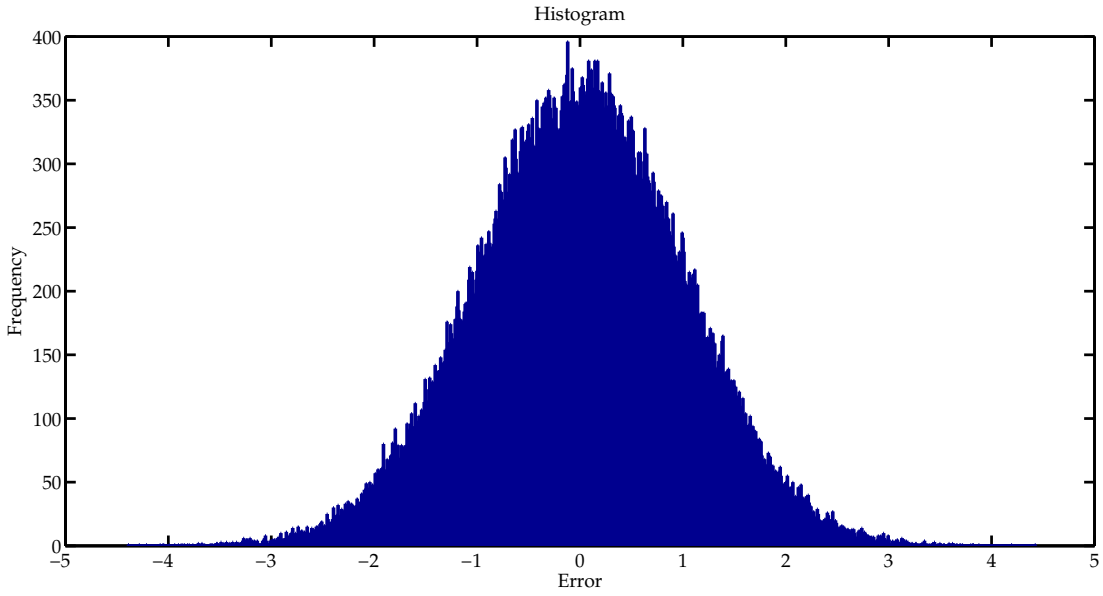

Figure 5.5: Normally distributed Histogram, with Zero Mean

A normal distribution can be completely characterized by the *mean* and *variance* of the data set. The function that describes the normal distribution is given by

$$f(x) = \frac{1}{\sigma\sqrt{2\pi}} e^{-(x-\mu)^2/2\sigma^2}$$

where $f(x)$ represents the frequency of occurrence of the value x, μ is the mean, σ^2 is the variance and σ is the standard variation.

Mean of the Normal Distribution

Mean of a normal distribution represents the center or the axis of symmetry for the distribution. In Figure 5.6 the approximate normal error distribution for two data set are plotted. The data set represented by dashed line is symmetric about zero indicating zero mean. For web guiding application, if the histogram is symmetric/centered about zero, then the system exhibits no steady state regulation error.

Spread of Normal Distribution

The spread of the normal distribution is due to the variance of the error. If the variance is large, then the normal distribution is broader at the base and shorter in height, while a low variance results in thinner distribution at the base. Figure 5.7 shows two data sets with different

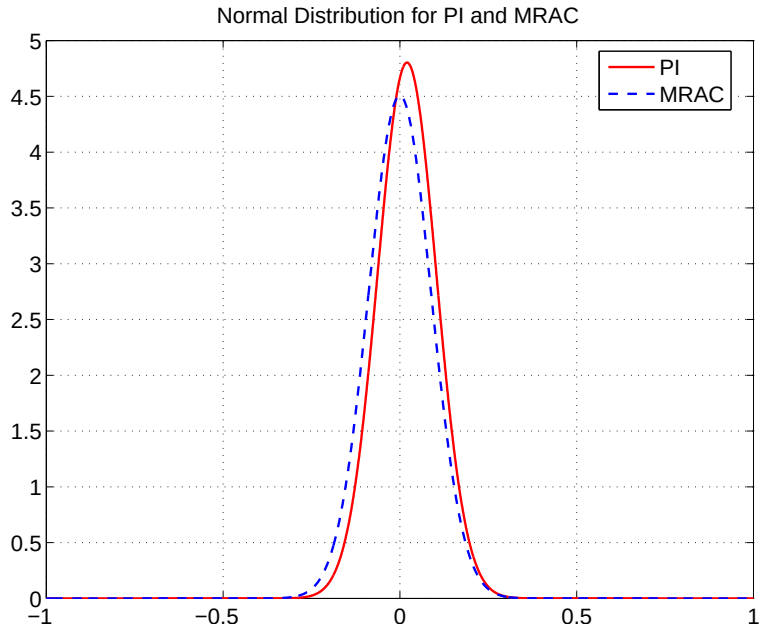

Figure 5.6: Mean of a Normal Distribution

variances.

Height of a Normal Distribution

The height of a normal distribution is the frequency of occurrence of the mean value. For guiding applications, it is desired to have the maximum height around zero. This implies that the frequency of error occurrence about mean is high, i.e., good guiding performance. Figure 5.7 shows two data sets with different heights.

Ideally one would like to see an impulse for the error distribution. But getting an impulse in practice is not possible. In fact the best possible distribution one could observe from any data set is a normal distribution.

A normally distributed histogram of error in web guiding indicates normal operation. This kind of distribution shows that there are no abnormalities in guiding. The regulation error can be considered as a *random variable*. Since the overall guiding process can be considered as a *stationary process*, a normally distributed error with zero mean indicates that the regulation error is *white*. Therefore, the regulation error is unpredictable and hence the guiding performance achieved does not exhibit any abnormalities. If the error is predictable, then the controller can be tuned to compensate for the predictable error to achieve better performance.

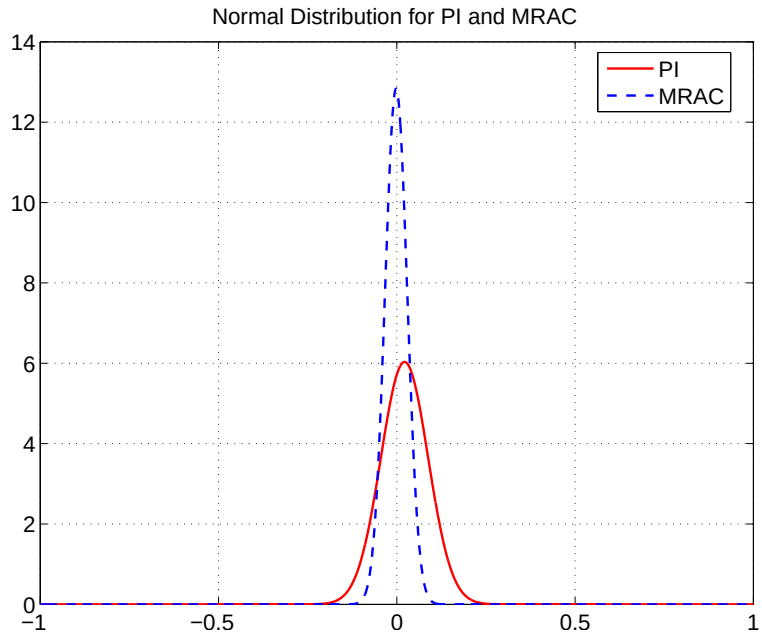

Figure 5.7: Variance of a Normal Distribution

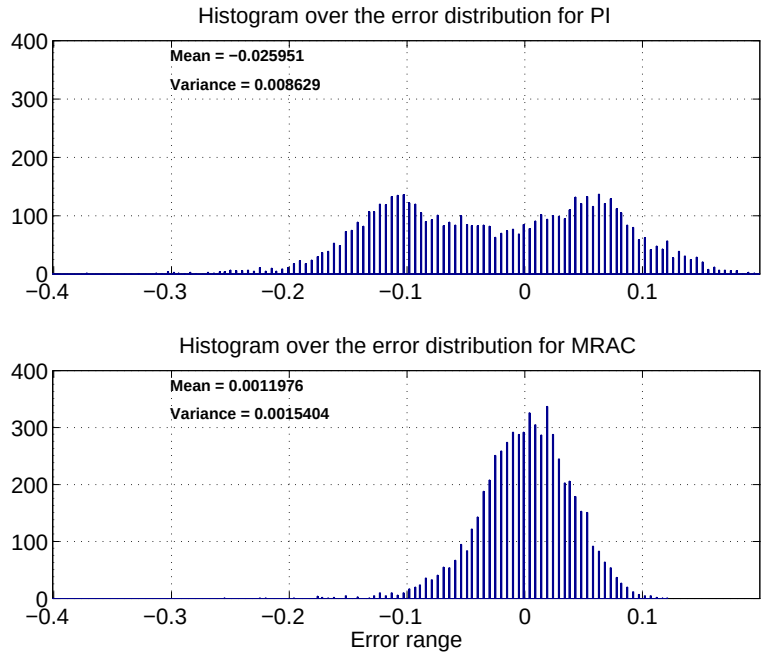

Figure 5.8: Experimental Data: Bottom Plot Shows Normal Distribution

5.1.2 Symmetric, Non-Normal, Short-Tailed Histograms

A short-tailed distribution is characterized by the tail which approaches zero quickly as shown in Figure 5.9. A classical short tailed distribution is a uniform distribution which has very short tails or in fact no tails.

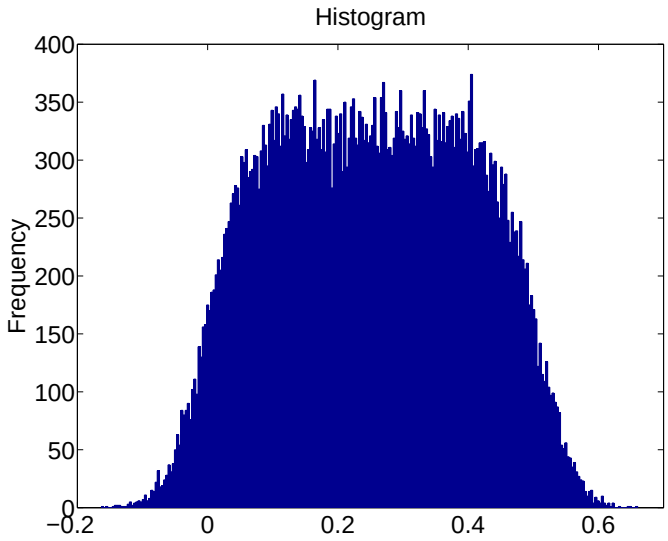

Figure 5.9: Short-Tailed Histogram Characteristic with "Fat" Body

A short-tailed histogram in web guiding indicates that the error is bounded between a small region in which it is uniformly distributed. The histogram shown in Figure 5.9 has the center located at around 0.2 which indicates steady state error of 0.2. Almost 90% of the error is distributed between 0.1 and 0.5. For applications where the error tolerance is known, a shorted tailed error distribution within the tolerance limit would result in satisfactory performance. A distribution with lean body and short tail would indicate an ideal guiding performance.

Unbiased and accurate estimation of center of a distribution is influenced by the length of the tails of the distribution. The center of the distribution obtained using sampled mean is generally misleading for short-tailed and long-tailed distributions. For example, a uniform distribution which varies between ± 0.1 will have its center at zero. This does not indicate that the error is zero predominantly. On the contrary, the error is equally likely to lie between 0.1 and -0.1. Observe the top plot in Figure 5.10 and assume that the mean is zero. Clearly this does not indicate good guiding performance compared to bottom plot. The histogram in the bottom plot clearly indicates that the error is predominantly zero. Also the frequency of

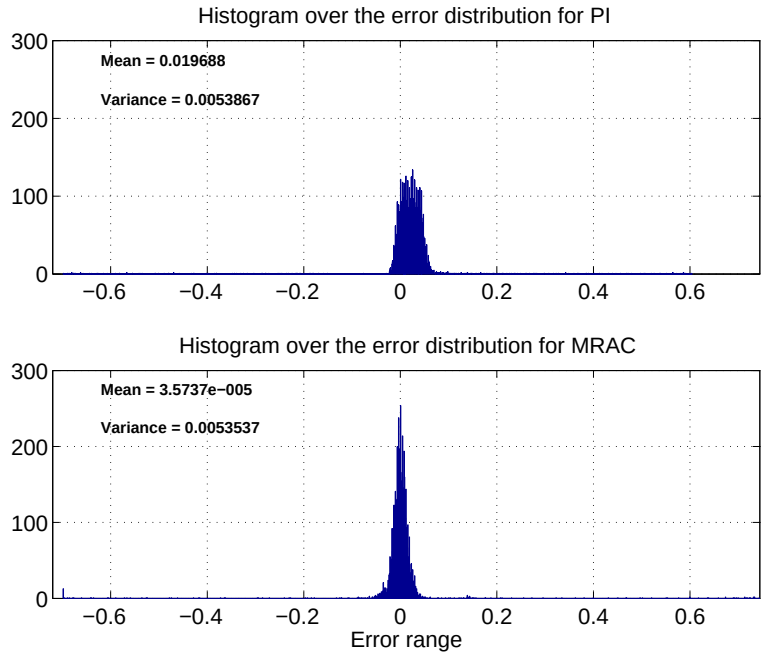

Figure 5.10: Experimental Data: Top Plot Indicates Short-Tailed Distribution

occurrence of the error rapidly decreases as we move away from zero; which is not the case with the histogram in the top plot.

5.1.3 Symmetric, Non-Normal, Long-Tailed Histograms

For a long-tailed distribution, the tails decline to zero very slowly as shown in Figure 5.11 and bottom plot of Figure 5.12. In this distribution the error is close to zero. The presence of a long-tail indicates that occasionally the error is large.

A symmetric long-tailed error distribution indicates poor guiding performance if the tail extends beyond the tolerance limits. In applications where the error cannot go beyond a certain value, a sampled data with long-tail would indicate how far the tail has to be reduced to achieve the required performance. Hence based on the tail length, the controller gains may be tuned to achieve the required performance. If the tail does not extend beyond the error tolerance limits, then the controller provides the required guiding performance.

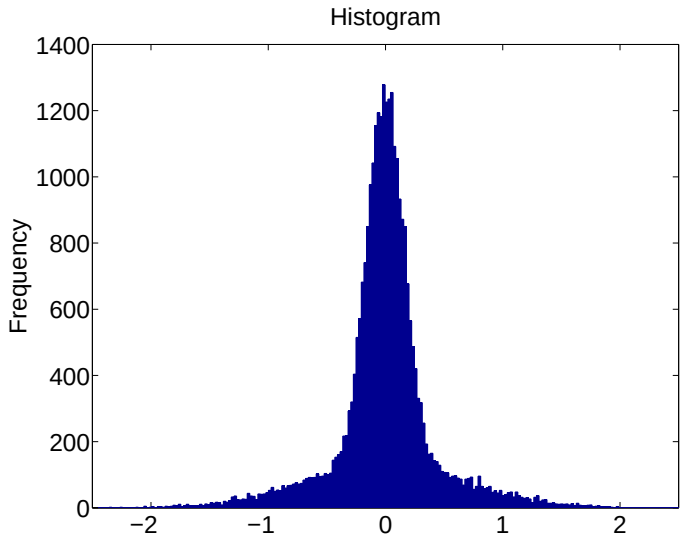

Figure 5.11: Long-Tailed Histogram Characterized by "Lean" Body and Long Tails

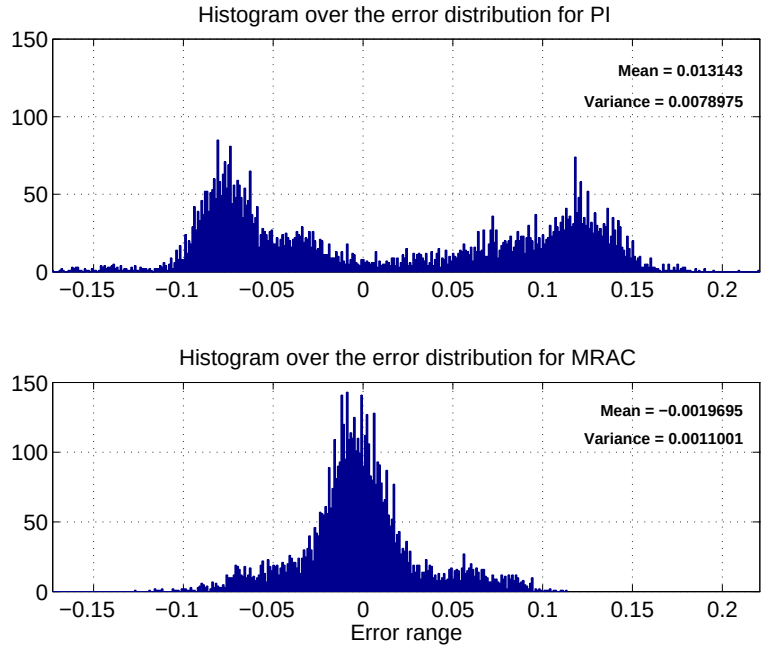

Figure 5.12: Experimental Data: Bottom Plot Shows Long-Tailed Distribution

5.1.4 Symmetric Bimodal histogram

The mode of a distribution is the value with high frequency of occurrence. Unimodal distributions are those with single mode around which the distribution is cluttered and gradually spreads out towards the tails. A normal distribution is a classical example of a unimodal distribution. Bimodal distributions have two modes around which the data is distributed as shown in Figure 5.13. An experimentally observed data is shown in Figure 5.14.

A bimodal error distribution is not an ideal distribution for web guiding applications. A bimodal distribution is usually seen in the presence of a periodic disturbance. This could mean that one or a few rollers upstream is severely misaligned or a periodic disturbance is being generated by some other process abnormalities.

The common statistical measures such as the mean (center of distribution) and variance (spread of the distribution) do not really indicate the true behavior of the guiding control system. For example, the top plot in Figure 5.14 shows the experimental data set with a bimodal error distribution. The mean for the data set is 0.02 and the variance is about 0.004. With just the mean and the variance statistics, it would not have been possible to deduce the presence of a periodic disturbance. Clearly, the use of histograms gives more information and captures several important characteristics of the web guiding control system.

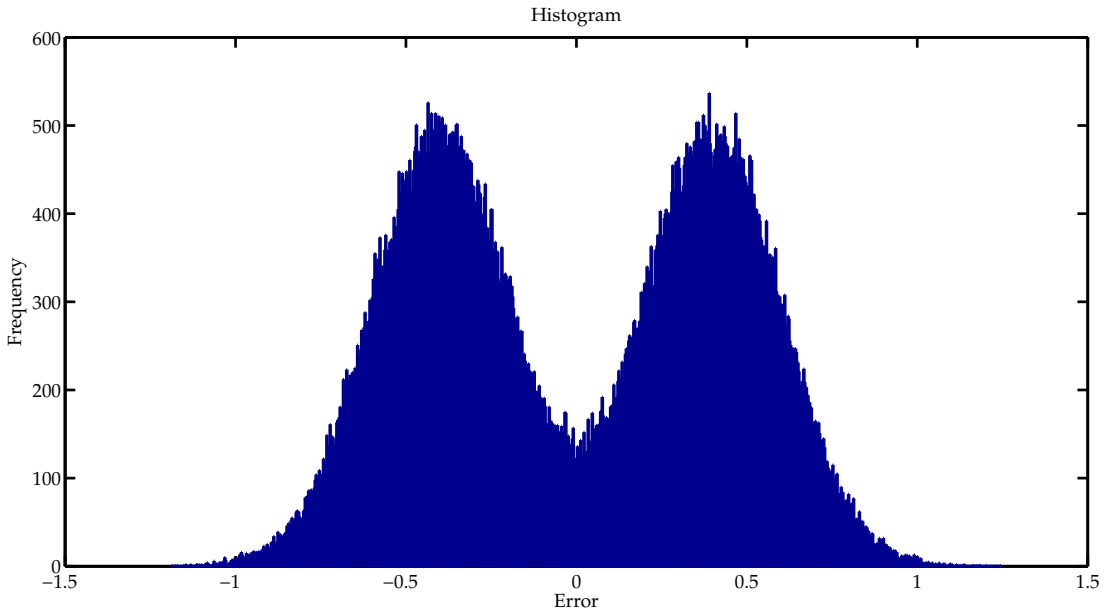

Figure 5.13: Symmetric Bimodal Distribution

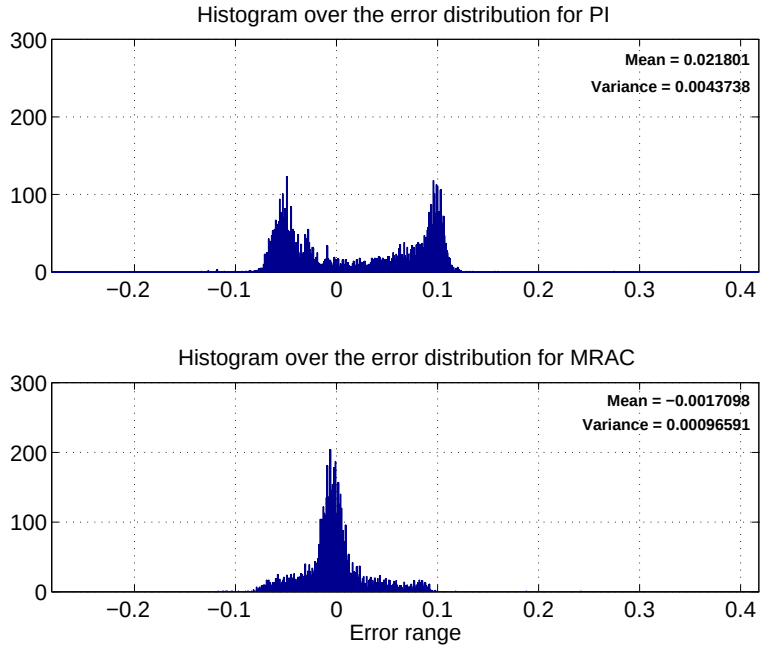

Figure 5.14: Experimental Data: Top Plot Indicates Bimodal Distribution

5.1.5 Skewed Non-Normal histogram

Until now all the histograms were symmetric about an axis. A skewed distribution is a distribution with no symmetry. Skewed histograms are characterized by a single tail, either to the left or to the right and are called "skewed left" and "skewed right" correspondingly.

For a skewed distribution obtaining a *measure of location*[2] becomes difficult. None of the measures like mean, median and mode can describe the characteristics of the distribution well. An example of a skewed distribution is shown in Figure 5.15.

Skewed distributions often occur when there is a lower bound and an upper bound on the data. A typical case in web guiding would be the case of sensor saturation. Based on the direction of the skew one can determine if the sensor gets saturated due to complete closure of the sensing window or if the web is completely away from the sensor window. The top plot in Figure 5.16 shows experimental data with sensor saturation. The flat surface observed is due to the saturation of the sensor. The bottom plot shows the corresponding histogram.

[2]Measure of location is a single representative value for a distribution [34]. Examples include mean, median, mode, etc.

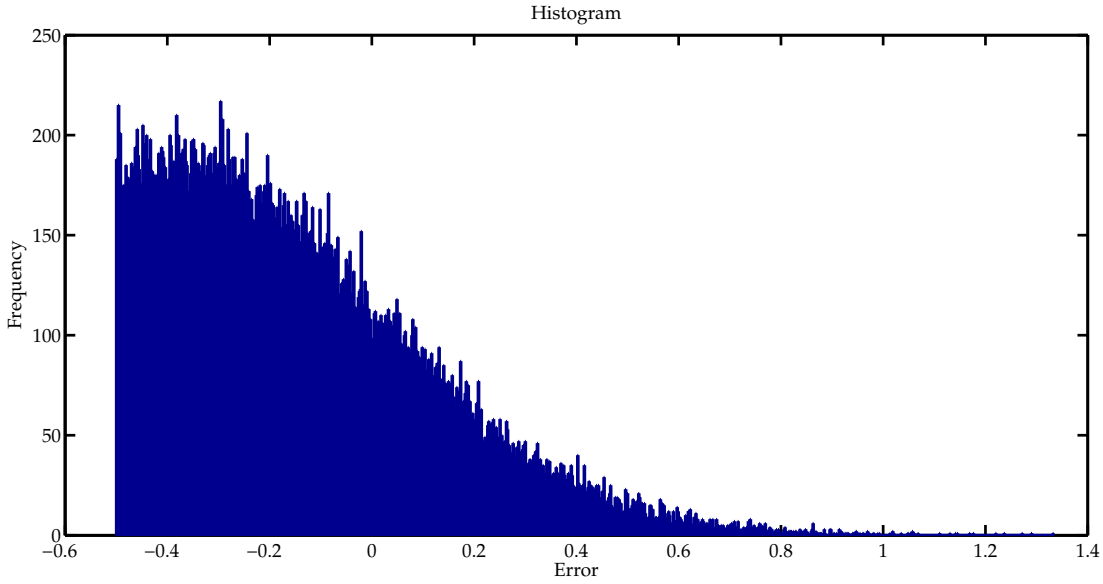

Figure 5.15: A Right Skewed Histogram

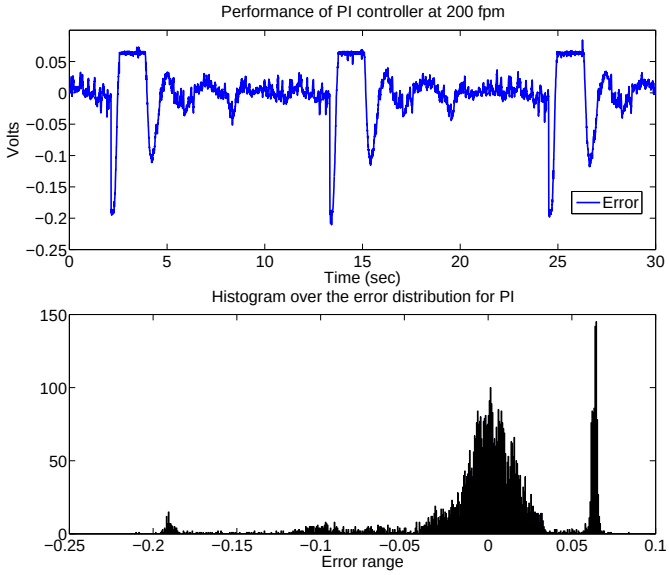

Figure 5.16: Experimental Data: Skewed Histogram

5.1.6 Symmetric Histogram with Outliers

Outliers are data points that appear from a distribution different (in location, scale, or distribution form) from the bulk of the data. A histogram with outliers is shown in Figure 5.17, Figure 5.18 shows the experimentally observed data.

Possible cause for outliers in web guiding applications are

- operator errors,
- web edge discontinuity,
- dust particles in a region of a transparent web,
- or a disturbance similar to a pulse disturbance, etc.

When histograms with outliers are observed in web guiding application, it is important to investigate the cause for their occurrence. The common practise of neglecting outliers, which are located at values greater than 4σ (σ is the standard deviation), should be avoided. The occurrence of outliers may indicate some machine or web induced abnormalities. The very fact that one can observe outliers indicates that the abnormality has occurred a considerable number of times. Therefore, the reason for their occurrence should be investigated. An experimental data with the presence of outliers is shown in Figure 5.18. The outliers are observed to the far left of the histograms. This indicates that a large error with a negative magnitude is observed quite frequently. Outliers in web guiding application may be observed when pulse disturbances are encountered.

5.1.7 Ideal Error Distribution

The ideal error distribution for guiding applications should be unimodal, with zero value for all measures such as mean, median and mode. The distribution should be normally distributed with a lean body. The variance of the distribution should be within the guiding tolerances. Such a distribution that is observed experimentally is shown in the bottom plot of Figure 5.19. A unimodal distribution indicates the absence of periodic disturbances while a lean distribution indicates good guiding performance.

In this chapter we have seen that histograms are useful in characterizing the guiding performance. In an event that visual displays are not available for operators, a possible alternative performance metric to histograms is presented in the following. This performance metric does

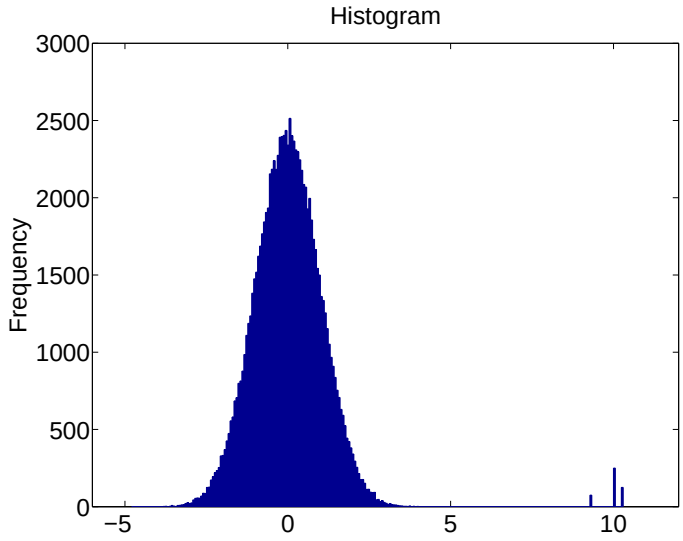

Figure 5.17: A Histogram with Outliers

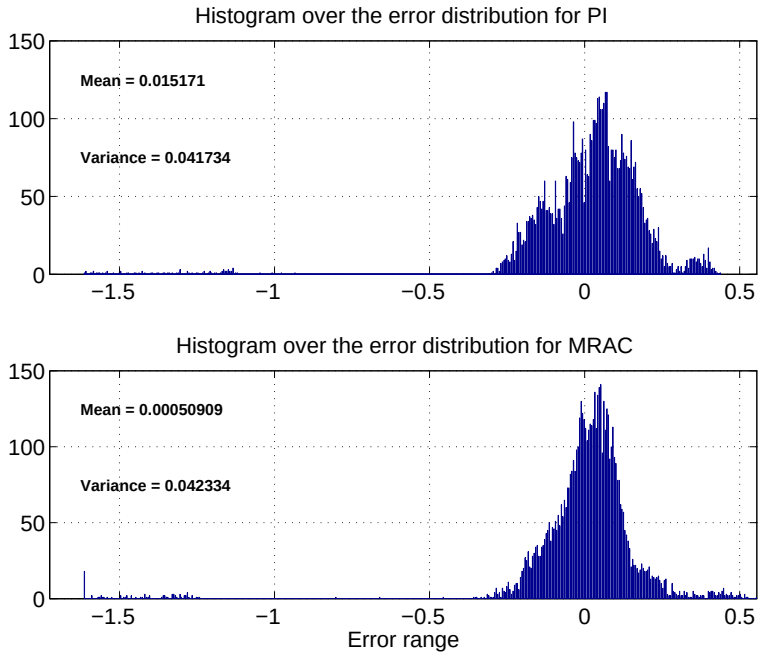

Figure 5.18: Experimental Data: Presence of Outliers

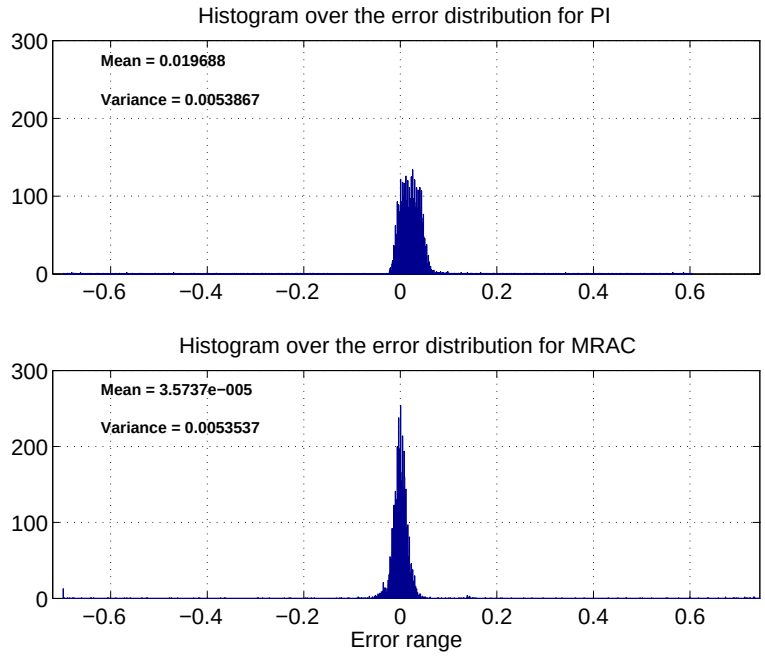

Figure 5.19: Experimental Data: The Ideal Distribution for Guiding Applications

not characterize the error distribution completely but can be used when no visual display is available.

A single measure of location is not capable of describing the characteristics of an error distribution completely. Hence a combination of these measures can be used to describe the guiding performance. From the observations with the type of histograms, we can deduce a few good performance characteristics based on the measures of location.

- Mean is desired to be close to zero.
- Median of the distribution is desired to be the mean of the distribution.
- Error distribution should be unimodal with mode value at zero.

The ideal statistical performance measure should be a combination of mean, median, mode, standard deviation and variance. All the common measures can be calculated using standard statistical tools and does not require any graphical visual unit for display. A good tracking performance would be a unimodal distribution with values for mean, median, mode all equal to zero. Also, the standard deviation has to be close to zero.

Chapter 6

Summary and Future Work

Maintaining the lateral position of the web on rollers is an important aspect of any web handling system. Inability to maintain the lateral position results in loss of productivity and poor quality of the finished products. In this thesis adaptive control strategies that can provide the specified lateral position regulation performance in the presence of process variations and uncertainty in web material properties were developed.

The lateral behavior of the web on rollers is affected by various process parameters such as transport velocity, web tension and material properties such as opacity and modulus. Industrial guiding control systems neglect the web lateral dynamics to simplify the controller design. While the control strategies developed in the literature assume that the process parameters are known and remain fixed. The adaptive control strategies developed in this thesis do not neglect the lateral web dynamics and do not assume the knowledge of the process parameters. Adaptive control strategies that are capable of adapting to variations in the process parameters were proposed in this work. A chapter by chapter summary of the thesis is given below.

In Chapter 2, design and formulation of a model reference adaptive controller suitable for web guiding were addressed. The chapter starts off with a basic introduction to adaptive control. Since the structure of the lateral dynamics of the web is well understood, a model reference adaptive control strategy was developed. The structure and complexity of the model reference adaptive control system depends on the structure and complexity of the lateral dynamics of the web. Two adaptive control strategies were developed by assuming a reduced order model for the lateral web dynamics. Another model reference adaptive controller was developed based on the complete model for the web dynamics. In all the three adaptive controller designs, the process parameters that affect the lateral dynamics of the web were considered to be unknown; the parameters of the actuator dynamics were also considered to be unknown. Computer sim-

ulations were conducted to evaluate the performance of the adaptive controllers. The results of the simulations indicated that the adaptive control strategies provide good guiding performance in the presence of disturbances and process variations.

In Chapter 3, the experimental results of the developed adaptive control strategies were presented and discussed. Experiments were conducted on an experimental web handling platform containing two intermediate web guides. Two different web materials of distinct physical characteristics were transported under different operating conditions on the experimental web handling platform. Several common disturbances observed in an industrial processing line were created. The effectiveness of the developed control strategies were evaluated with sinusoidal, step, and pulse disturbances and a number of process variations such as changes in web opacity, web tension, and transport velocity. All three adaptive controllers were able to cope with the process variations and provided good guiding performance in the presence of disturbances. The performance of the adaptive controllers were compared with an industrial PI controller.

One of the significant performance characteristic of the adaptive controller was its ability to cope with sensor gain variations. Industrial controllers fail to provide good guiding performance when the sensor gain changes. Experimental results clearly indicate that the adaptive controllers are able to provide good guiding performance with sensor gain variations.

A systematic procedure for choosing various design parameters in the adaptive control schemes were provided in Chapter 3. From the experimental observations of the simplified adaptive controllers, some key characteristics of the adaptive controllers for web guiding applications were noted. Based on these observations guidelines for practical implementation were presented.

In Chapter 4, adaptive fiction compensation strategies suitable for web guiding application were proposed. Experiments were carried out to identify static friction coefficients of a guide mechanism. An adaptive friction compensation strategy was proposed to compensate for friction in web guides. This compensation technique can be used as an inner loop of a control strategy used for lateral guiding. Another adaptive control strategy which considers the coefficients of friction and the parameters of web dynamics to be unknown was proposed. The controller was shown to be globally asymptotically stable. But such a controller design needs prior information about the friction parameters in order to implement it practically. Finally, a recursive least square (RLS) algorithm for static friction compensation was presented. The RLS

algorithm can be used as an inner loop of an existing lateral guiding strategy. The proposed RLS algorithm was implemented as an inner loop for the adaptive control schemes presented in Chapter 2. Experimental results indicate that the friction compensation based on RLS algorithm is capable of providing improved performance.

In Chapter 5, a new performance metric for web guiding applications was proposed. Common performance metrics such as the two norm of the regulation error, visual plots of regulation error as a function of time, etc., do not completely describe the performance characteristics of the guide control system. A new performance metric based on histograms which can clearly indicate the guide performance was discussed. Several different types of histograms and their significance in identifying lateral performance characteristics were discussed.

The adaptive strategies proposed in this thesis exhibit good guiding performance in the presence of process variations and disturbances. Several improvements to the adaptive control algorithm can be made to enhance its robustness. Projection of estimated parameters based on parameter bounds is one way of improving the robustness of the adaptive controller which has to be investigated in the future.

The control algorithms in this thesis were developed for intermediate guides. This algorithm can be extended to unwind and rewind guides. Future work should also focus on implementing adaptive control strategies for unwind and rewind guiding.

In some industrial applications the edge sensor is positioned one span downstream of the guide roller. The transfer function from the lateral displacement of the web at the guide to the lateral displacement at the subsequent roller (free span lateral dynamics) is non-minimum phase. Therefore, placement of the edge sensor one or more spans downstream of the guide roller would require consideration of the additional dynamics in the analysis. Future work should investigate the effects of placement of the sensor in spans downstream of the guide roller. To improve robustness of the guiding control system feedforward control should also be investigated.

Friction compensation based on RLS algorithm has shown improvements in guiding performance. Additional theoretical work has to be conducted in order to investigate the possibility of simultaneous compensation of unknown parameters in the web lateral dynamics and friction models.

BIBLIOGRAPHY

[1] K. I. Hopcus, "Unwind and Rewind Guiding," in *Proceedings of the Second International Conference on Web Handling*. Stillwater: Oklahoma State University, 1993, pp. 34 – 45. 4

[2] D. P. Campbell, *Process Dynamics*. Wiley, 1958. 6

[3] J. J. Shelton, "Lateral dynamics of a moving web," Ph.D. dissertation, Oklahoma State University, Stillwater, 1968. 6

[4] J. J. Shelton and K. N. Reid, "Lateral Dynamics of an Idealized Web," *ASME Journal of Dynamic Systems, Measurment, and Control*, vol. 93, no. 3, pp. 187 – 192, September 1971. 6

[5] ——, "Lateral Dynamics of Real Moving Web," *ASME Journal of Dynamic Systems, Measurment, and Control*, vol. 93, no. 3, pp. 180 – 186, September 1971. 6

[6] L. A. Sievers, "Modeling and control of lateral web dynamics," Ph.D. dissertation, Rensselaer Polytechnic Institute, 1987. 6

[7] C. E. Kardamilas, "Stochastic modeling and control of lateral web dynamics," Ph.D. dissertation, Oklahoma State University, 1990. 6, 9

[8] G. E. Young and K. N. Reid, "Lateral and Longitudinal Dynamic Behavior and Control of Moving Webs," *Journal of Dynamic Systems, Measurement, and Control*, vol. 115, pp. 309 – 317, June 1993. 6

[9] A. K. Abbaraju, Master's thesis, Oklahoma State University, Stillwater, 2007, to be submitted. 6, 9

[10] P. R. Pagilla, K. N. Reid, K. Hopcus, and J. Haque, "Adaptive control of web guides," Oklahoma Center for Advancement of Science and Technology, Tech. Rep. AR032-049, 2005. 6

[11] L. Sievers, M. J. Balas, and A. von Flotow, "Modeling of web conveyance systems for multivariable control," *IEEE Transactions on Automatic Control*, vol. 33, no. 6, pp. 524 – 531, June 1988. 9, 10

[12] G. E. Young, J. J. Shelton, and C. E. Kardamilas, "Modeling and Control of Multiple Web Spans using State Estimation," *ASME Journal of Dynamic Systems, Measurement, and Control*, vol. 111, pp. 505 – 510, 1989 1989. 10

[13] M. J. Balas and S. C. Liang, "Disturbance Accommodating Control of Web Processes," in *Proceedings of ASME Winter Annual Meeting*, vol. 22, Dallas, 1990, pp. 137 – 141. 10

[14] P. R. Pagilla, R. V. Dwivedula, Y. L. Zhu, S. S. Mandal, K. I. Hopcus, and J. Haque, "Lateral Control of a Web using Estimated Velocity Feedback," in *Proceedings of the Sixth International Conference on Web Handling*. Stillwater: Oklahoma State University, 2001, pp. 34 – 45. 10

[15] S. S. Mandal, "Lateral Control of a Web using Estimated Velocity Feedback," Master's thesis, Oklahoma State University, Stillwater, 2000. 10

[16] J. B. Yerashunas, J. A. D. Abreu-Garcia, and T. T. Hartley, "Control of lateral motion in moving webs," *IEEE Transactions on Control Systems Technology*, vol. 11, no. 5, pp. 684 – 693, September 2003. 10

[17] K. J. Åström and B. Wittenmark, *Adaptive Control*, 2nd ed. Prentice-Hall, 1994. 13, 22, 52, 90

[18] P. A. Ioannou and J. Sun, *Robust Adaptive Control*. Prentice-Hall, 1996. 15, 17, 18, 22, 23, 34, 39, 41, 42, 52, 120

[19] C. H. Edwards and D. E. Penney, *Elementary Differential Equations with Boundary Value Problems*, 4th ed. Prentice-Hall, 2000.

[20] W. E. Boyce and R. C. DiPrima, *Elementary Differential Equations*, 7th ed. John Wiley & Sons (ASIA) Pte. Ltd., 2002.

[21] R. C. Dorf and R. H. Bishop, *Modern Control Systems*, 8th ed. Addison-Wesley, 1997.

[22] K. S. Narendra and A. M. Annaswamy, *Stable Adaptive Systems*. Dover Publications, 2005. 22, 29, 34, 39

[23] K. S. Narendra and L. S. Valavani, "Stable adaptive controller design–direct control," *IEEE Transactions on Automatic Control*, vol. 23, no. 4, pp. 570 – 583, August 1978. 28, 29

[24] P. R. Pagilla, R. V. Dwivedula, Y. Zhu, and L. P. Perera, "Periodic Tension Disturbance Attenuation in Web Process Lines using Active Dancers," *ASME Journal of Dynamic Systems, Measurement, and Control*, vol. 125, pp. 361 – 371, September 2003. 45

[25] R. V. Dwivedula, Y. Zhu, and P. R. Pagilla, "Characteristics of active and passive dancers: A comparative study," *Control Engineering Practice, A Journal of the International Federation of Automatic Control*, vol. 14, no. 4, pp. 409 – 423, 2006. 45, 47

[26] B. Armstrong-Hélouvry, P. Dupont, and C. C. de Wit, "A Survey of Models, Analysis Tools and Compensation Methods for the Control of Machines with Friction," *Automatica*, vol. 30, no. 7, pp. 1083–1138, 1994. 65, 66

[27] B. Friedland and Y.-J. Park, "On Adaptive Friction Compensation," *IEEE Transactions on Automatic Control*, vol. 37, no. 10, pp. 1609 – 1612, October 1992. 69

[28] J. W. Gilbart and G. C. Winston, "Adaptive compensation for an optical tracking telescope," *Automatica*, vol. 10, no. 2, pp. 125–131, March 1974. 69

[29] Y. Zhu, "Adaptive Control of Mechanical Systems with Static and Dynamic Friction Compensation," Master's thesis, Oklahoma State University, Stillwater, 2001. 69

[30] S. Haykin, *Adaptive Filter Theory*, 3rd ed. Prentice-Hall, 1996. 89, 91

[31] C. Canudas, K. J. Åström, and K. Braun, "Adaptive Friction Compensation in DC-Motor Drives," *IEEE Journal Robotics and Automation*, vol. 3, no. 6, pp. 681 – 685, December 1987. 90

[32] J. Wang, S. J. Qin, C. Bode, and M. Purdy, "Recursive Least Squares Estimation and Its Application to Shallow Trench Isolation," *Advanced Process Control and Automation, Proceedings of SPIE*, vol. 5044, pp. 109 – 120, 2003. 90

[33] J. M. Mendel, *Lessons in Digital Estimation Theory*. Prentice-Hall, 1987. 91

[34] I. M. Chakravarthi, R. G. Laha, and J. Roy, *Handbook of Methods of Applied Statistics*. John Wiley & Sons, 1967, vol. I. 105

[35] C. A. Desoer and M. Vidyasagar, *Feedback Systems: Input-Output Properties*. Academic Press, 1975. 120

[36] C. T. Chen, *Linear System Theory and Design*. Saunders HBJ, 1984. 120

APPENDIX A

Offset Adaptation

For an infrared sensor, the opacity variation in web material affects the sensor output. Experimental results in chapter 3 indicate that the developed adaptive controller is able to cope with the sensor gain variation. Apart from the sensor gain variation, whenever the web opacity changes guide-point also changes. In this section we present an automatic reference detection (guide-point detection) algorithm called offset adaptation which can determine the appropriate reference position based on the opacity of the web material.

The infrared sensor provides a larger sensing window when compared to the ultrasonic sensor. In some applications, because of larger web edge errors, infrared sensors are desired. An ideal infrared sensor gives full scale voltage when it is completely uncovered and zero voltage when completely covered by an ideal opaque material. Therefore, the lower limit of the output voltage increases based on the web material used and its opacity. One does not have knowledge of this lower limit of the sensor output when different web materials are used. Figure A.1 shows the output voltage as a function of sensor window width for a typical infrared sensor of 0.7 *in* physical sensing window width. The abscissa represents the width of blocked portion of sensor window the ordinate represents the output voltage. A completely opaque web would have the voltage range between 0 to 6 volts (full scale reading) while a semi-transparent web has a lesser voltage range, for example, in the range of $5 - 6$ volts as shown.

As seen from the Figure A.1, if the opacity of the material changes, then the guide point also changes, i.e., it is offset. Hence, it becomes important to know this offset value for each web material used. At present, one simple solution is suggested that can ascertain the offset value using adaptation. The following is the procedure for implementing offset adaptation.

- Run MRAC and set the reference to 97% of the full scale sensor reading.
- As soon as the web edge reaches the reference, reduce the reference by a small step size

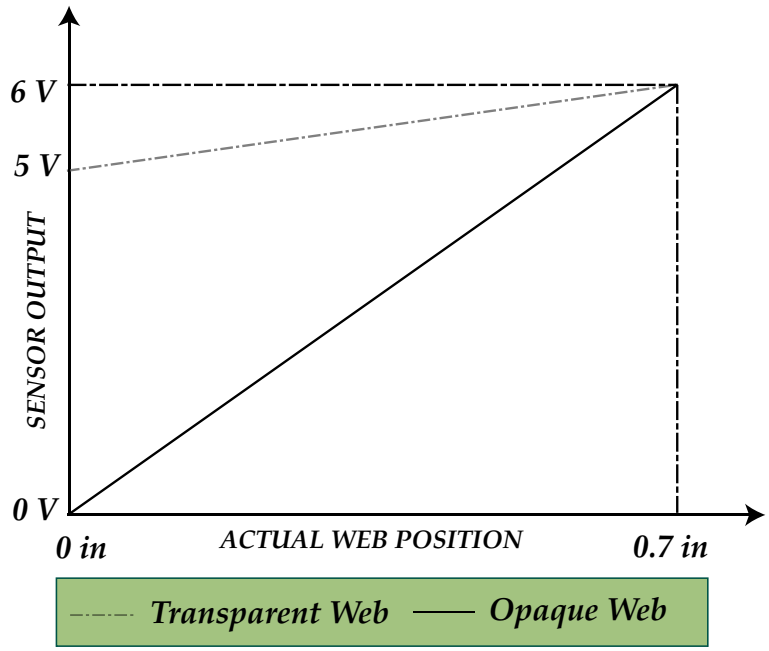

Figure A.1: Output voltage range and typical curves for opaque and transparent webs

(step size was considered as 0.1 volt and can be varied based on the full scale reading of the sensor and the application).

- Repeat the above step until the sensor output saturates.
- The output of the edge sensor gives the current position of the web when the web completely covers the sensor window.
- The new reference is set by taking the average of current web position and the full scale sensor reading.
- Stop offset adaptation and start the regular adaptation with the new reference.

Figures A.2, and A.3 show the offset adaptation when implemented with the opaque web and the transparent web. For both the experiments on offset adaptation, the web is kept stationary.

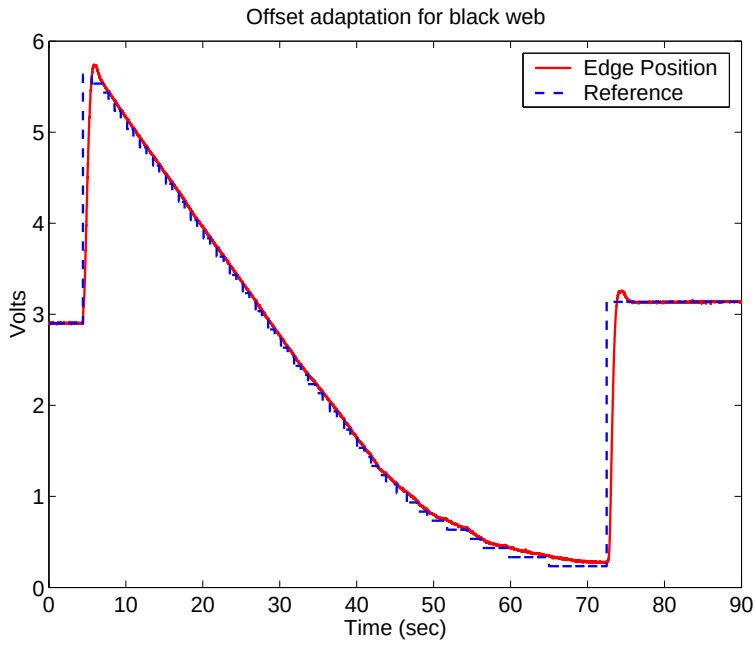

Figure A.2: Offset adaptation on the opaque web

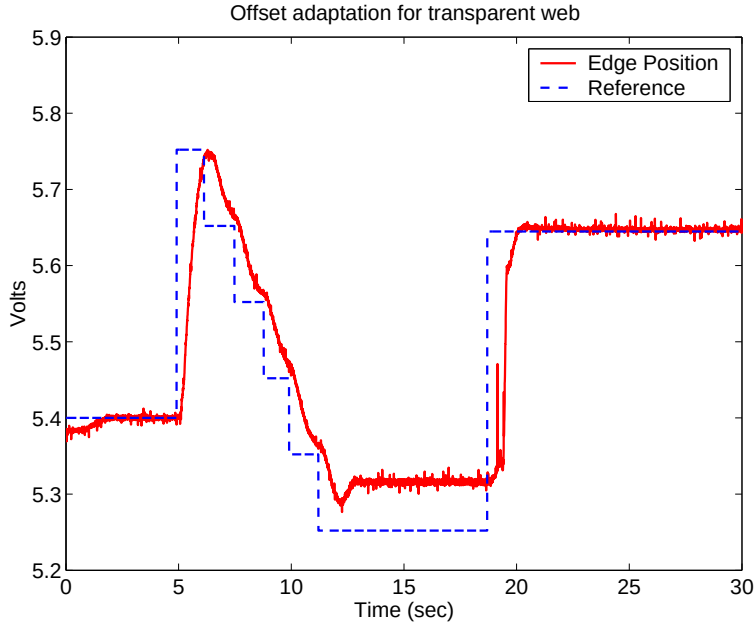

Figure A.3: Offset adaptation on the transparent web

APPENDIX B

Mathematical Preliminaries

Definitions, theorems, lemmas, and some important results which are helpful in understanding the design and analysis of the adaptive control developed in this thesis, is presented in this chapter. Proofs for the theorems are not within the scope of this work and hence they are omitted. The mathematical preliminaries in this chapter are from [18], [35], and [36].

B.1 Continuous Functions and their Limits

Definition B.1 (norm) *The **norm** $|x|$ of a vector x is a real valued function with the following:*

- $|x| \geq 0$ *with* $|x| = 0$ *if and only if* $x = 0$
- $|\alpha x| = |\alpha||x|$ *for any scalar* α
- $|x + y| \leq |x| + |y|$

Definition B.2 ($\mathcal{L}_p$ norm) *For functions of time, $\mathcal{L}_p$ norm can be defined as*

$$||x||_p \triangleq \left(\int_0^\infty |x(\tau)|^p d\tau \right)^{1/p}$$

for $p \in [0, \infty)$ and say that $x \in \mathcal{L}_p$ when $||x||_p$ exists (i.e., x is locally integrable and $||x||_p < \infty$)

Definition B.3 ($\mathcal{L}_\infty$ norm) *$\mathcal{L}_\infty$ norm can be defined as*

$$||x||_\infty \triangleq \sup_{t \geq 0} |x(t)|$$

and say that $x \in \mathcal{L}_\infty$ when $||x||_\infty$ exists (i.e., $||x||_\infty$ is finite.)

Definition B.4 (Continuity) *A function $f : [0, \infty) \longmapsto \mathcal{R}$ is **continuous** on $[0, \infty)$ if for any given $\epsilon_0 > 0$ $\exists$ a $\delta(\epsilon_0, t_0)$ such that $\forall\ t_0, t \in [0, \infty)$ for which $|t - t_0| < \delta(\epsilon_0, t_0)$ we have $|f(t) - f(t_0)| < \epsilon_0$.*

Definition B.5 (Uniform Continuity) *A function $f : [0,\infty) \longmapsto \mathcal{R}$ is **uniformly continuous** on $[0,\infty)$ if for any given $\epsilon_0 > 0$ $\exists$ a $\delta(\epsilon_0)$ such that $\forall\ t_0, t \in [0,\infty)$ for which $|t - t_0| < \delta(\epsilon_0)$ we have $|f(t) - f(t_0)| < \epsilon_0$.*

Remark B.1 *A function f with $\dot{f} \in \mathcal{L}_\infty$ is uniformly continuous on $[0,\infty)$.*

Fact 1 $\lim_{t\to\infty} \dot{f}(t) = 0$ does not imply that $f(t)$ has a limit as $t \to \infty$.

Fact 2 $\lim_{t\to\infty} f(t) = c$ for some constant $c \in \mathcal{R}$ does not imply that $\dot{f}(t) \to 0$ as $t \to \infty$.

Lemma B.1 *The following is true for scalar-valued functions:*

- *A function $f(t)$ that is bounded from below and is nonincreasing has a limit as $t \to \infty$.*
- *Consider the nonnegative scalar functions $f(t), g(t)$ defined for all $t \geq 0$. If $f(t) \leq g(t) \forall\ t \geq 0$ and $g \in \mathcal{L}_p$, then $f \in \mathcal{L}_p\ \forall p \in [1,\infty]$*

Lemma B.2 *If $f, \dot{f} \in \mathcal{L}_\infty$ and $f \in \mathcal{L}_p$ for some $p \in [1,\infty]$, then $f(t) \to 0$ as $t \to \infty$.*

Lemma B.3 (Barbălat's Lemma) *If $\lim_{t\to\infty} \int_0^t f(\tau)d\tau$ exists and is finite, and $f(t)$ is uniformly continuous function, the $\lim_{t\to\infty} f(t) = 0$.*

B.2 Input-Output Stability

Consider an LTI system described by the convolution of two functions $u, h : \mathcal{R}^+ \to \mathcal{R}$ defined as

$$y(t) = u * h \triangleq \int_0^t h(t-\tau)u(\tau)d\tau = \int_0^t u(t-\tau)h(\tau)d\tau \tag{B.1}$$

where u, y is the input and output of the system. Let $H(s)$ be a Laplace transform of the $h(.)$. $H(s)$ is called the transfer function and $h(t)$ is called the impulse response of the system.

Let D ne an open interval in the real line $\mathcal{R}$ and let f(.) be a function defined on D.

Definition B.6 (Analytic) *A function of a real variable, $f(.)$, is said to be **analytic** on D if $f \in C^\infty$ and if $\forall\ t_0 \in D$ $\exists$ a positive real number ϵ_0 such that, $\forall\ t \in (t_0 - \epsilon_0, t_0 + \epsilon_0)$, $f(t)$ is representable by a Taylor series expansion about the point t_0:*

$$f(t) = \sum_{n=0}^{\infty} \frac{(t-t_0)^n}{n!} f^{(n)}(t_0)$$

Theorem B.1 *Let $H(s)$ be a strictly proper[1] rational transfer function of s. Then $H(s)$ is analytic in $Re[s] \geq 0$ if and only if $h \in \mathcal{L}_1$*

Corollary B.1 *If $h \in \mathcal{L}_1$, then*

- *h decays exponentially, i.e., $|h(t)| \leq \alpha_1 e^{-\alpha_0 t}$ for some $\alpha_0, \alpha_1 > 0$*
- *$u \in \mathcal{L}_1 \Rightarrow y \in \mathcal{L}_1 \cap \mathcal{L}_\infty, \dot{y} \in \mathcal{L}_1, y$ is continuous and $\lim_{t\to\infty} |y(t)| = 0$*
- *$u \in \mathcal{L}_2 \Rightarrow y \in \mathcal{L}_2 \cap \mathcal{L}_\infty, \dot{y} \in \mathcal{L}_2, y$ is continuous and $\lim_{t\to\infty} |y(t)| = 0$*
- *For $p \in [1, \infty], u \in \mathcal{L}_p \Rightarrow y, \dot{y} \in \mathcal{L}_p$ and y is continuous*

Corollary B.2 *Let $H(s)$ be a biproper[2] and analytic in $Re[s] \geq 0$. Then $u \in \mathcal{L}_2 \cap \mathcal{L}_\infty$ and $\lim_{t\to\infty} |u(t)| = 0$ imply that $y \in \mathcal{L}_2 \cap \mathcal{L}_\infty$ and $\lim_{t\to\infty} |y(t)| = 0$.*

B.3 Lyapunov Stability

Consider a system described by

$$\dot{x} = f(t, x), \qquad x(t_0) = x_0 \tag{B.2}$$

where $x \in \mathcal{R}, f : \mathcal{T} \times \mathcal{B}(r), \mathcal{T} = [t_0, \infty)$ and $\mathcal{B}(r) = \{x \in \mathcal{R}^n \mid |x| < r\}$. Assume that f is of that for every $x_0 \in \mathcal{B}(r)$ and every $t_0 \in \mathcal{R}^+$, B.2 possesses one and only one solution $x(t; t_0, x_0)$. The system is autonomous if f does not depend on t,

$$\dot{x} = f(x) \tag{B.3}$$

otherwise, it is non-autonomous.

Definition B.7 *A state x_e is said to be an equilibrium state of the system described by B.2 if*

$$f(t, x_e) \equiv 0 \qquad \forall\, t \geq t_0$$

Definition B.8 *The equilibrium state x_e is said to be **stable (in the sense of lyapunov)** if for arbitrary t_0 and $\epsilon > 0$ $\exists$ a $\delta(\epsilon, t_0)$ such that $|x_0 - x_e| < \delta$ implies $|x(t; t_0, x_0) - x_e| < \epsilon\ \forall t \geq t_0$.*

Definition B.9 *The equilibrium state x_e is said to be **uniformly stable** if it is stable and if $\delta(\epsilon, t_0)$, in the above definition, does not depend on t_0.*

[1] For a strictly proper transfer function the degree of the numerator polynomial is less than the degree of the denominator polynomial.

[2] A biproper transfer function has equal number of poles and zeros.

Definition B.10 *The equilibrium state x_e is said to be **asymptotically stable** if (i) it is stable, and (ii) $\exists\ \delta(t_0)$ such that $|x_0 - x_e| < \delta(t_0)$ implies $\lim_{t\to\infty} |x(t; t_0, x_0) - x_e| = 0$.*

Definition B.11 *The equilibrium state x_e is said to be **uniformly asymptotically stable** if (i) it is stable, (ii) for every $\epsilon > 0$ and any $t_0 \in \mathcal{R}^+, \exists a \delta_0 > 0$ independent of t_0 and ϵ and a $T(\epsilon) > 0$ independent of t_0 such that $|x(t; t_0, x_0) - x_e| < \epsilon\ \forall t \geq t_0 + T(\epsilon)$ whenever $|x_0 - x_e| < \delta_0$.*

Definition B.12 *The set of all $x_0 \in \mathcal{R}^n \mid x(t; t_0, x_0) \to x_e$ as $t \to \infty$ for some $t_0 \geq 0$ is called the **region of attraction** of the equilibrium state x_e. If condition (ii) of the above definition is satisfied, then the equilibrium state x_e is said to be **attractive**.*

Definition B.13 *The equilibrium state x_e is said to be **exponentially stable** if there exists an $\alpha > 0$, and for every $\epsilon > 0$ there exists a $\delta(\epsilon) > 0$ such that*

$$|x(t; t_0, x_0) - x_e| \leq \epsilon e^{-\alpha(t-t_0)} \qquad \forall\ t \geq t_0$$

whenever $|x_0 - x_e| < \delta(\epsilon)$.

Definition B.14 *The equilibrium state x_e is said to be **unstable** if it is not stable.*

Definition B.15 *A solution $x(t; t_0, x_0)$ of B.2 is **bounded** if $\exists$ a $\beta > 0$ such that $|x(t; t_0, x_0)| < \beta\ \forall\ t \geq t_0$, where β may depend on each solution.*

Definition B.16 *The solutions of B.2 are **uniformly bounded** if for any $\alpha > 0$ and $t_0 \in \mathcal{R}^+$, there exists a $\beta = \beta(\alpha)$ independent of t_0 such that if $|x_0| < \alpha$, then $|x(t; t_0, x_0)| < \beta\ \forall\ t \geq t_0$.*

Definition B.17 *The solutions of B.2 are **uniformly ultimately bounded** (with bound B) if $\exists$ a $B > 0$ and if corresponding to any $\alpha > 0$ and $t_0 \in \mathcal{R}^+$, $\exists$ a $T = T(\alpha) > 0$ (independent of t_0) such that $|x_0| < \alpha$ implies $|x(t; t_0, x_0)| < B\ \forall\ t \geq t_0 + T$.*

Definition B.18 *The equilibrium point x_e of B.2 is **asymptotically stable in the large** if it is stable and every solution of B.2 tends to x_e as $t \to \infty$ (i.e., the region of attraction of x_e is for all $\mathcal{R}^n$).*

Definition B.19 *The equilibrium point x_e of B.2 is **uniformly asymptotically stable in the large** if (i) it is uniformly stable, (ii) the solutions of B.2 are uniformly bounded, and (iii) for any $\alpha > 0$, any $\epsilon > 0$ and $t_0 \in \mathcal{R}^+, \exists\ T(\epsilon, \alpha) > 0$ independent of t_0 such that if $|x_0 - x_e| < \alpha$ then $|x(t; t_0, x_0)| < \epsilon\ \forall\ t \geq t_0 + T(\epsilon, \alpha)$.*

Definition B.20 *The equilibrium point x_e of B.2 is **exponentially stable in the large** if there exists $\alpha > 0$ and for any $\beta > 0$, there exists $k(\beta) > 0$ such that*

$$|x(t; t_0, x_0)| \leq k(\beta)e^{-\alpha(t-t_0)} \quad \forall\, t \geq t_0$$

whenever $|x_0| < \beta$.

Definition B.21 *A continuous function $\varphi : [0, r] \to \mathcal{R}^+$ (or a continuous function $\varphi : [0, \infty) \to \mathcal{R}^+$) is said to belong to **class** $\mathcal{K}$, i.e., $\varphi \in \mathcal{K}$ if, (i) $\varphi(0) = 0$, (ii)φ is strictly increasing on $[0, r]$ (or on $[0, \infty)$).*

Definition B.22 *A continuous function $\varphi : [0, r] \to \mathcal{R}^+$ is said to belong to **class** $\mathcal{KR}$, i.e., $\varphi \in \mathcal{KR}$ if, (i) $\varphi(0) = 0$, (ii)φ is strictly increasing on $[0, \infty)$, and, (iii) $\lim_{r\to\infty} \varphi(r) = \infty$.*

Definition B.23 *A function $V(t, x) : \mathcal{R}^+ \times \mathcal{B}(r) \to \mathcal{R}$ with $V(t, 0) = 0\ \forall\ t \in \mathcal{R}^+$ is **positive definite** if there exists a continuous function $\varphi \in \mathcal{K}$ such that $V(t, x) \geq \varphi(|x|)\ \forall\ t \in \mathcal{R}^+, x \in \mathcal{B}(r)$ and some $r > 0$. $V(t, x)$ is called **negative definite** if $-V(t, x)$ is positive definite.*

Definition B.24 *A function $V(t, x) : \mathcal{R}^+ \times \mathcal{B}(r) \to \mathcal{R}$ with $V(t, 0) = 0\ \forall\ t \in \mathcal{R}^+$ is said to be **positive (negative) semidefinite** if $V(t, x) \geq 0 (V(t, x) \leq 0) \forall\ t \in \mathcal{R}^+$ and $x \in \mathcal{B}(r)$ for some $r > 0$.*

Definition B.25 *A function $V(t, x) : \mathcal{R}^+ \times \mathcal{B}(r) \to \mathcal{R}$ with $V(t, 0) = 0\ \forall\ t \in \mathcal{R}^+$ is said to be **decrescent** if $\exists\ \varphi \in \mathcal{K}$ such that $|V(t, x)| \leq \varphi(|x|)\ \forall\ t \geq 0$ and $\forall\ x \in \mathcal{B}(r)$ for some $r > 0$.*

Definition B.26 *A function $V(t, x) : \mathcal{R}^+ \times \mathcal{R}^n \to \mathcal{R}$ with $V(t, 0) = 0\, \forall\, t \in \mathcal{R}^+$ is said to be **radially unbounded** if $\exists\ \varphi \in \mathcal{KR}$ such that $V(t, x) \geq \varphi(|x|)\ \forall\ x \in \mathcal{R}^n$ and $t \in \mathcal{R}^+$.*

Theorem B.2 *Suppose there exists a positive definite function $V(t, x) : \mathcal{R}^+ \times \mathcal{B}(r) \to \mathcal{R}$ for some $r > 0$ with continuous first-order partial derivatives with respect to x, t, and $V(t, 0) = 0\ \forall\ t \in \mathcal{R}^+$. Then the following statements are true:*

- *if $\dot{V} \leq 0$, then $x_e = 0$ is **stable**.*
- *if V is decrescent and $\dot{V} \leq 0$, then $x_e = 0$ is **uniformly stable**.*
- *if V is decrescent and $\dot{V} < 0$, then $x_e = 0$ is **uniformly asymptotically stable**.*
- *if V is decrescent and $\exists\ \varphi_1, \varphi_2, \varphi_3 \in \mathcal{K}$ of the same order of magnitude such that*

$$\varphi_1(|x|) \leq V(t, x) \leq \varphi_2(|x|), \quad \dot{V}(t, x) \leq -\varphi_3(|x|)$$

*$\forall\ x \in \mathcal{B}(r)$ and $t \in \mathcal{R}^+$, then $x_e = 0$ is **exponentially stable**.*

Theorem B.3 *Suppose that B.2 possesses unique solutions for all $x_0 \in \mathcal{R}^n$. Suppose $\exists$ a positive definite, decrescent and radially unbounded function $V(t,x) : \mathcal{R}^+ \times \mathcal{R}^n \rightarrow \mathcal{R}^+$ with continuous first-order partial derivative with respect to t, x and $V(t,0) = 0 \; \forall \; t \in \mathcal{R}^+$. Then the following statements are true:*

- *if $\dot{V} < 0$, then $x_e = 0$ is **uniformly asymptotically stable in the large**.*
- *if $\exists \; \varphi_1, \varphi_2, \varphi_3 \in \mathcal{KR}$ of the same order of magnitude such that*

$$\varphi_1(|x|) \leq V(t,x) \leq \varphi_2(|x|), \quad \dot{V}(t,x) \leq -\varphi_3(|x|)$$

*then $x_e = 0$ is **exponentially stable in the large**.*

Theorem B.4 *Assume that B.2 possesses unique solution $\forall \; x_0 \in \mathcal{R}^n$. If $\exists$ a function $V(t,x)$ defined on $|x| \geq R$ (where R may be large) and $t \in [0, \infty)$ with continuous first-order partial derivatives with respect to x, t and if $\exists \; \varphi_1 \varphi_2 \in \mathcal{KR}$ such that*

- $\varphi_1(|x|) \leq V(t,x) \leq \varphi_2(|x|)$
- $\dot{(V)}(t,x) \leq 0$

$\forall \; |x| \geq R$ and $t \in [0, \infty)$, then, the solution of B.2 are uniformly bounded. If in addition $\exists \varphi_3 \in \mathcal{K}$ defined on $[0, \infty)$ and

- *$\dot{V}(t,x) \leq -\varphi_3(|x|) \; \forall |x| \geq R$ and $t \in [0, \infty)$*

then, the solution of B.2 are uniformly ultimately bounded.

Definition B.27 *A set Ω in $\mathcal{R}^n$ is **invariant** with respect to equation B.3 if every solution of B.3 starting in Ω remains in $\Omega \; \forall \; t$.*

Theorem B.5 *Assume that B.3 possesses unique solutions $\forall \; x_0 \in \mathcal{R}^n$. Suppose there exists a positive definite and radially unbounded function $V(x) : \mathcal{R}^n \rightarrow \mathcal{R}^+$ with continuous first-order derivatives with respect to x and $V(0) = 0$. If*

- *$\dot{V} \leq 0 \; \forall \; x \in \mathcal{R}^n$*
- *The origin $x = 0$ is the only invariant subset of the set*

$$\Omega = \{x \in \mathcal{R}^n | \dot{V} = 0\} \tag{B.4}$$

*then the equilibrium $x_e = 0$ of B.3 is **asymptotically stable in the large**.*

B.4 Positive Real and Strictly Positive Real Transfer Functions

Definition B.28 *A rational transfer function $G(s)$ of the complex variables $s = \sigma + j\omega$ is called PR if*

- *$G(s)$ is real for real s.*
- *$Re[G(s)] \geq 0 \; \forall \; Re[s] > 0$.*

Lemma B.4 *A ration proper transfer function $G(s)$ is PR if and only if*

- *$G(s)$ is real for real s.*
- *$G(s)$ is analytic in $Re[s] > 0$, and the poles on the $j\omega$-axis are simple and such that the associated residues are real and positive.*
- *For all real value of ω for which $s = j\omega$ is not a pole of $G(s)$, one has $Re[G(j\omega)] \geq 0$.*

Definition B.29 *Assume that $G(s)$ is not identically zero for all s. Then $G(s)$ is SPR if $G(s-\epsilon)$ is PR for some $\epsilon > 0$.*

Theorem B.6 *Assume that a rational function $G(s)$ of the complex variable $s = \sigma + j\omega$ is real for real s and is not identically zero for all s. Let n^* be the relative degree[3] of $G(s) = Z(s)/R(s)$ with $|n^*| \leq 1$. Then, $G(s)$ is SPR if and only if*

- *$G(s)$ is analytic in $Re[s] \geq 0$*
- *$Re[G(j\omega)] > 0, \forall \; \omega \in (-\infty, \infty)$*
- 1. *When n^* = 1, $\lim_{|\omega| \to \infty} \omega^2 Re[G(j\omega)] > 0$.*
  2. *When n^* = -1, $\lim_{|\omega| \to \infty} \dfrac{G(j\omega)}{j\omega} > 0$.*

Corollary B.3

1. *$G(s)$ is PR (SPR) if and only if $1/G(s)$ is PR (SPR)*
2. *If $G(s)$ is SPR, then, $|n^*| \leq 1$, and the zeros and poles of $G(s)$ lie in $Re[s] < 0$.*
3. *if $|n^*| > 1$, then $G(s)$ is not PR.*

Lemma B.5 (Kalman-Yakubovich-Popov (KYP) Lemma) *Given a square matrix A with all eigenvalues in the closed left half complex plane, a vector B such that (A,B) is controllable, a vector C and a scalar $d \geq 0$, the transfer function defined by*

$$G(s) = d + C^\top (sI - A)^{-1} B \tag{B.5}$$

[3] relative degree is the difference between, the degree of denominator polynomial and the degree of numerator polynomial

is PR if and only if there exist a symmetric positive definite matrix P and a vector q such that

$$A^\top P + PA = -qq^\top \tag{B.6}$$

$$PB - C = \pm q\sqrt{2d} \tag{B.7}$$

Lemma B.6 (Meyer-Kalman-Yakubovich (MKY) Lemma) *Given a stable matrix, vector B, C and a scalar $d \geq 0$, we have the following:*

$$G(s) = d + C^\top (sI - A)^{-1} B \tag{B.8}$$

is SPR, then for any given $L = L^\top > 0$, there exists a scalar $\nu > 0$, a vector q and a positive definite matrix $P = P^\top$ such that

$$A^\top P + PA = -qq^\top - \nu L \tag{B.9}$$

$$PB - C = \pm q\sqrt{2d} \tag{B.10}$$

Theorem B.7 *If A_c is stable matrix and $G(s) = C^\top (sI - A_c)^{-1} B_c$ is SPR, then $e, \theta, \omega \in \mathcal{L}_\infty; e, \dot{\theta} \in \mathcal{L}_\infty \cap \mathcal{L}_2$ and $e(t), e_1(t), \dot{\theta}(t) \to 0$ as $t \to \infty$*

APPENDIX C

Model Reference Adaptive Control: Supplement

This appendix provides additional material for the adaptive control designs in Chapter 2. A brief discussion on model reference adaptive control design for a relative degree one system is discussed. This appendix also includes the necessary and sufficient condition for the choice of the parameter p_0 in the ploynomial $L(s)$. The polynomial $L(s)$ is added to the system to satisfy the SPR condition.

C.1 MRAC for Relative Degree 1 System

In this section the model reference adaptive controller design for relative degree one systems is described in detail. This design procedure can be extended to relative degree two systems as long as the SPR condition is satisfied. The design and analysis in this section forms the basis for the model reference adaptive controllers designed in chapter 2.

Consider a system and a desired reference model both having relative degree one.

$$\dot{y} = Ay + Bu, \quad y_L = C^\top y \tag{C.1a}$$

$$\dot{x} = A_c x + B_c r, \quad y_m = C_c^\top x \tag{C.1b}$$

Assuming that it is possible to find a parametrized control law $u = {\theta^*}^\top \omega$ which could result in a closed-loop system having the same dynamics of the reference model, then the error equation $\dot{\epsilon} = \dot{y} - \dot{x}$ and hence the tracking error is given by

$$\dot{\epsilon} = A_c \epsilon + B\tilde{\theta}^\top \omega, \quad \tilde{\theta} = \theta - \theta^* \tag{C.2a}$$

$$e_1 = y_L - y_m = [1 \quad 0]\epsilon = C_c^\top \epsilon \tag{C.2b}$$

Let us define the estimate of tracking error to be

$$\hat{e}_1 = W_m(s)\rho\left[u - \theta^\top \omega\right] \tag{C.3}$$

where ρ is an estimate of ρ^*, θ is the estimate of the parameter vector θ^*. Notice that

$$\hat{e}_1 = W_m(s)\rho\left[u - \theta^\top \omega\right] = W_m(s)\rho[0], \quad \because u = \theta^\top \omega \tag{C.4}$$

Notice that since $W_m(s)$ is SPR, when $\hat{e}_1(0) = 0, \hat{e}_1 = 0, \forall t \geq 0$. Hence there is no need to generate $\hat{e}_1 \Rightarrow \epsilon_1 = e_1 - \hat{e}_1 = e_1$. Hence the error dynamics reduces to

$$\dot{\epsilon} = A_c\epsilon + B_c\rho^*[\theta^\top\omega - {\theta^*}^\top\omega] = A_c\epsilon + B_c\rho^*\tilde{\theta}^\top\omega \tag{C.5a}$$

$$e_1 = W_m(s)\rho^*\tilde{\theta}^\top\omega, \qquad \tilde{\theta} \triangleq \theta(t) - \theta^* \tag{C.5b}$$

This error dynamics is suitable for SPR-Lyapunov design since the output tracking error e_1 is related to the parameter error $\tilde{\theta}$ by a SPR transfer function.

Consider a lyapunov function candidate as

$$V(\tilde{\theta}, \epsilon) = \frac{\epsilon^\top P_c \epsilon}{2} + \frac{\tilde{\theta}^\top \Gamma^{-1}\tilde{\theta}|\rho^*|}{2} \tag{C.6}$$

where $\Gamma = \Gamma^\top > 0, P_c = P_c^\top > 0$ satisfies the following algebric equations

$$P_c A_c + A_c^\top P_c = -qq^\top - \nu L_c \tag{C.7}$$

$$P_c B_c = C_c \tag{C.8}$$

for some matrix $L_c = L_c^\top > 0$, some vector q, and a small positive constant. $\because A_c$ is stable using the MKY lemma (B.6) we can always find a positive definited matrix P_c. Taking the time derivative of V in equation C.6 along the trajectories of C.5.

$$\dot{V} = \underbrace{\frac{\epsilon^\top A_c^\top P_c \epsilon}{2}} + \underbrace{\frac{(B_c\rho^*\tilde{\theta}^\top\omega)^\top P_c\epsilon}{2}} + \underbrace{\frac{\epsilon^\top P_c A_c \epsilon}{2}} + \underbrace{\frac{\epsilon^\top P_c(B_c\rho^*\tilde{\theta}^\top\omega)}{2}} + \dot{\tilde{\theta}}^\top\Gamma^{-1}\tilde{\theta}|\rho^*| \tag{C.9}$$

$$= \underbrace{-\frac{\epsilon^\top qq^\top\epsilon}{2} - \frac{\epsilon^\top\nu_c L_c^\top\epsilon}{2}} + \underbrace{\epsilon^\top P_c B_c\rho^*\tilde{\theta}^\top\omega} + \dot{\tilde{\theta}}^\top\Gamma^{-1}\tilde{\theta}|\rho^*| \tag{C.10}$$

if

$$\dot{\tilde{\theta}}^\top\Gamma^{-1}\tilde{\theta}|\rho^*| = \epsilon^\top P_c B_c\rho^*\tilde{\theta}^\top\omega \tag{C.11}$$

then, $\dot{V} \leq 0$. Notice that in equation C.11 ρ^* can be written as $\rho^* = |\rho^*|\text{sgn}(\rho^*)$ and the equation reduces to

$$\dot{\tilde{\theta}}^\top\Gamma^{-1}\tilde{\theta}|\rho^*| = -\epsilon^\top P_c B_c\omega^\top\tilde{\theta}|\rho^*|\text{sgn}(\rho^*) \tag{C.12}$$

using the fact that $\tilde{\theta}^\top \omega = \omega^\top \tilde{\theta} \in \mathcal{R}$. Hence the adaptive law is given by

$$\dot{\tilde{\theta}}^\top = -\text{sgn}(\rho^*)\epsilon^\top \underbrace{P_c B_c}\omega^\top \Gamma \tag{C.13}$$

$$= -\text{sgn}(\rho^*)\underbrace{\epsilon^\top C_c}\omega^\top \Gamma \tag{C.14}$$

$$\dot{\tilde{\theta}} = -e_1 \text{sgn}(\rho^*)\Gamma\omega \quad (\because \Gamma = \Gamma^\top) \tag{C.15}$$

$$\dot{\tilde{\theta}} = \dot{\theta} - \dot{\theta}^* = \dot{\theta} = -e_1 \text{sgn}(\rho^*)\Gamma\omega \tag{C.16}$$

C.1.0.1 Analysis

Because $V > 0$ and $\dot{V} \leq 0$, V is bounded or $V \in \mathcal{L}_\infty \Rightarrow \epsilon, \theta, \tilde{\theta} \in \mathcal{L}_\infty$. With $\epsilon \in \mathcal{L}_\infty$ we get $y, x \in \mathcal{L}_\infty$. ω being the states or the filtered version of the states along with the reference trajectory, $\because y \in \mathcal{L}_\infty, \Rightarrow \omega \in \mathcal{L}_\infty \Rightarrow u = \theta^\top \omega \in \mathcal{L}_\infty$. Therefore all the signals in the closed-loop system are bounded. As seen in section **??** on page **??**, it can been shown that $\epsilon \in \mathcal{L}_2$ and hence $e_1 = C_c^\top \epsilon \in \mathcal{L}_2$. From the error, since the matirx A_c is stable and the input $\tilde{\theta}^\top \omega \in \mathcal{L}_\infty$, $\Rightarrow \dot{\epsilon} \in \mathcal{L}_\infty \Rightarrow \dot{e}_1 = C_c^\top \dot{\epsilon} \in \mathcal{L}_\infty$. Therefore from $e_1, \dot{e}_1 \in \mathcal{L}_\infty$ and $e_1 \in \mathcal{L}_2$, using lemma B.2 we have $e_1(t) \to 0$ as $t \to \infty$.

C.2 Choice of parameter p_0

This section formulates the necessary and sufficient condition for the choice of the design parameter p_0 in $L(s) = s + p_0$ which makes $W_m(s)L(s)$ SPR. The relative degree of the reference model and the plant model is 2. In order to use the SPR lyapunov design a relative degree $n^* = -1$ transfer function, $(s + p_0)$, is cascaded with the reference model so that the relative degree of the combined system is one[1].

$$K(s) = G(s)(s + p_0)$$

where,

$$G(s) = \frac{\omega_n^2}{(s^2 + 2\zeta\omega_n s + \omega_n^2)}$$

Applying theorem corollary B.3 we find that $p_0 > 0$. Applying theorem B.6 we find the following.

[1]Note that a transfer function $G(s)$ can be SPR only if its relative degree is less than or equal to one and $1/G(s)$ is SPR (Corollary B.3).

- If $G(s)$ is stable and $p_0 > 0$, then $K(s)$ is analytic in $Re[s] \geq 0$.

- For $Re[K(j\omega)] > 0, \forall\, \omega \in (-\infty, \infty)$

$$\begin{aligned} K(s) &= \frac{(s+p_0)\omega_n^2}{s^2 + 2\zeta\omega_n s + \omega_n^2} \\ K(j\omega) &= \frac{(j\omega+p_0)\omega_n^2}{-\omega^2 + 2\zeta\omega\omega_n j + \omega_n^2} \\ &= \frac{\omega_n^2(j\omega+p_0)[(\omega_n^2-\omega^2) - 2\zeta\omega_n\omega j]}{(\omega_n^2-\omega^2)^2 + (2\zeta\omega_n\omega)^2} \\ Re[K(j\omega)] &= \frac{\omega_n^2 p_0(\omega_n^2-\omega^2) + 2\zeta\omega_n^3\omega^2}{(\omega_n^2-\omega^2)^2 + (2\zeta\omega_n\omega)^2} \end{aligned}$$

$$\omega_n^2 p_0(\omega_n^2-\omega^2) + 2\zeta\omega_n^3\omega^2 > 0 \text{ for } Re[K(j\omega)] > 0$$

$$\text{if } (2\zeta\omega_n^3 - p_0\omega_n^2)\omega^2 > 0 \text{ then, } Re[K(j\omega)] > 0$$

  Hence, p_0 has to be less than $2\zeta\omega_n$.

- For the third condition i.e., When n^* = 1, $\lim_{|\omega|\to\infty} \omega^2 Re[K(j\omega)] > 0$

$$\begin{aligned} \lim_{|\omega|\to\infty} \omega^2 Re[K(j\omega)] &= \lim_{|\omega|\to\infty} \omega^2 \frac{\omega_n^2 p_0(\omega_n^2-\omega^2) + 2\zeta\omega_n^3\omega^2}{(\omega_n^2-\omega^2)^2 + (2\zeta\omega_n\omega)^2} \\ &= \lim_{|\omega|\to\infty} \frac{[2\zeta\omega_n^3 - p_0\omega_n^3] + p_0\omega_n^4/\omega^2}{1 + \omega_n^4/\omega^4 + (4\zeta\omega_n^2 - 2\zeta\omega_n^2)/\omega^2} \\ &= 2\zeta\omega_n^3 - p_0\omega_n^3 \end{aligned}$$

$$\Rightarrow 2\zeta\omega_n > p_0 \text{ to satisfy the above condition.}$$

Hence p_0 has to be chosen based on the reference model such that $0 < p_0 < 2\zeta\omega_n$.

APPENDIX D

Additional Experimental Results

D.1 Three Parameter Guide Adaptive Controller

D.1.1 Experiments with opaque web

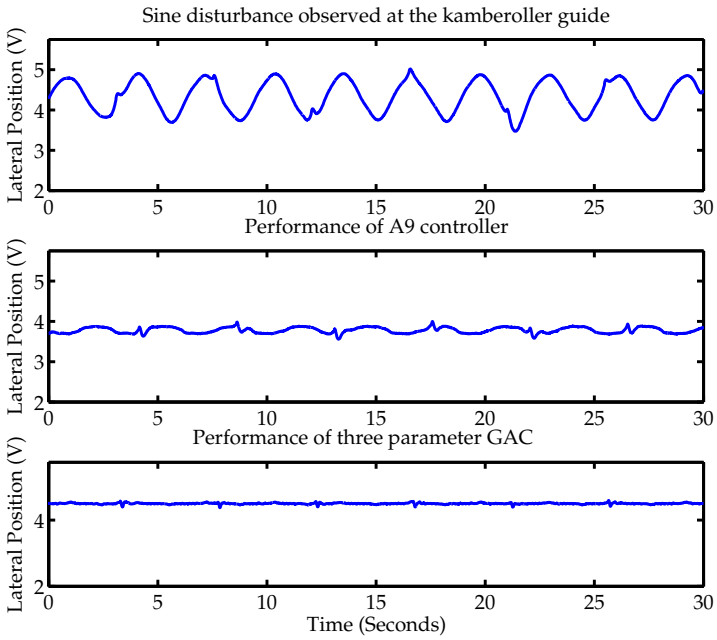

Figure D.1: Performance Comparison: 3-Parameter, 500 fpm, Sine Disturbance, Opaque Web

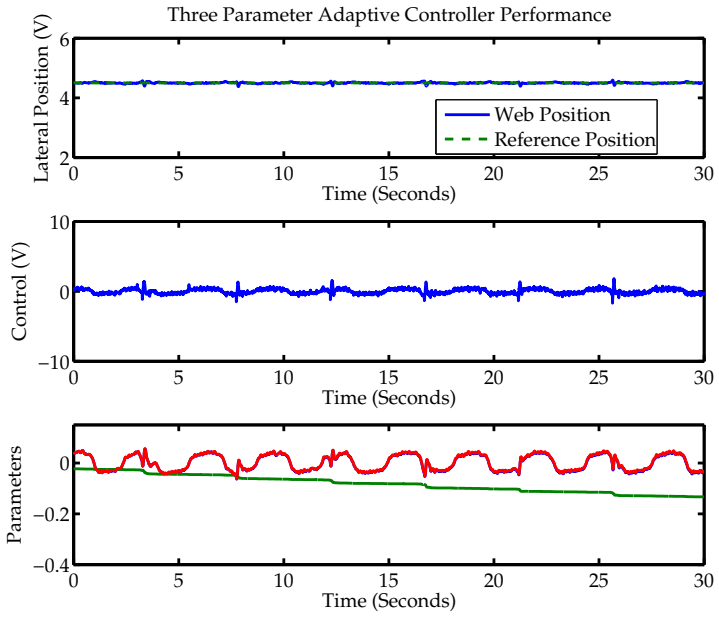

Figure D.2: Adaptive Controller: 3-Parameter, 500 fpm, Sine Disturbance, Opaque Web

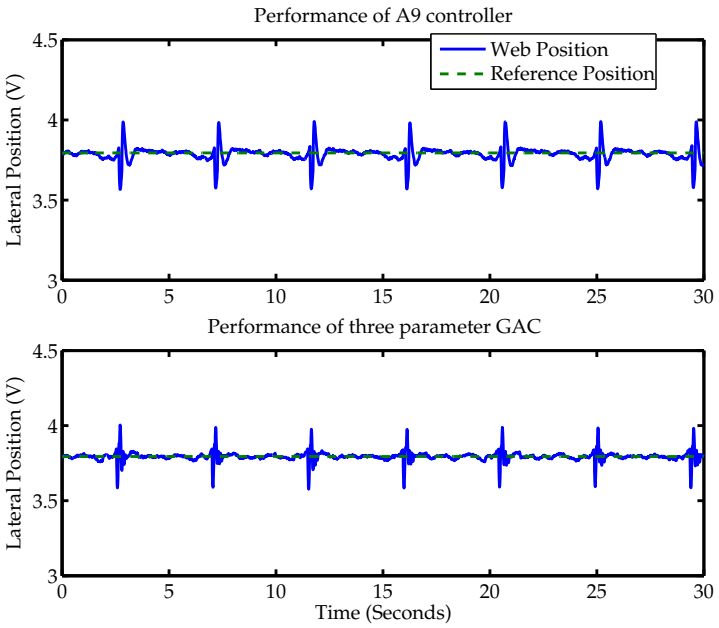

Figure D.3: Performance Comparison: 3-Parameter, 500 fpm, Pulse Disturbance, Opaque Web

D.1.2 Experiments with transparent web

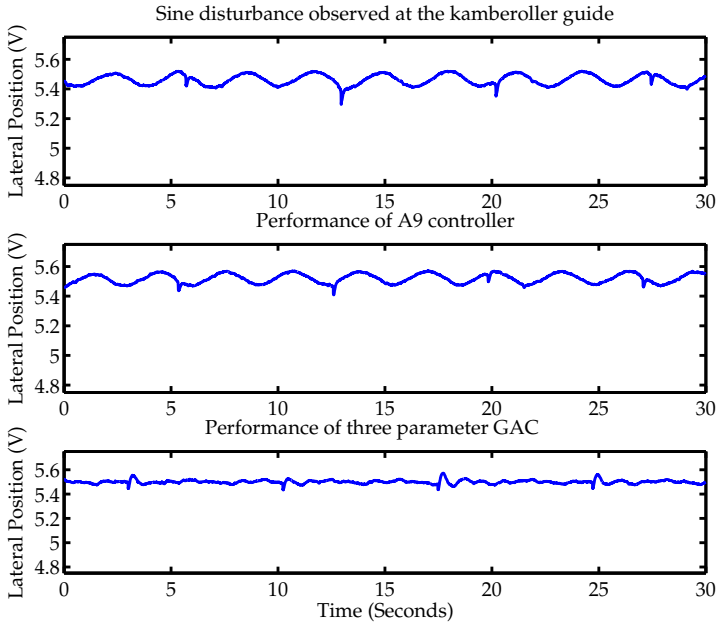

Figure D.4: Performance Comparison: 3-Parameter, 300 fpm, Sine Disturbance, Transparent Web

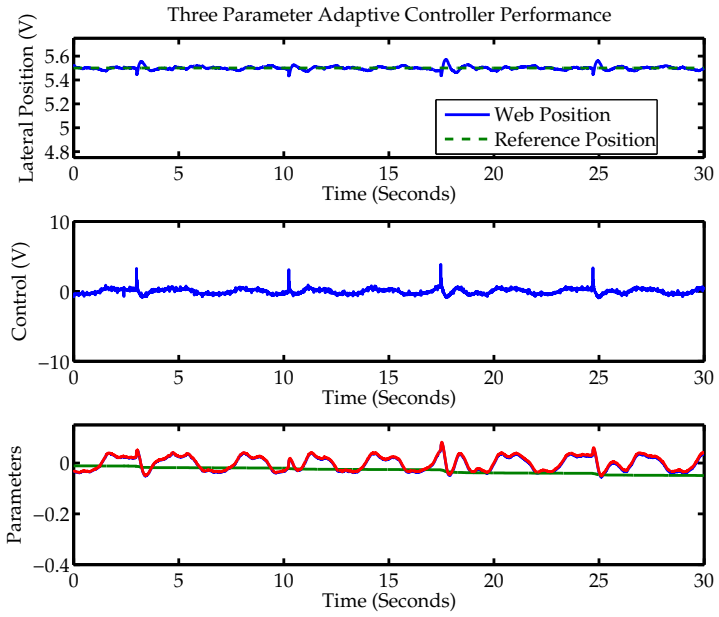

Figure D.5: Adaptive Controller: 3-Parameter, 300 fpm, Sine Disturbance, Transparent

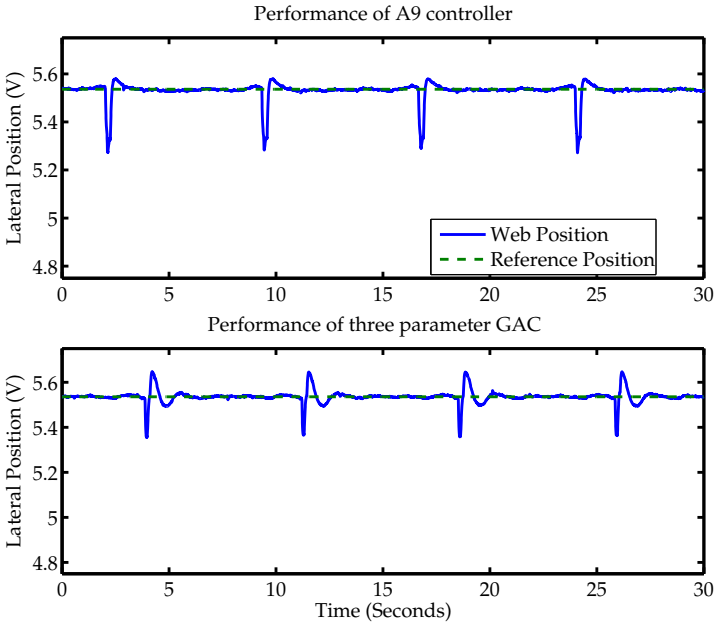

Figure D.6: Performance Comparison: 3-Parameter, 300 fpm, Pulse Disturbance, Transparent

D.2 Four Parameter Guide Adaptive Controller

D.2.1 Experiments with opaque web

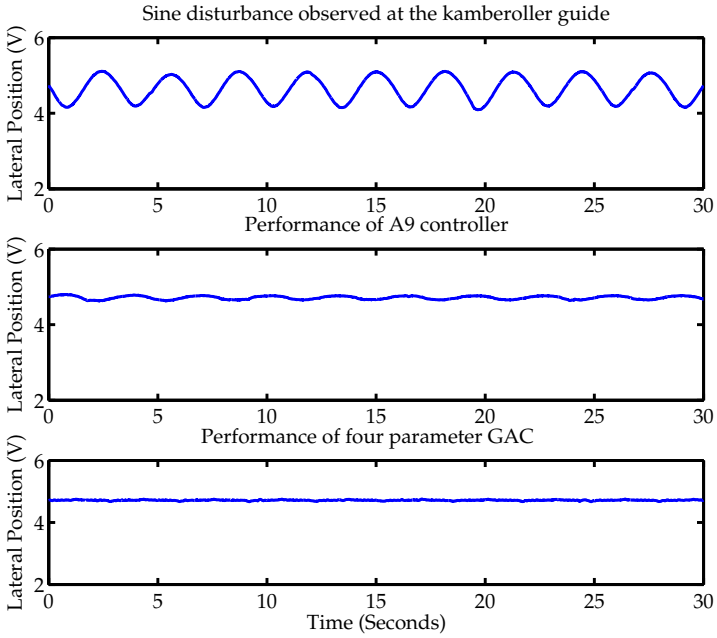

Figure D.7: Performance Comparison: 4-Parameters, 300 fpm, Sine Disturbance, Opaque Web

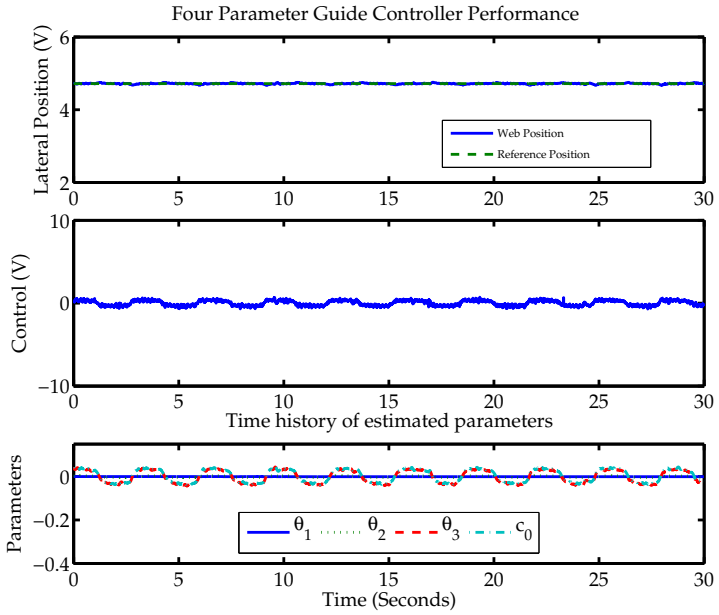

Figure D.8: Adaptive Controller: 4-Parameters, 300 fpm, Sine Disturbance, Opaque Web

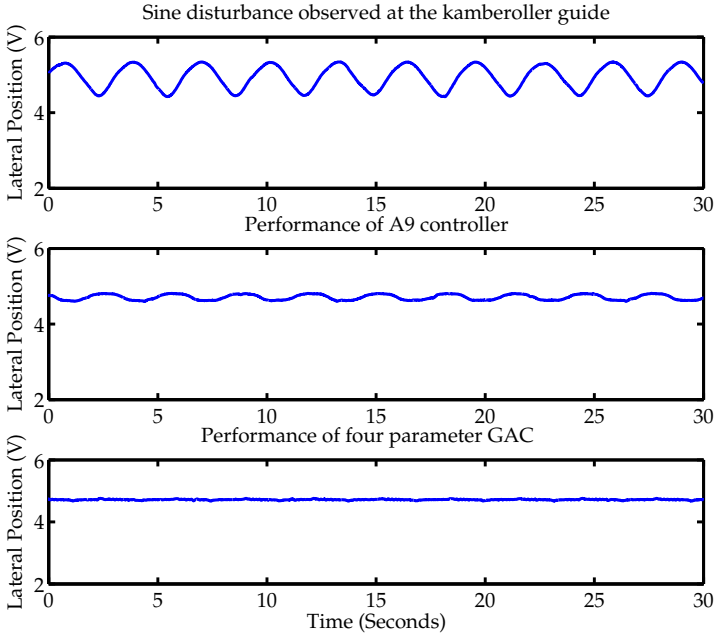

Figure D.9: Performance Comparison: 4-Parameters, 500 fpm, Sine Disturbance, Opaque Web

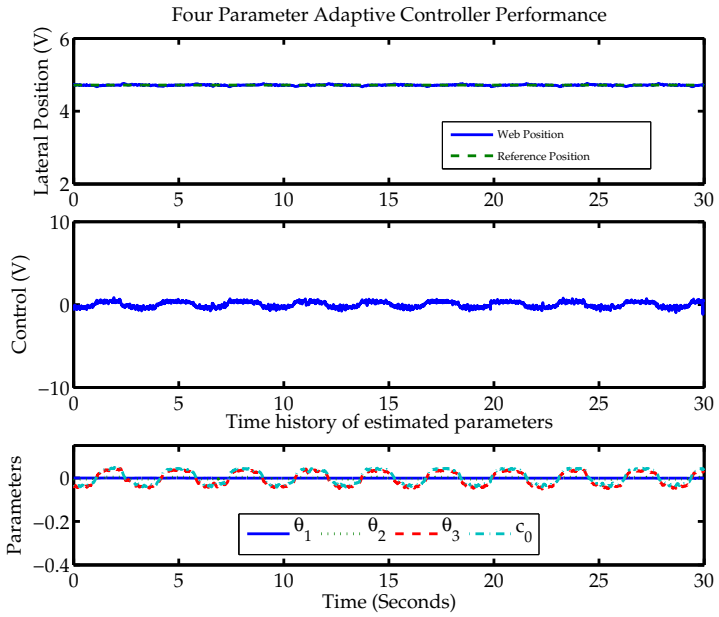

Figure D.10: Adaptive Controller: 4-Parameters, 500 fpm, Sine Disturbance, Opaque Web

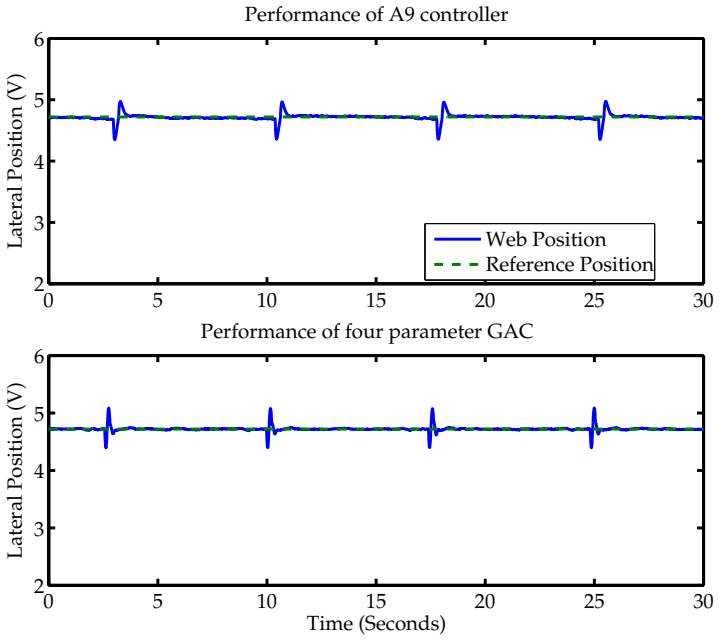

Figure D.11: Performance Comparison: 4-Parameters, 300 fpm, Pulse Disturbance, Opaque Web

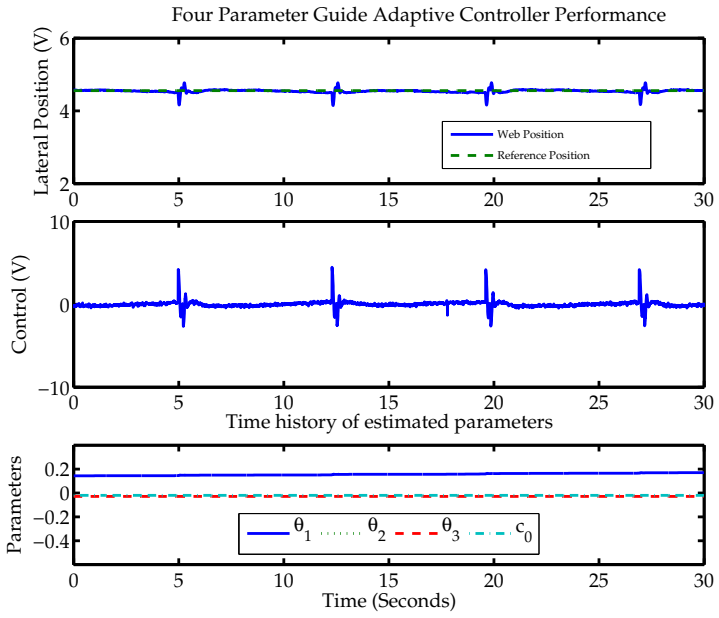

Figure D.12: Adaptive Controller : 4-Parameters, 300 fpm, Pulse Disturbance, Steady-State, Opaque Web

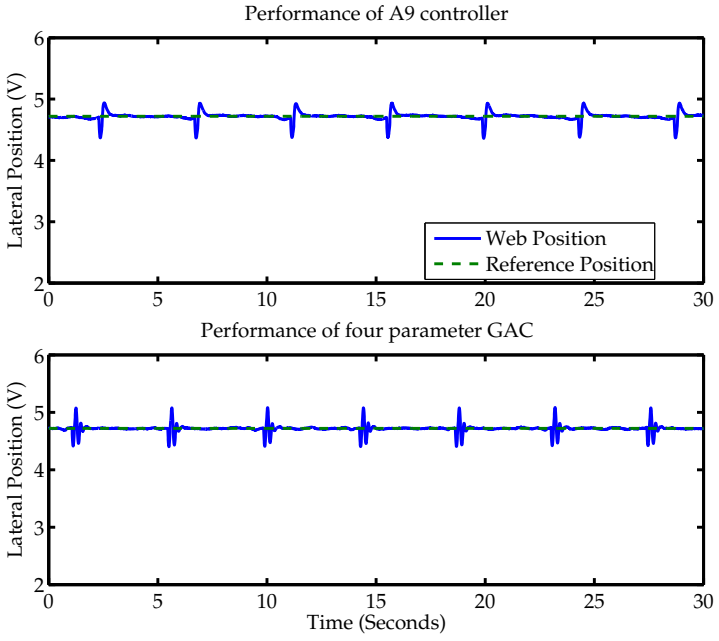

Figure D.13: Performance Comparison: 4-Parameters, 500 fpm, Pulse Disturbance, Opaque Web

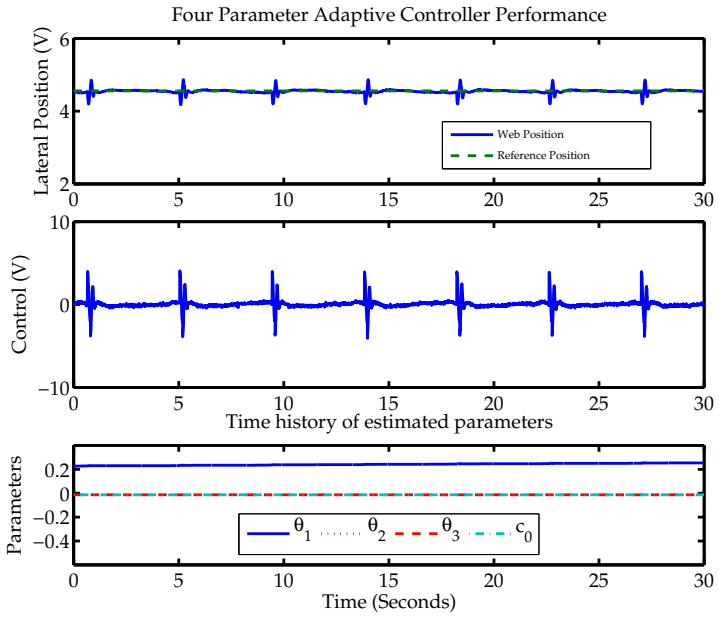

Figure D.14: Performance Comparison: 4-Parameters, 500 fpm, Pulse Disturbance, Steady-State, Opaque Web

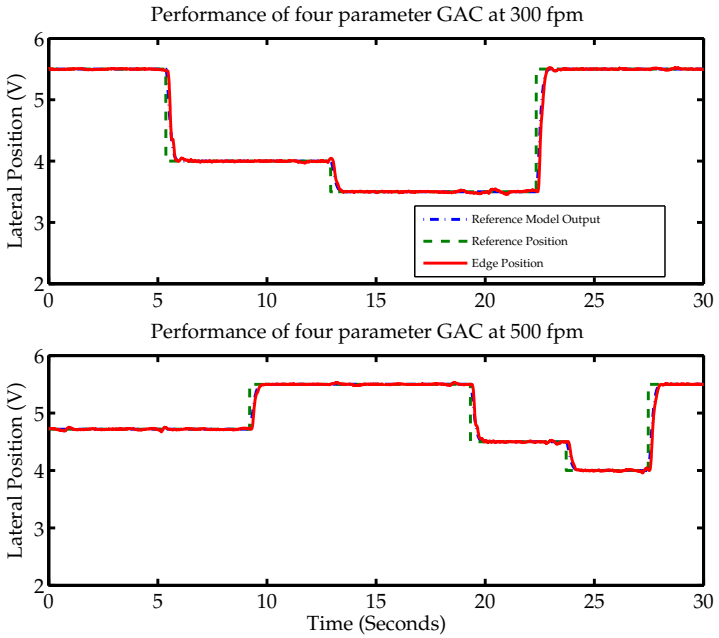

Figure D.15: Adaptive Controller: 4-Parameter, 300 and 500 fpm, Step Reference Changes, Opaque Web

D.2.2 Experiments with transparent web

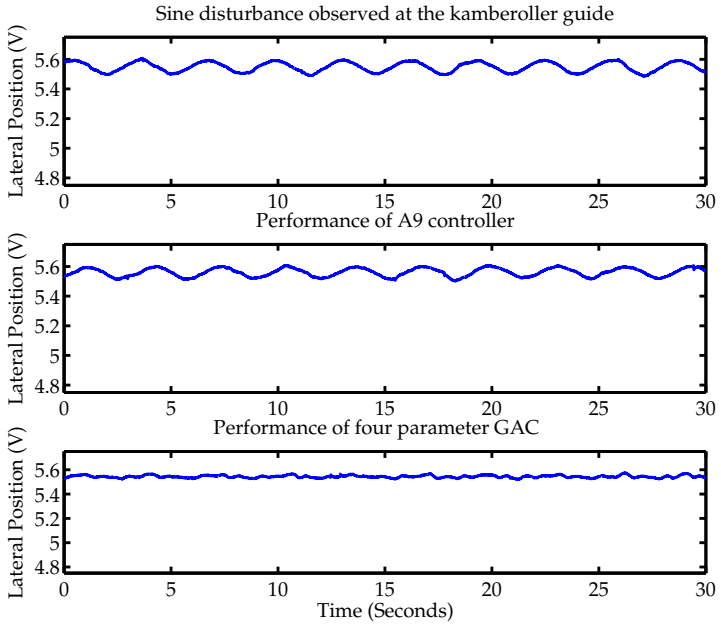

Figure D.16: Performance Comparison: 4-Parameters, 300 fpm, Sine Disturbance, Transparent Web

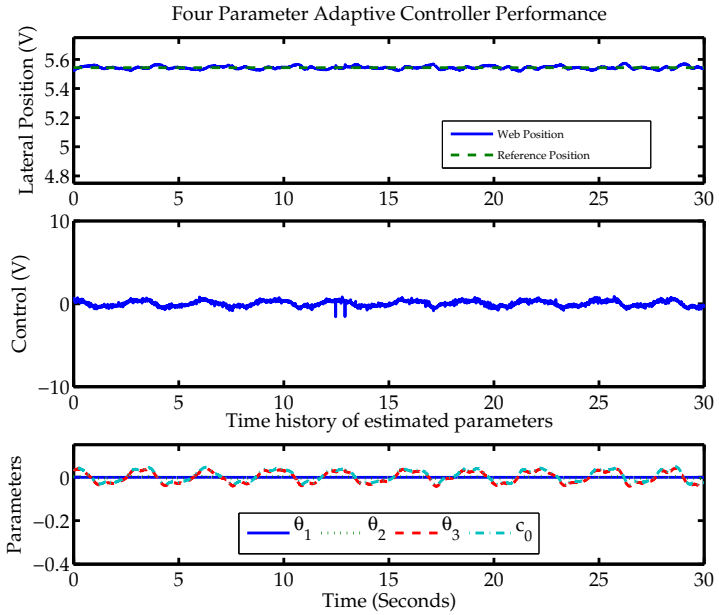

Figure D.17: Adaptive Controller: 4-Parameters, 300 fpm, Sine Disturbance, Transparent Web

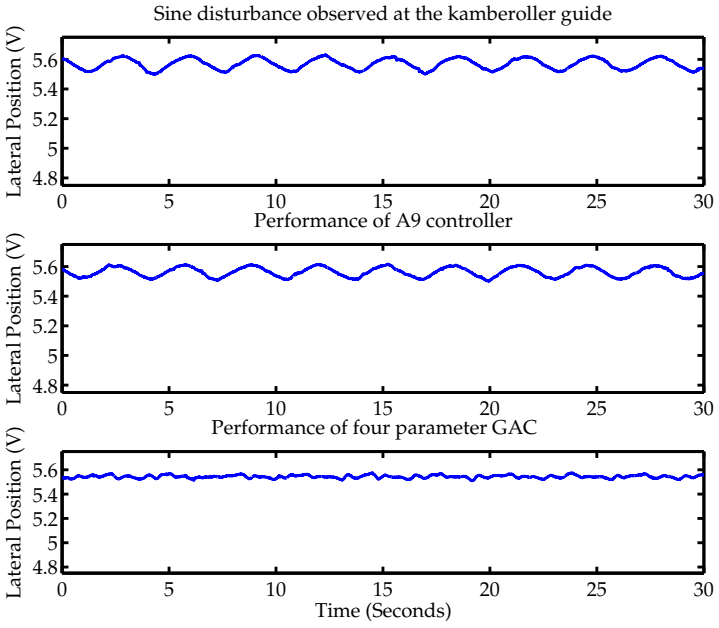

Figure D.18: Performance Comparison: 4-Parameters, 500 fpm, Sine Disturbance, Transparent Web

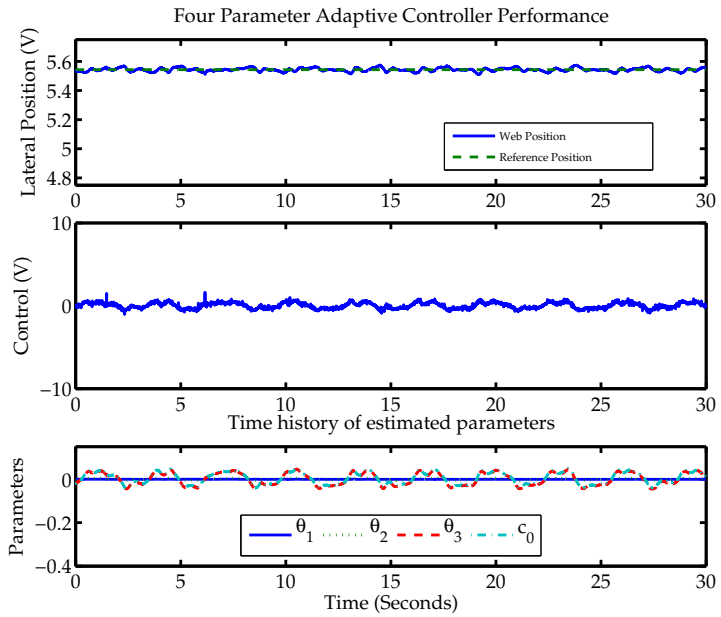

Figure D.19: Adaptive Controller: 4-Parameters, 500 fpm, Sine Disturbance, Transparent Web

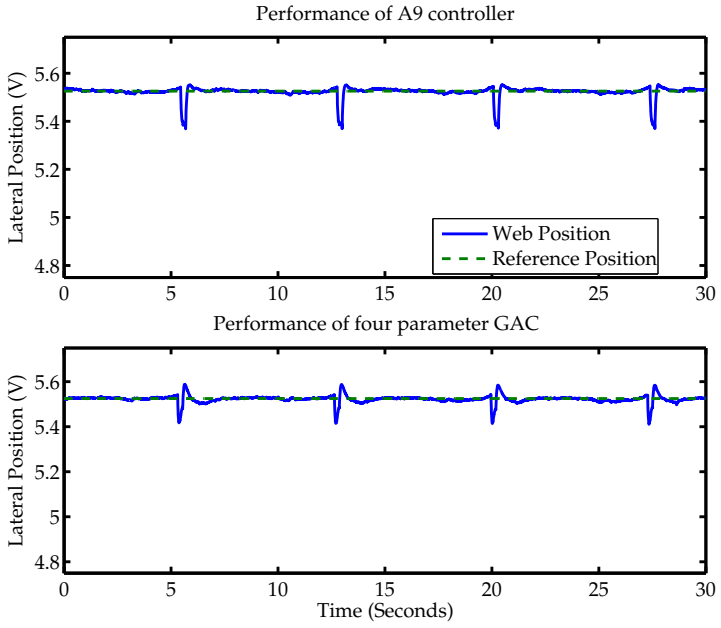

Figure D.20: Performance Comparison: 4-Parameters, 300 fpm, Pulse Disturbance, Transparent Web

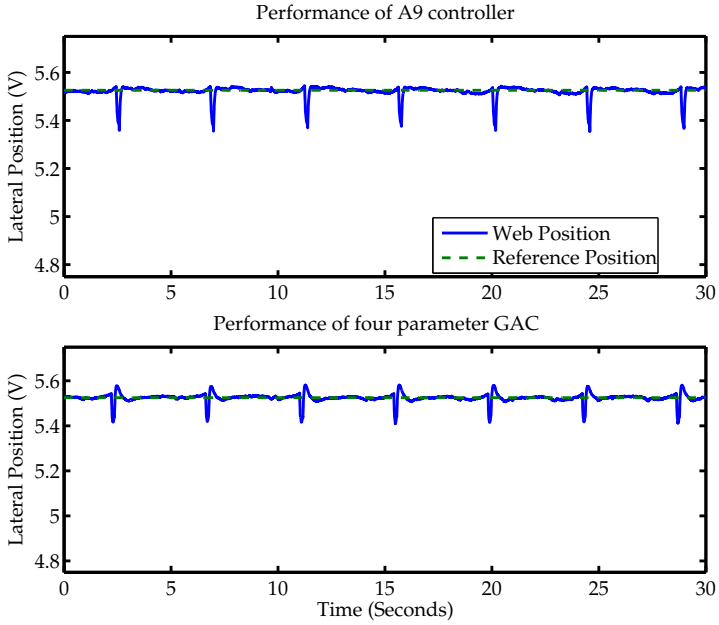

Figure D.21: Performance Comparison: 4-Parameters, 500 fpm, Pulse Disturbance, Transparent Web

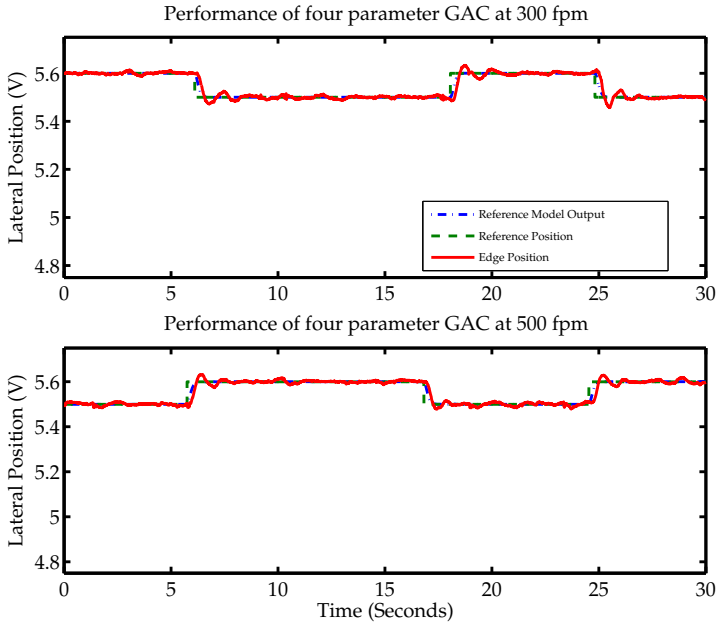

Figure D.22: Adaptive Controller: 4-Parameters, 300 and 500 fpm, Step Reference Changes, Transparent Web

D.3 Guide Adaptive Controller

D.3.1 Experiments with opaque web

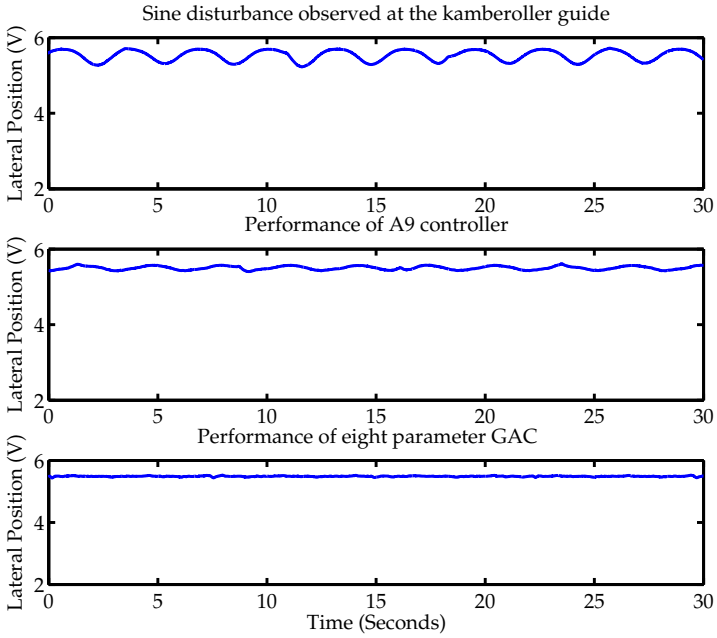

Figure D.23: Performance Comparison: 8-Parameters, 300 fpm, Sine Disturbance, Opaque Web

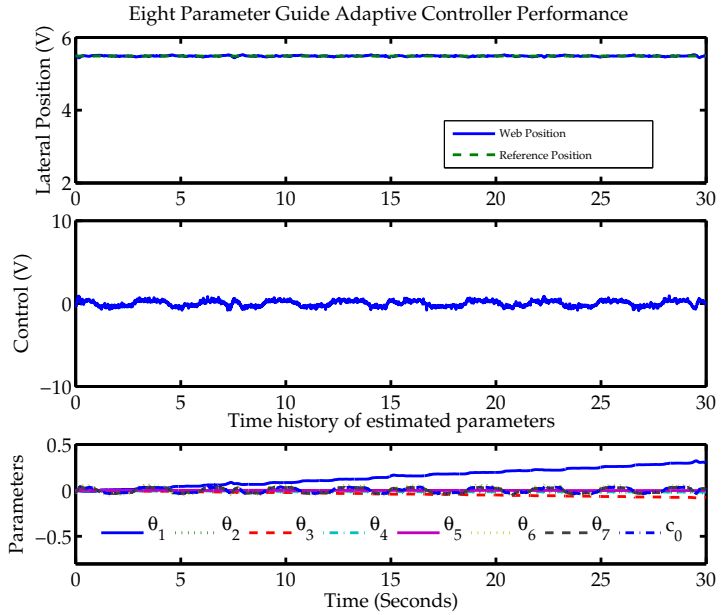

Figure D.24: Adaptive Controller: 8-Parameters, 300 fpm, Sine Disturbance, Opaque Web

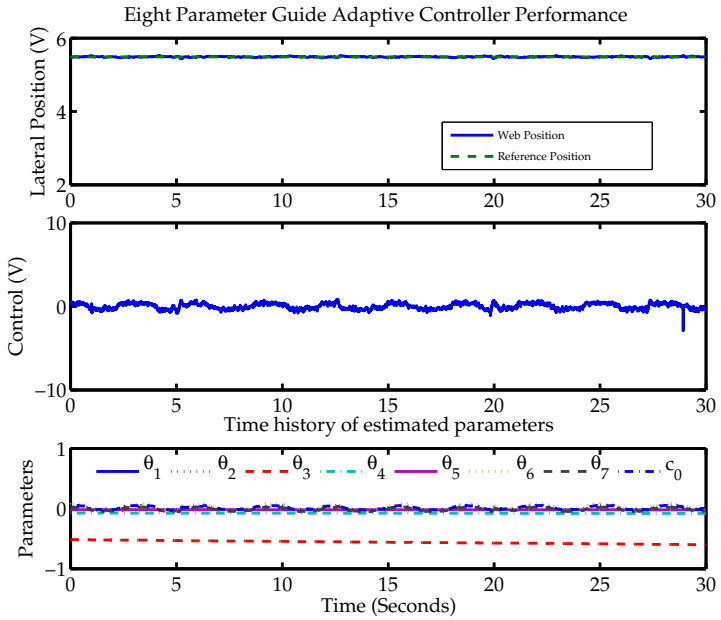

Figure D.25: Adaptive Controller: 8-Parameters, 300 fpm, Sine Disturbance, Setady-State, Opaque Web

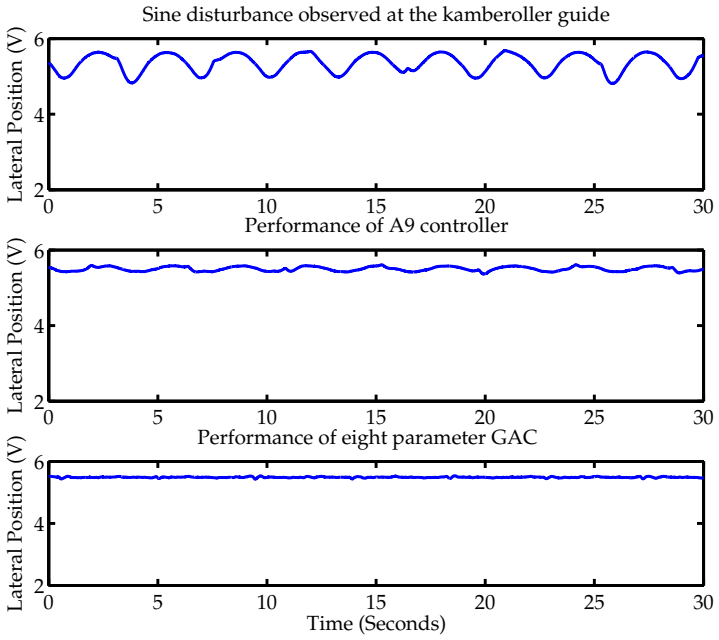

Figure D.26: Performance Comparison: 8-Parameters, 500 fpm, Sine Disturbance, Opaque Web

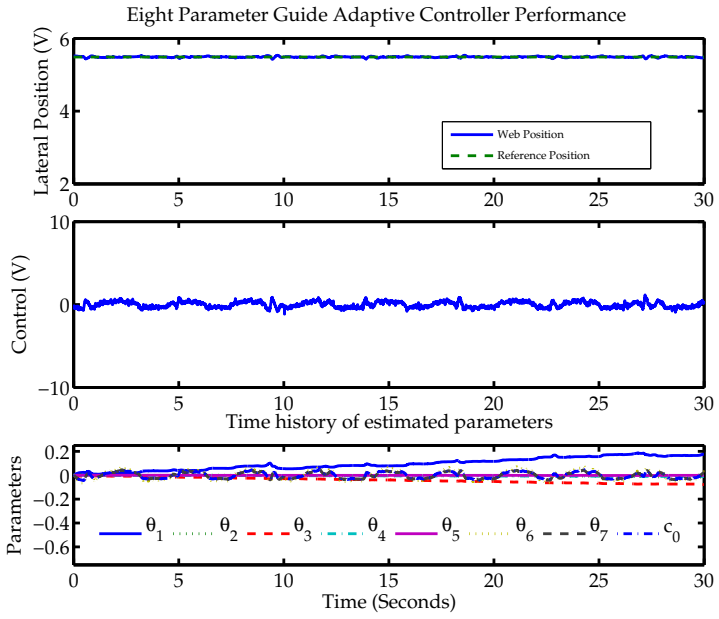

Figure D.27: Adaptive Control: 8-Parameters, 500 fpm, Sine Disturbance, Opaque Web

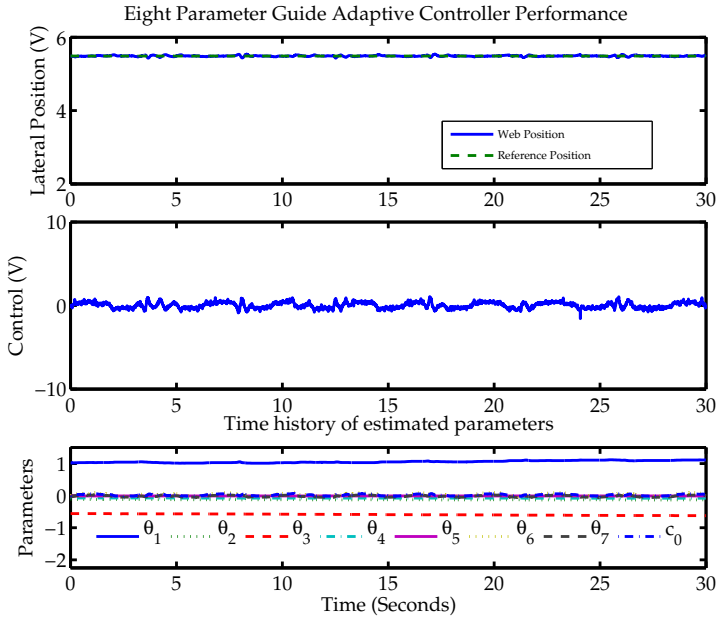

Figure D.28: Adaptive Control: 8-Parameters, 500 fpm, Sine Disturbance, Steady-State, Opaque Web

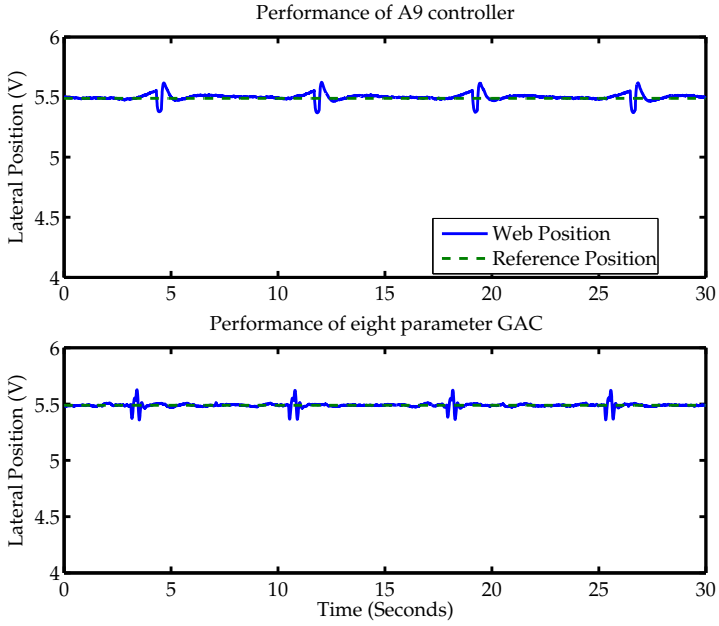

Figure D.29: Performance Comparison: 8-Parameters, 300 fpm, Pulse Disturbance, Opaque Web

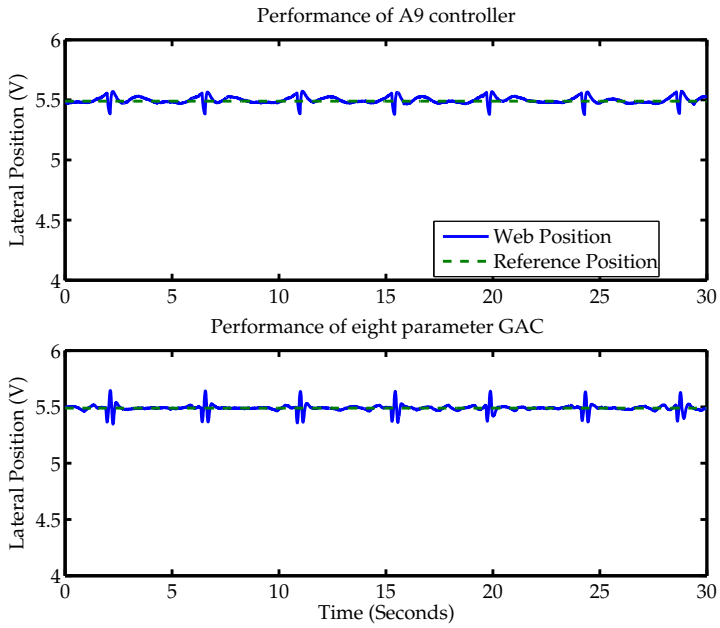

Figure D.30: Performance Comparison: 8-Parameters, 500 fpm, Pulse Disturbance, Opaque Web

D.3.2 Experiments with transparent web

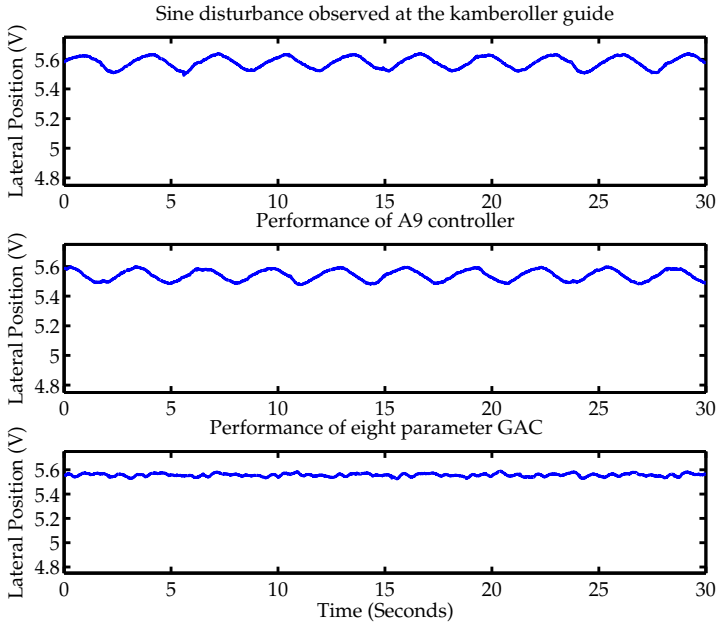

Figure D.31: Performance Comparison: 8-Parameters, 500 fpm, Sine Disturbance, Transparent Web

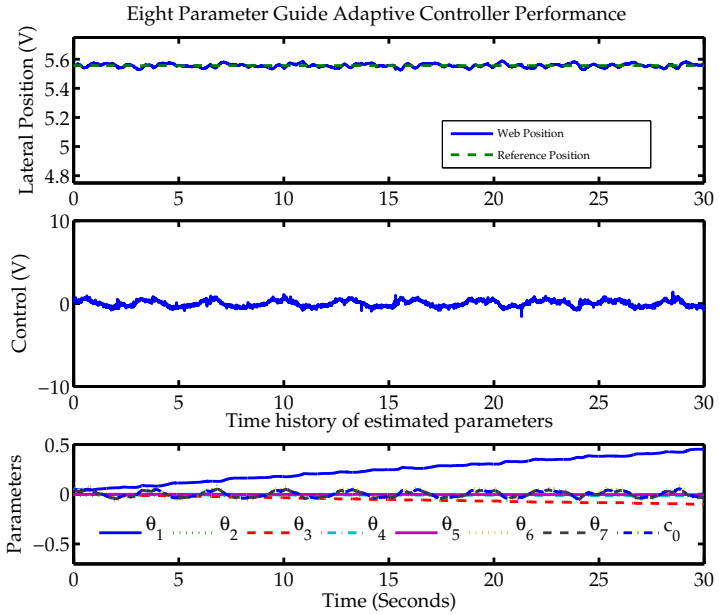

Figure D.32: Adaptive Controller: 8-Parameters, 500 fpm, Sine Disturbance, Transparent Web

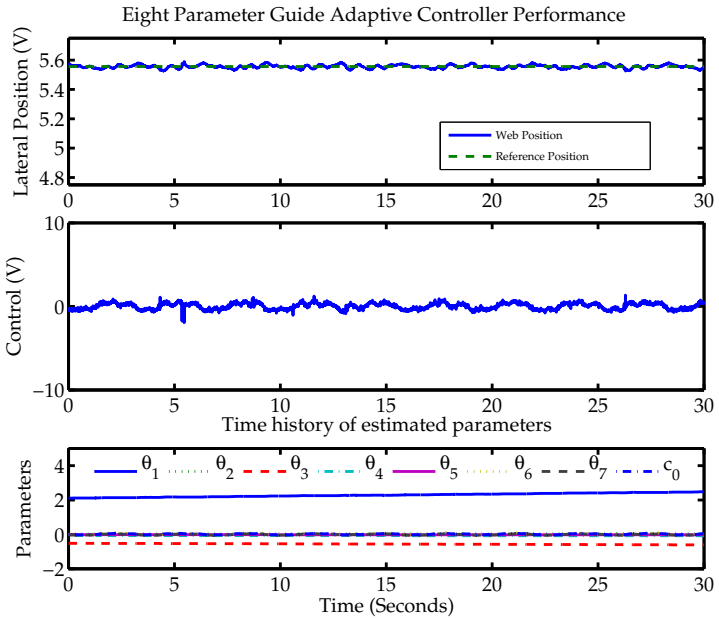

Figure D.33: Adaptive Controller: 8-Parameters, 500 fpm, Sine Disturbance, Steady-State, Transparent Web

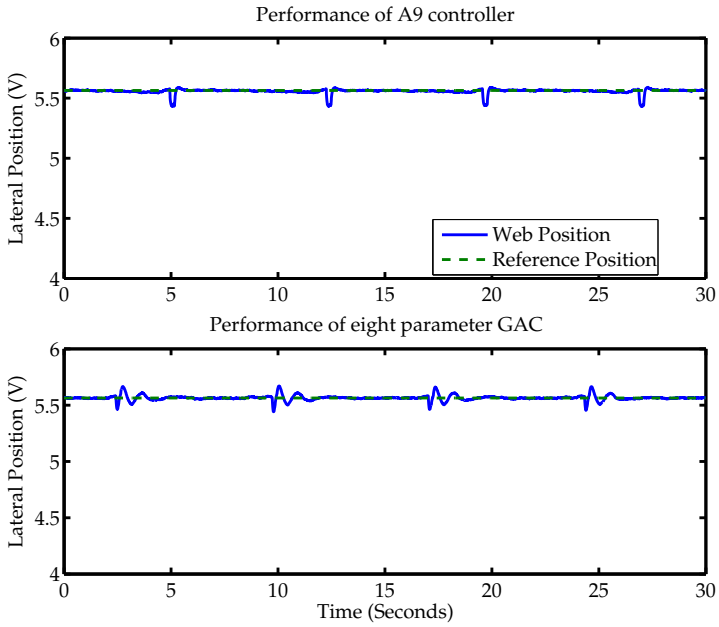

Figure D.34: Performance Comparison: 8-Parameters, 300 fpm, Pulse Disturbance, Transparent Web

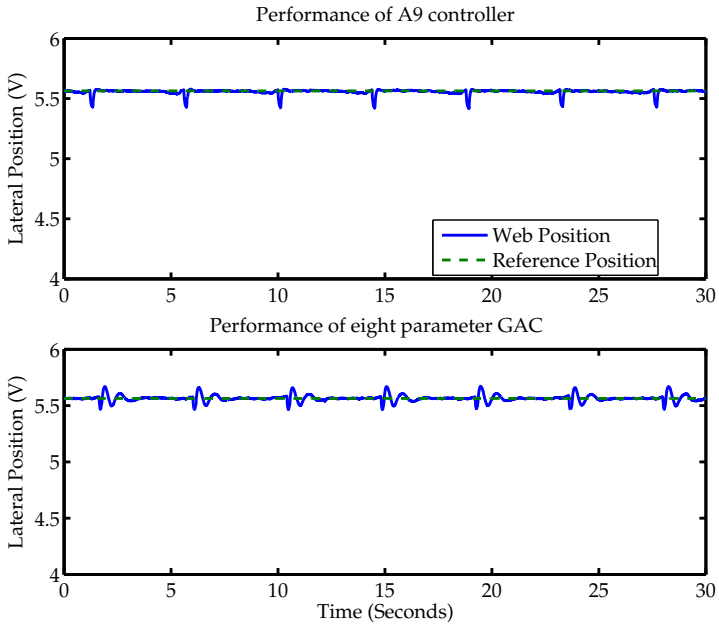

Figure D.35: Performance Comparison: 8-Parameters, 500 fpm, Pulse Disturbance, Transparent Web

VITA

Aravind Seshadri

Candidate for the Degree of

Master of Science

Thesis: MODEL REFERENCE ADAPTIVE CONTROL OF WEB GUIDES

Major Field: Mechanical Engineering

Biographical:

Personal Data: Born in Chennai (Madras), India, on August 4, 1982, the youngest son of Seshadri Krishnamachari and Vijayalakshmi Seshadri.

Education: Receive Bachelor of Engineering in Mechanical Engineering from University of Madras, Chennai, India, in 2003; Completed the requirements for the Master of Science degree with a major in Mechanical Engineering and a minor in Mathematics at Oklahoma State University in May, 2007.

Experience: Research Assistant at Oklahoma State University from June 2004 - present; Teaching Assistant at Oklahoma State University from August 2004 - December 2005.

Professional Memberships:

- American Society of Mechanical Engineers (ASME)
- Institute of Electrical and Electronics Engineers (IEEE)
- IEEE Computational Intelligence Society (IEEE CIS)
- IEEE Control Systems Society (IEEECSS)
- IEEE Robotics & Automation Society (IEEE RAS)
- International Society for Optical Engineering (SPIE)
- Society for Industrial and Applied Mathematics (SIAM)